SALINTY TOLERANCE IN THE SINGLE-CELL C_4 SPECIES *BIENERTIA SINUSPERSICI* AND THE KRANZ-TYPE C_4 SPECIES *SUAEDA ELTONICA* (CHENOPODIACEAE)

BY

COURTNEY PRICE LEISNER

A thesis submitted in partial fulfillment of
the requirements for the degree of

MASTER OF SCIENCE IN BOTANY

WASHINGTON STATE UNIVERSITY
Department of Biological Sciences

AUGUST 2009

To the Faculty of Washington State University:

The members of the Committee appointed to examine the thesis of COURTNEY PRICE LEISNER find it satisfactory and recommend it be accepted.

Gerald E. Edwards, PhD., Chair

Mechthild Tegeder, PhD.

Asaph Cousins, PhD.

ACKNOWLEDGMENTS

I would like to express my gratitude to my advisor, Gerry Edwards, for his continual support and patience. He gave me the opportunity to develop my own skills in scientific inquiry and discover my passion for botanical science. I have learned the most about myself and scientific investigation from this experience.

I would also like to extend thanks to my committee members, Mechthild Tegeder and Asaph Cousins, for their guidance and valuable insight. I would also like to thank Valerie Lynch-Holm and Chris Davitt for their help with my microscopy work in the Franceschi Microscopy and Imaging Center, and their guidance during my time as a teaching assistant there. I would also like to thank Chuck Cody, Elena Voznesenskaya and Nouria Koteeva for their extensive knowledge and assistance in growing the plants needed for my project. I would also like to thank Ray Lee and the Cousin's lab for their assistance in completing various analyses needed in my project. I would like to thank Marc Evans for his extensive help with all of my statistical questions related to this project.

I have had the privilege of working in a lab with a group of helpful and inventive students and scientists. I would like to thank Monica Smith, JoonHo Park, Yasuko Nagai, Olavi Kiirats, Josh Rosnow, and Sascha Offermann for helping with experimental protocols, research questions, and for having great scientific queries related to my research project. Their friendship, knowledge and support were essential components to the success of my research project. Finally, I would like to acknowledge all of my friends and family for their never-ending support and encouragement.

SALINITY TOLERANCE IN THE SINGLE-CELL C_4 SPECIES *BIENERTIA SINUSPERSICI* AND THE KRANZ-TYPE C_4 SPECIES *SUAEDA ELTONICA* (CHENOPODIACEAE)

Abstract

By Courtney Price Leisner, MS
Washington State University
August 2009

Chair: Gerald E. Edwards

Beginning in 2001, research on the photosynthetic mechanisms of plant species in the Chenopodiaceae family revealed these plants can carry out C_4 photosynthesis within individual photosynthetic cells, through the development of two cytoplasmic domains having dimorphic chloroplasts. This dispelled the 35 year paradigm that Kranz-type anatomy is required for C_4 photosynthesis. The single-cell C_4 species being studied are halophytes, but the effect of high salinity levels on the developmental transition from C_3 to C_4, and plant functions remain to be determined. The response of the single-cell C_4 species to increasing salinity was investigated to determine optimal growth and tolerance, using microscopic, biochemical and physiological techniques. *Bienertia sinuspersici* and a related Kranz type C_4 species, *Suaeda eltonica* were grown in growth chambers in an aerated hydroponic system with modified Hoagland's solution (adapted from a previous method used with *Arabidopsis*), with exposure to varying levels of NaCl. Salinity treatments (0 to 400 mM NaCl) show *B. sinuspersici* has optimum growth under 50-200 mM NaCl, while growth is severely impaired in 400 mM NaCl (near sea water levels). Differences were observed in growth, chlorenchyma cell morphology, carbon isotope values as a measure of C_4

efficiency, content of selected photosynthetic enzymes and rates of carbon assimilation. Under all salt levels, mature leaves develop the C_4 type of chlorenchyma cells and express C_4 enzymes, showing salt is not required for C_4 development, but is required for optimum growth.

TABLE OF CONTENTS

LIST OF FIGURES

Dedication

This thesis is dedicated to all the great ‘bears’ in my life.

CHAPTER ONE

GENERAL INTRODUCTION

Single-Cell C_4 Photosynthesis

Kranz anatomy requires the spatial separation of fixation of atmospheric CO_2 and the donation of CO_2 to the carboxylation enzyme in the Calvin cycle, Rubisco (ribulose-1,5-bisphosphate carboxylase-oxygenase). Rubisco is a dual substrate enzyme; it can catalyze reactions with either CO_2 or O_2. While the carboxylase reaction (CO_2) produces the necessary building blocks for carbon skeletons needed for plant metabolism, the oxygenase reaction (O_2) initiates photorespiration. Oxygenation is considered a wasteful side reaction of Rubisco because it uses active sites that otherwise would be used for carboxylation, it consumes RuBP, and the recovery of carbon in phosphoglycolate metabolism consumes ATP and reducing equivalents while releasing previously fixed CO_2 (Sharkey, 1985). The spatial separation between the initial capture of atmospheric CO_2 and its donation to Rubisco in C_4 photosynthesis creates a CO_2-concentrating mechanism that largely eliminates the oxygenase reaction, allowing CO_2 levels to be close to saturation even under conditions where stomatal conductance is lowered to prevent water loss (i.e., high temperatures, drought, and saline conditions).

In Kranz-type C_4 photosynthesis, the enzyme required for fixation of atmospheric CO_2 (PEPC, phospho*enol*pyruvate carboxylase) is found in the mesophyll cells. The mesophyll cells surround the bundle sheath cells, where exclusively Rubisco is located. Atmospheric CO_2 is fixed into C_4 acids (malate and aspartate) which are shuttled into the bundle sheath cells, where they are used as donors of CO_2 to Rubisco. Until recently, it was believed that without this

spatial separation between two cell types, the CO_2 concentrating mechanism in C_4 photosynthesis would not efficiently function. With the discovery of single-cell C_4 photosynthesis, it was found that sufficient spatial separation of the initial CO_2 fixation and donation of CO_2 to Rubisco can be achieved in one chlorenchyma cell type.

Research on species in the Chenopodiaceae revealed this novel type of single-cell C_4 photosynthesis. In the single-cell C_4 system, spatial separation of the C_4 enzymes is accomplished between dimorphic chloroplasts in individual chlorenchyma cells, as opposed to different cell types in Kranz anatomy. In *Bienertia sinuspersici* and *B. cycloptera* (Chenopodiaceae), these dimorphic chloroplasts are located around the periphery of the cell (peripheral chloroplasts, PC) and in the central cytoplasmic compartment (CCC chloroplasts). The peripheral chloroplasts are functionally analogous to mesophyll chloroplasts, while the CCC chloroplasts are analogous to bundle sheath chloroplasts in Kranz type C_4 plants. Also located in the CCC are the mitochondria, which contain the decarboxylating enzyme (NAD-malic enzyme) necessary to release CO_2 from the C_4 acids and concentrate it around Rubisco (see Edwards *et al*., 2004). (Figure 1)

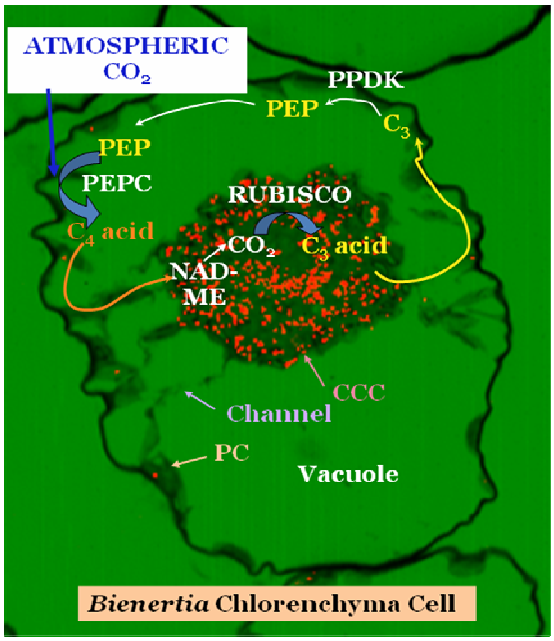

Figure 1. Model of C_4 photosynthesis in *Bienertia*.

B. sinuspersici is a NAD-ME type C_4 species, which relates to the decarboxylating enzyme which releases CO_2 around Rubisco. In NAD-ME type C_4 species, alanine plus atmospheric CO_2 is converted to aspartate in one compartment through alanine aminotransferase,

pyruvate Pi dikinase (PPDK), PEP carboxylase (PEPC) and aspartate aminotransferase reactions (Kanai and Edwards, 1999). Then aspartate is metabolized to alanine plus CO_2 in another compartment (through aspartate aminotransferase, malate dehydrogenase, NAD-malic enzyme, and alanine aminotransferase), where the CO_2 is assimilated by Rubisco. This results in a shuttle of aspartate and alanine in the C_4 cycle. The relative enzymatic activities of PEPC, PPDK, NAD-ME and Rubisco can all greatly affect the capacity of net CO_2 assimilation rates.

While there is a model for the overall biochemistry of C_4 photosynthesis in *B. sinuspersici* (Figure 1), how this species may utilize this unique photosynthetic system and other adaptations to tolerate highly saline and desert conditions in the Persian Gulf is unknown. Kranz-type C_4 photosynthesis is known to confer some level of drought and high temperature tolerance due to its CO_2 concentrating mechanism. This concentrating mechanism allows plants to lower their stomatal conductance and prevent water loss. In areas where water loss must be minimized, such as high temperature and drought, C_4 photosynthesis can be advantageous. The focus of the current research investigation was to study the growth, morphological and photosynthetic response of the single-cell C_4 species *B. sinuspersici* to saline conditions compared to the related Kranz type species *Suaeda eltonica*.

Halophytes versus Glycophytes.

Salinity is a major environmental factor limiting plant growth and productivity. During the onset and development of salt stress within a plant, the major processes such as photosynthesis, protein synthesis, and energy and lipid metabolism are affected due to the toxic effect of salt on plant metabolism (Parida and Das, 2005). Salt stress reduces the soil water

potential and causes ion imbalance or disturbances in ion homeostasis and toxicity in the soil. Lowered soil water potential can prevent a plant from taking up water unless it lowers its own water potential through the accumulation of solutes. This altered water status leads to initial growth reduction and limitation of plant productivity. Since salt stress involves both osmotic and ionic stress, growth suppression is directly related to the total concentration of soluble salts, or the osmotic potential of soil water (Parida and Das, 2005). Some plant species however, have developed the ability to grow in areas with soil containing high levels of salt by utilizing mechanisms that allow them to take up or exclude ions from the soil, which in turn, allow them to take up sufficient water.

Salt tolerance is the ability of plants to grow and complete their life cycle on a substrate that contains high concentrations of soluble salt. Plants that can survive on high concentrations of salt in the rhizosphere and grow well are called halophytes. Halophytes are either obligate or facultative depending on their salt-tolerating capacity. Obligate halophytes have constitutive features for salt tolerance and are characterized by low morphological and taxonomical diversity with relative growth rates increasing in salt concentrations equal to 50% sea water (approx. 250 mM) (Parida and Das, 2005). In facultative halophytes, some tolerance to salt is inducible; they are found in less saline habitats along the border between saline and nonsaline upland and are characterized by broader physiological diversity which enables them to cope with saline and nonsaline conditions (Parida and Das, 2005).

Although they represent only 2% of terrestrial plant species, halophytes are present in about half the higher plant families and represent a wide diversity of plant forms (Glenn *et al*., 1999). Halophytic species have evolved the necessary mechanisms to persist in areas with saline soils, marshes, and wetlands. However, almost all our modern crops are derived from

glycophytes, which are plants apparently lacking the genetic basis for salt tolerance (Glenn *et al*., 1999). Glycophytes and halophytes can have a wide range of salt tolerance and sensitivity. Greenway and Munns (1980) divided the large range of salinity tolerance in glycophytes and halophytes into three groups (Figure 2). Group I (A and B) represented halophytes which continue to grow rapidly at 200-500 mM NaCl (Greenway and Munns, 1980). In this group is *Suaeda maritima*, also a member of the Chenopodiaceae, which occurs in subfamily Suaedoideae along with *B. sinuspersici*. Group II represents halophytes that grow very slowly above 200 mM NaCl. This group includes halophytes and nonhalophytes that show a mid-range of tolerance, from intermediate to sensitive, and are represented by red fescue (*Festuca rubra* supsp. *littoralis*), tomato (*Lycopersicon esculentum*), and soybean (*Glycine max*) (Greenway and Munns, 1980). Finally, group III represents very salt sensitive non-halophytes. This includes fruit trees such as avocado and citrus (Greenway and Munns, 1980).

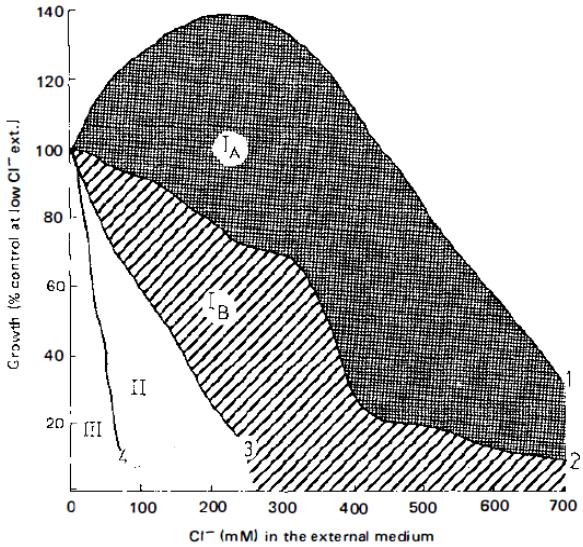

Figure 2. Growth response of different species to salinity. Growth after 1-6 months at high external Cl^-. Curve 1: *Suaeda maritima*; Curve 2: sugar beet and *Spartina townsendii*; Curve 3: cotton; Curve 4: beans (Greenway and Munns, 1980).

Halophytes: General mechanisms of salinity tolerance.

Despite their polyphyletic origins, halophytes appear to have evolved the same basic method of osmotic adjustment: accumulation of inorganic salts, mainly NaCl, in the vacuole and accumulation of organic solutes in the cytoplasm (Glenn *et al*., 1999). Osmotic adjustment, at the physiological level, is an adaptive mechanism involved in drought or salinity tolerance. This permits the maintenance of turgor under conditions of water deficit, as it can counteract the effects of a rapid decline in leaf water potential (Chen *et al*., 2009). A plant must have a more negative water potential in order to take up water from the soil. When the soil contains a high level of solutes (i.e., NaCl), the plant must take up more solutes in order to have a more negative water potential than the soil. Halophytes have developed the ability to accumulate inorganic and

organic solutes within the cell, as well as the ability to excrete these salts through salt glands and other excretory mechanisms.

Halophytic plant species have also developed the ability to accumulate compatible solutes in order to have a more negative water potential than the saline soils they inhabit. If Na^+ and Cl^- are sequestered in the vacuole of a cell, organic solutes that are compatible with metabolic activity even at high concentrations (hence 'compatible solutes') must accumulate in the cytosol and organelles to balance the osmotic pressure of the ions in the vacuole (Munns and Tester, 2008). These compatible solutes can also prevent ion toxicity by allowing plants to change their osmotic potential without accumulating high levels of Na^+ or Cl^- ions. The compounds that accumulate most commonly are sucrose, proline, and glycine betaine, although other molecules can accumulate to high concentrations in certain species (Munns and Tester, 2008). The ATP requirement for the accumulation of Na^+ in the vacuole has been estimated at 3.5, and for synthesis of compatible solutes at 34 for mannitol, 41 for proline, 50 for glycine betaine, and approximately 52 for sucrose (Munns and Tester, 2008). The synthesis of these compounds occurs at the expense of plant growth, but may allow the plant to survive and recover from the presence of high external concentrations of salt (Munns and Tester, 2008).

Salt tolerance of plants may also depend on a High-affinity K^+ Transporter (HKT), which mediates Na^+-specific transport or Na^+-K^+ transport, and plays a key role in the regulation of Na^+ homeostasis (Chen *et al*., 2009; Munns and Tester, 2008). HKTs are proposed to function in the root (Laurie *et al*., 2002). Different patterns of gene expression within the plant also affect the role of these transporters in net cation uptake to the shoot; expression of a protein that catalyzes influx in the outer half of the root (epidermis and cortex) increases influx into the plant, but an influxer in the stele reduces net influx into the plant (Munns and Tester, 2008). Additionally,

there is evidence that in salt-tolerant plants, the compartmentation of Na^+ into vacuoles is accomplished by operation of a Na^+/H^+ anitporter in the tonoplast (Glen *et al*., 1999). This provides an efficient mechanism to avert the deleterious effects of Na^+ in the cytosol and maintains osmotic balance by using Na^+ (and chloride) accumulated in the vacuole to drive water into the cells (Apse *et al*., 1999). This Na^+/H^+ anitporter transports Na^+ into the vacuole by using the electrochemical gradient of protons generated by the vacuolar H^+-translocating enzymes, H^+-adenosine triphosphatase (ATPase) and H^+-inorganic pyrophosphatase (PP_iase) (Apse, *et al*., 1999). These transporters allow for the necessary osmotic adjustment to avoid drought-like effects from saline soils.

While plants may take up NaCl into the vacuole to avoid toxic cytosolic level of Na^+/Cl^- ions, some plants also accumulate NaCl in salt glands. It is assumed that glands export ions directly from the cytoplasmic space, controlling ion concentration in the [cytoplasmic] phase (Lüttge, 1971). Work done on *Limonium* demonstrated the salt export mechanism was subject to metabolic induction in response to the external medium concentration of ions, and thus it is highly adaptive to varied degrees of salinity (Lüttge, 1971). Salt glands allow plants to tolerate higher levels of NaCl in the soil while still maintaining cellular turgor pressure and lower ionic concentrations.

These general mechanisms of salinity tolerance enable halophytic species to persist in areas other species would find intolerable. Plants may utilize a medley of tolerance mechanisms to prevent ion toxicity and allow for water uptake. While more species-specific tolerance mechanisms are documented, these general mechanisms give a background of the major problems encountered by plants growing in saline soils and how they manage them.

Methods of salt tolerance in the Chenopodiaceae.

High salt levels, combined with the arid climate of a desert ecosystem, create a difficult environment for most plants. However, a few plant families have however developed adaptations that allow them to persist in such a harsh environment. In many semi-arid deserts, Chenopodiaceae is the most important plant family (Schmida, 1985). In addition to being members of the desert community, Chenopodiaceae is also a dominant family in coastal salt-marshes located in the Irano-Turanian region, as well as other regions of Asia (Shmida, 1985). Chenopods have adapted to the high salt levels and high temperatures of the desert environments of Iran and other parts of Asia and the Persian Gulf; these adaptations have allowed them to become dominants in desert and saline communities. An important group of Chenopods is a succulent clade consisting of subfamilies Suaedoideae, Salsoloideae, and Salicornioideae, which have semi-terete or terete (tapered or cylindrical) leaves with large water/salt storage cells (Kapralov *et al*., 2006).

The Chenopodiaceae may have originated in the huge salt-desertic areas of the drained Tethyan Ocean during the Miocene-Pliocene Period (Shmida, 1985). Since the salty habitat is widespread over vast areas of coast, the species of this family were distributed across coastal biotopes (areas with uniform abiotic conditions) and to other continental coasts by long-distance dispersal (Shmida, 1985). Similarities found between coastal habitats and desert habitats have allowed Chenopods to survive this long-distance dispersal into coastal habitats. Both environments are typified by their salty and sandy biotopes (Shmida, 1985), and both contain such harsh growing conditions that eliminate most species. The proposed evolution of Chenopods in saline habitats has facilitated the development of adaptations for low water, high salt and arid soil and atmospheric conditions. Along with the adaptation of C_4 photosynthesis,

these adaptations have allowed Chenopods to become a dominant species in arid desert communities (Figure 3).

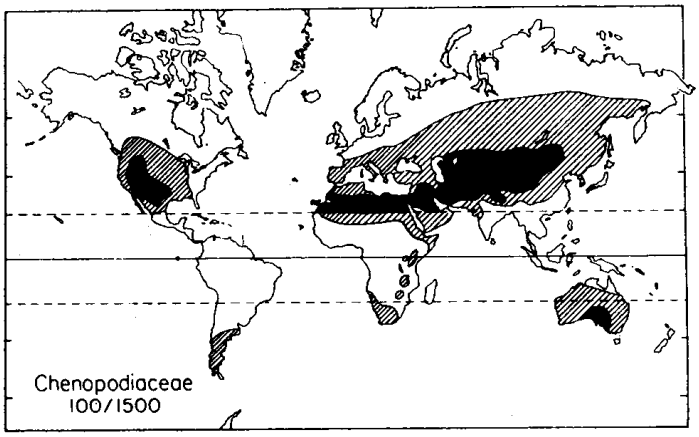

Figure 3. Distribution map of the Chenopodiaceae (100 genera, 1500 species). Black areas represent desert, lined areas represent Chenopod distribution. (Shmida, 1985).

The diverse halophytic vegetation of the Chenopodiaceae is supported by saline habitats formed by salty rivers in the Irano-Turanian region (Akhani, 2004). The Irano-Turanian region (including the area around the Persian Gulf, Makran and West Pakistan) could be considered a center of origin or center of diversity for many halophytic genera of Chenopodiaceae, e.g. *Halimoncnemis*, *Halanthium*, *Piptoptera*¸ *Climacoptera*, *Petrosimonia*, *Gamanthus*, *Bienertia*, *Kalidium*, *Halostachys*, *Salsola*, and *Suaeda*. Formation of these saline habitats in Iran was caused by low rainfall, transport of salt by wind and river flow, salt spray in the littoral and marsh zones, the geologic origin of salt in various soil deposition layers, and anthropogenic and agricultural activities (Akhani, 2004).

Plant species within the Chenopodiaceae in the Irano-Turanian region can be categorized as leaf succulent halophytes. These species occur on moderate to high salty soils in habitats influenced by natural disturbances (temporal inundation or leaching of high salty soils by flooding) or human disturbances and nitrification of habitats (e.g., wetlands, roadsides). Specifically, succulent C_4 Chenopods are located in shrubby, semi-woody or hemicrytophytic communities on salty and dry soils (Akhani, 2004). These halophytic plant species form associations with many other types of halophytes within the desert community. Halophytic C_4 Chenopods form ecological associations with stem-succulent C_3 Chenopods in semi-woody or perennial halophytic communities on muddy or coastal salt flats. In addition, the C_4 Chenopods form associations with salt-excreting halophtyes and obligatory hygro-halophytes in salt marsh and riverine burchwood communities located by the sea, lakes and rivers (Akhani, 2004).

Species in the Chenopodiaceae can be characterized as arido-active perennials and bi-seasonal annuals (Shmida, 1985), i.e. these plants remain metabolically active (to some degree) during the entire year, even the dry season. To accomplish year-round metabolic activity, several morphological and developmental strategies have evolved. As the level of water in the soil solution decreases, the water soil potential increases (becomes more negative). This increases the propensity of water to move from the roots into the soil. Consequently, plants must prevent desiccation and decrease transpiration. The development of xeromorphic traits, such as excessive development of fibrous tissue, thickened or otherwise covered epidermis, sunken and protected stomata, and reduction or 'waxing' of the transpiring surface (Polunin, 1960) allows a plant to withstand arid conditions. Chenopods can also reduce their metabolically active surface area, which decreases the distance photosynthates and other nutrients must be transported. A reduction in the metabolically active surface is accomplished by having a small surface area in

relation to dry weight, and seasonal surface reduction as a function of increasing water stress by leaf and branch shedding, and by "partial death" (Evenari, 1985).

Additional xeromorphic traits include an increase in root to shoot biomass ratio and a change in root morphology in response to soil water levels. Roots can exploit a relatively large volume of water, have large horizontal extension, and reach great depths when needed (Evenari, 1985). Chenopods can also reduce heat stress caused by the elevated solar radiation and temperature by leaf movements (i.e. curling), leaf hairs and high reflectivity of incoming radiation (Evenari, 1985). Finally, members of the Chenopodiaceae may not flower in years of extreme drought, which decreases the water and energy needed to support the plant.

These morphological and developmental adaptations allow for physiological adaptations in Chenopods that are beneficial for persistence in deserts and saline habitats. These plants also decrease transpiration rates through regulation of the stomatal opening. Variable movement of the stomates prevents excess water loss and gas exchange during periods of drought, high light intensity and elevated temperatures. Additionally, Chenopods have the capacity to reduce salt loads by excreting excess salt through glands, or take in high levels of saline water in order to tolerate the high levels of salt in the soil solution of the Irano-Turanian deserts. Members of the Chenopodiaceae also have the capacity to control independently the rate of transpiration and photosynthesis (known as "flexible coupling") and the capacity to change the diurnal pattern of net photosynthesis as a function of decreasing water potential (Evenari, 1985).

In addition to "flexible coupling," Chenopods utilize C_4 photosynthesis to decrease their rate of photorespiration and the futile cycling of CO_2. The CO_2 concentrating mechanism in C_4 photosynthesis allows the plant to have high-temperature optima of net photosynthesis and

temperature acclimation of photosynthesis (Evenari, 1985). The novel single-cell C_4 photosynthesis may also confer some level of salinity or drought tolerance, which is the focus of this study.

These physiological and morphological adaptations have created the ecological amplitudes of Chenopods that allow them to occupy arid desert climates, as well as saline soils. The use of C_4 (and possibly single-cell C_4 photosynthesis) has also given these plant species higher water use efficiency, which makes them ideally suited for arid ecosystems (Evenari, 1985). Adaptations conferring increased water use efficiency and decreased transpiration rates allow Chenopods to also occupy saline habitats. More than half of the halophytic and salt-tolerant plant species in Iran are Chenopods (Akhani *et al*., 1993), making them a dominant halophyte in the Irano-Turanian region. The dominance exhibited by the Chenopodiaceae in arid and saline communities makes this family a good indicator species for increased aridization and desertification resulting from global warming. Additionally, the development of single-cell C_4 photosynthesis exclusively in such a halophyte-dominated family such as Chenopodiaceae, is ideal for understanding if this novel type of photosynthesis confers some level of salinity tolerance for these plants.

Research Aim

As global temperature and CO_2 levels increase, understanding how plants respond to these altered environmental conditions will become increasingly important for predicting broader ecosystem-wide changes. C_4 plants are noted for having higher rates of photosynthesis under CO_2 limited conditions, and higher water and nitrogen use efficiency. Succulent C_4 species have

morphological features which may increase tolerance to drought and saline conditions. Rising global temperatures decrease global freshwater availability due to glacier retreat, which, in turn, causes coastal salt intrusion. Halophytic vegetation with higher photosynthetic efficiencies under salt stress could be important in maintaining ecosystems in these future saline environments. Furthermore, the presence of halophytic C_4 species may be an indicator for salt intrusion and an overall increase in arid climates and global temperatures.

The succulent C_4 species in the Chenopodiaceae are not only dominant members of their communities but also important filters for the abiotic environment. Halophytic vegetation in arid climates can be used to prevent salt intrusion by improving the quality of saline soils. The high intake of salt, coupled with the release of nutrients and gases into the environment by these plants, improves soil conditions (Evenari, 1985). These activities in turn, create microhabitats that allow other plant species to enter the community as well as microorganisms and desert animals. As a result, a community forms, despite the challenging habitat.

In addition to their role in altering soil conditions, Chenopods may play an important role in the face of global warming. Rising temperatures due to elevated greenhouse gases in the atmosphere have created more arid environments world-wide. The ability of Chenopods to remain metabolically active under extreme temperatures and low water availability allows them to persist in these arid environments. Changes in the habitat range of the Chenopodiaceae may therefore be used as a possible indicator of salt intrusion and/or climate aridization. Areas previously unoccupied by Chenopods that now contain these species may indicate increased atmospheric temperatures and possible salt intrusion into these habitats. Similar to the advancement of the timberline in mountainous regions, the habitat range of the Chenopodiaceae may act as an indicator for the advancement of climate change due to global warming.

The focus of this research is on the single-cell C_4 species *B. sinuspersici* and how this novel photosynthetic mechanism is affected by NaCl. If having a single-cell system aids the plant in accumulating or coping with high levels of NaCl, what about the single-cell system confers salinity tolerance? Also, does the formation of the single-cell C_4 system require NaCl? All of these questions are pertinent to understanding more about this unique photosynthetic mechanism and what relationship it might have with the halophytic properties in *B. sinuspersici*. Understanding the development and stress tolerance mechanisms in this halophytic species may shed light on its overall ecological role, especially in light of current global climate aridization and soil salinization.

References

Akhani, H (2004) Halophytic vegetation of Iran: towards a syntaxonomical classification. Annali Di Botanica 4: 65-82.

Akhani H, and Ghorbanli, M (1993) A contribution to the halophytic vegetation and flora of Iran. Towards the rational use of high salinity tolerant plants 1: 35-44.

Apse MP, Aharon GS, Snedden WA, and Blumwald, E (1999) Salt tolerance conferred by overexpression of a vacuolar Na^+/H^+ antiport in *Arabidopsis*. Science 285: 1256–1258.

Chen S, Gollop N, and Heuer B (2009) Proteomic analysis of salt-stressed tomato (*Solanum lycopersicum*) seedlings: effect of genotype and exogenous application of glycinebetaine. J. of Expt. Bot. 60: 2005-1019.

Edwards GE, Franceschi VR, and Voznesenskaya EE (2004) Single-cell C_4 photosynthesis versus the dual-cell (Kranz) paradigm. Annu. Rev. Plant Biol. 55: 173-196.

Evenari, M (1985) Adaptations of plants and animals to the desert environment. *in* M. Evenari, I. Noy-Meir, and D. W. Goodall, editors. Ecosystems of the world: hot deserts and arid shrublands, A. Elsevier Science Publishers B.V., New York, New York, USA. pp. 79-92.

Glenn EP, Brown JJ, and Blumwald E (1999) Salt tolerance and crop potential of halophytes. Crit. Rev. Plant Sci. 18: 227-255.

Greenway H and Munns R (1980) Mechanisms of salt tolerance in nonhalophytes. Annu. Rev. Plant Physiol. 31: 149-190.

Kanai R and Edwards G (1999) The Biochemistry of C_4 Photosynthesis. *in* Sage, R. and R. Monson, editors. C_4 Plant Biology. Academic Press, San Diego, CA, USA. pp. 49-80.

Kapralov MV, Akhani H, Voznesenskaya EV, Edwards G, Franceschi V, and Roalson EH (2006) Phylogenic relationships in the Salicornioideae / Suaedoideae / Salsoloideae s.l.

(Chenopodiaceae) clade and a clarification of the phylogenetic position of *Bienertia* and *Alexandra* using multiple DNA sequence datasets. Sys. Bot. 31: 571-585.

Laurie S, Feeney KA, Maathuis FJM, Heard PJ, Brown SJ, and Leigh RA (2002) A role for HKT1 in sodium uptake by wheat roots. Plant J. 32: 139-149.

Lüttge, U (1971) Structure and function of plant glands. Annu. Rev. Plant Physiol. 22: 23-44.

Munns R and Tester M (2008) Mechanisms of salinity tolerance. Annu. Rev. Plant Biol. 59: 651-81.

Parida, AK, and Das AB (2005) Salt tolerance and salinity effects on plants: a review. Ecotox. Environ. Safe. 60: 324-349.

Polunin, N (1960) Introduction to plant geography and some related sciences. McGraw-Hill, New York, New York, USA.

Sharkey, TD (1985) O_2-insensitive photosynthesis in C_3 plants. Its occurrence and a possible explanation. Plant Physiol. 78: 71-75.

Shmida, A (1985) Biogeography of the desert flora. *in* M. Evenari, I. Noy-Meir, and D. W. Goodall, editors. Ecosystems of the world: hot deserts and arid shrublands, A. Elsevier Science Publishers B.V., New York, New York, USA. pp. 23-78.

CHAPTER TWO

SALINITY TOLERANCE IN THE SINGLE-CELL C_4 SPECIES *BIENERTIA SINUSPERSICI* (CHENOPODIACEAE)

Abstract

Recent research on the photosynthetic mechanisms of plant species in the Chenopodiaceae family revealed that three species, including *Bienertia sinuspersici*, can carry out C_4 photosynthesis within individual photosynthetic cells, through the development of two cytoplasmic domains having dimorphic chloroplasts. These unusual single-cell C_4 species are halophytes which have semi-terete succulent leaves. The effects of salinity (0 up to 400 mM NaCl) on growth and photosynthesis of *B. sinuspersici* were studied. The results show that this species can grow and develop the single-cell C_4 system without NaCl. Growth is enhanced by NaCl (50 to 200 mM), while severe inhibition of growth and photosynthesis occurs at 400 mM NaCl. Analysis of chlorenchyma cells by microscopy showed formation of the single-cell C_4 type photosynthetic cells in all treatments. Carbon isotope analysis of leaf biomass, western blots on key C_4 pathway enzymes, and measurements by gas exchange (including the CO_2 compensation point, and level of CO_2 required to saturate CO_2 assimilation) show function of C_4 type photosynthesis, although salinity had quantitative affects on these parameters, and on growth. With increasing salinity the carbon isotope values of leaves ($\delta^{13}C$) became more positive (up to 2.5 ‰), suggestive of increased efficiency of C_4 function under saline conditions. Saline conditions up to 200 mM NaCl resulted in an increase in the size and fresh weight of leaves (reflecting an increased succulence), and an apparent increase in shoot and root biomass.

Treatment with moderate levels of salt resulted in the highest CO_2-saturated rates of photosynthesis on a per leaf and per unit leaf dry weight basis. With increasing salinity, there was an apparent decline in the maximum rates of CO_2 assimilation and the maximum carboxylation efficiency on a leaf area basis as leaves became more succulent. At the same time, western blot data showed there was an increase in PEPC and PPDK, and a slight decrease in NAD-ME and Rubisco on a protein basis with increasing NaCl. The influence of salinity on plant development and the C_4 system in *Bienertia* is discussed.

Introduction

An effective means for minimizing photorespiration in terrestrial settings is the C_4 CO_2-concentrating mechanism, involving the carboxylation of PEP and the shuttling of four and three carbon acids between two specialized compartments. In Kranz type C_4 anatomy this includes the mesophyll tissue, where initial fixation of inorganic carbon occurs, and an inner ring of 'bundle-sheath' cells, surrounding the vascular bundle (Sage, 1999). C_4 photosynthesis was believed to require this characteristic type anatomy in order to effectively spatially separate the initial fixation of atmospheric CO_2 and the carboxylation reaction of Rubisco with CO_2. However, research on plants in the Chenopodiaceae family, revealed plants that can carry out C_4 photosynthesis within a single photosynthetic cell.

Initial investigations on these plants has shown the functioning of single-cell C_4 photosynthesis, through spatial compartmentalization of dimorphic chloroplasts and other organelles (Edwards *et al*., 2004; Voznesenskaya *et al*., 2002). During leaf development, there is conversion of young C_3 like chlorenchyma cells (with a single type of chloroplast) to the spatial

development of two cytoplasmic compartments having dimorphic chloroplasts. In *Bienertia sinuspersici* (the species of interest in this study), the dimorphic chloroplasts are partitioned between peripheral chloroplasts and a central cytoplasmic compartment (CCC) (Edwards *et al*., 2004; Voznesenskaya *et al*., 2002).

The single-cell C_4 system has a CO_2 concentrating mechanism which increases photosynthetic rates by restricting photorespiration, which can occur through O_2 competition with CO_2 in binding to RuBP during catalysis by Rubisco. Due to this mechanism, C_4 plants in general are known to perform better than C_3 plants under CO_2 limited conditions, especially under high temperatures or water deficits. Also, the rate of CO_2 assimilation per unit nitrogen in C_4 plants is greater than C_3 plants because high CO_2 partial pressure in the bundle sheath cells enables Rubisco to operate near its maximum catalytic rate and suppresses photorespiration (Evans and von Caemmerer, 2000). The innate properties of C_4 photosynthesis, among various structural forms in Chenopodiaceae, is thought to contribute to the persistence of C_4 Chenopods in high temperatures and saline soils in semi-arid deserts of Central Asia and the Persian Gulf (Akhani *et al*., 2005; Voznesenskaya *et al*., 2002; Voznesenskaya *et al*., 2001).

B. sinuspersici ranges from the westernmost coasts of Pakistan and extends westward all along the coastal areas in southern Iran (Baluchestan, Hormozgan, Fars, Bushehr, and Khuzestan Provinces) and countries surrounding the Persian Gulf, including the United Arab Emirates, northern Saudi Arabia, Qatar, Kuwait, and Iraq (Ahkani *et al* ., 2005). Its ability to thrive in areas of low water content and highly saline soils makes this plant's halophytic and xeromorphic characteristics of great interest. Work on the ecology of *B. cycloptera* determined the soil salinity (measured as the electric conductivity) to be approximately 51.6 dS/m, which is slightly lower than the electric conductivity of seawater (Akhani *et al*., 2003). Coupled with its novel

photosynthetic mechanism, *B. sinuspersici* is an ideal species to study to understand the possible relationship between salinity tolerance and photosynthesis.

As global temperature and CO_2 levels increase, understanding how plants respond to these altered environmental conditions is extremely important for predicting broader ecosystem-wide changes. In addition to possessing a novel form of photosynthesis, single-cell C_4 species have morphological features which may increase tolerance to elevated temperatures, drought and soil salinity. They also serve as an alternative model to the Kranz system in considering the potential to convert C_3 crops to C_4. The aim of this research, which may be useful in efforts to improve tolerance to crops for growth in unfavorable climates, was to address three main questions about the effects of salinity on *B. sinuspersici*: 1) Is it an obligate halophyte; 2) Is there an optimal salinity level for C_4 function and growth; and 3) How is the mechanism of photosynthesis affected by salinity?

Materials and Methods

Plant Material.

Bienertia sinuspersici was propagated from cuttings grown in 2MS Media. This consisted of 8.6 g/L complete MS salt (Plant Media),10 ml/L 100X MS vitamin stock, 20 g/L sucrose, 1.95 g/L MES buffer (10 mM MES free acid), 10 mM NaCl, pH 5.8, and 0.4 % gelrite. Once roots were formed, the cuttings were placed into the hydroponics system. Cuttings were placed in modified sterile plastic test tubes (50 ml) (#227261, Cell Star, Greiner Bio-One North America Inc., Monroe, NC, USA) which had the top half removed and three 25.4 x 1 mm slits, cut in the narrow bottom of the tube. The tubes (with rooted cuttings) were placed in 3 liter

plastic containers (GladWare, Glad Products Co., Oakland, CA, USA) that were spray painted black and covered with aluminum foil to prevent algal growth. Each 3 liter container held 5 tubes. In addition, the containers were fitted with an air hose and aquarium bubbler (MillionAire MA300, Commodity Axis, Inc., Camarillo, CA, USA) to oxygenate the water. The hydroponics solution used was a modified 1/4X Hoagland's solution, as described for growth of *Arabidopsis* (Toqcuin *et al*., 2003). Plants were grown in a growth chamber (model GC-16l Econair Ecological Chambers Inc., Wiinipeg, Canada) under a maximum photosynthetic flux density of 500 μmole quanta m^{-2} s^{-1} (PPFD) during a 14/10 hr, 25/18 °C, day/night cycle. Atmospheric CO_2 was used and the relative humidity was 40%. The lights in the chamber were programmed to come on and off in a stepwise increase and decrease over a 3 hour period at the beginning and the end of the photoperiod, respectively.

Gas exchange.

Rates of photosynthesis under varying ambient CO_2 concentrations were measured using a LI-6400 portable photosynthesis system from LI-COR Biosciences (Lincoln, NE, USA). Mature leaves were removed from the plant and the individual incident leaf area was measured. Detached leaves were placed in the 6400-02B LED Light Source chamber (maximum leaf area 6 cm^2). A modified leaf chamber cuvette was used; detached leaves were placed on a mesh screen that was glued to the cuvette gasket with silicon epoxy. A slit was made in the center of the mesh screen to allow for the thermocouple to have contact with the detached leaves. Once in the chamber, the detached leaves were allowed to acclimate under 1000 PPFD, a leaf temperature of 25 °C, and 353 μbars CO_2 for 20 min until steady state photosynthesis was achieved.

Preliminary tests showed that photosynthesis of the succulent detached leaves was stable for approximately 1 hour. After this acclimation period, CO_2 response measurements were made in decreasing intervals from 353 µbars to 46 µbars and then increasing intervals to 1578 µbars atmospheric CO_2. Rates of photosynthesis were measured on a leaf area, per leaf, µg chlorophyll, mg of soluble protein and mg dry weight basis.

From response curves, the CO_2 compensation point (Γ), maximum carboxylation efficiency from the initial slope (C_E), A_{max} values (level of CO_2 assimilation under saturating photosynthesis), and stomatal conductance (g_s) were determined. Additionally, the intercellular CO_2 concentration (Ci) was calculated. After the CO_2 response curve was completed, the detached leaves were removed and partitioned for $\delta^{13}C$, chlorophyll and western blot analysis. At least 2 leaves were partitioned for $\delta^{13}C$ analysis. These leaves were put a 55 °C oven and dried for 24 hours. The remaining leaves were frozen whole in liquid nitrogen and stored in microfuge tubes at -80 °C for subsequent chlorophyll and western blot analysis.

Chlorophyll and soluble protein determination.

Total chlorophyll and soluble protein were determined from crude extracts of material used in gas exchange analysis that was frozen in liquid nitrogen and stored at -80 °C. Leaf material was homogenized with a mortar and pestle in liquid nitrogen and then equally aliquoted into separate microfuge tubes for chlorophyll and protein extraction. For chlorophyll extraction, 1 ml of 80% (v/v) acetone was added. Material was kept in the dark to prevent chlorophyll degradation. Leaf material was incubated for 3 days in 80% (v/v) acetone, with a removal and renewal of the acetone each day following centrifugation at 16,000 g for 5 minutes. The

removed acetone was stored at room temperature in the dark until the chlorophyll content was determined. After the incubation period the supernatants of all three acetone extractions were combined and an aliquot was used for the total chlorophyll measurement. Measurements were made at 663.2 and 646.8 nm in a Shimadzu UV-240 Spectrophotometer (Shimadzu Scientific Instruments, Columbia, MD, USA) using constants from Porra *et al*., (1989).

Total protein was measured from the remaining frozen leaf material previously aliquoted. The pellet was resuspended in 200 µl of the total protein extraction buffer (TBEB) (2% SDS, 10% glycerol, 5% 2-mercaptoethanol, 0.0625M Tris-HCl, pH = 6.8) and immediately boiled for 5 minutes. The extract was then centrifuged for 5 minutes at 16,000 g, the supernatant removed, placed in a new microfuge tube and assayed for total protein using the RD DC Bio-Rad Protein Assay (#500-0121, Bio-Rad Laboratories, Hercules, CA, USA) according to the manufacturer's protocol. A standard curve of bovine serum albumin (BSA) (F. Hoffman La-Roche Ltd., Basel, Switzerland) was used for calibration.

For western blots, supernatant fractions from the crude extracts from different salt treatments were adjusted to the same protein concentration, and 10 and 5 µg of protein were loaded per lane. The samples were loaded onto a 10% polyacrylamide-SDS gel and separated through gel electrophoresis (10 V/cm for 1 h in a Bio-Rad Mini-PROTEAN Tetra Electrophoresis System (Bio-Rad Laboratories, Hercules, CA, USA)). After electrophoresis, the gel was transblotted onto a nitrocellulose membrane (Bio-Rad Laboratories, Hercules, CA, USA) that was presoaked in 1X transblotting buffer (20 mM Tris base, 150 mM glycine, 0.025% SDS, and 20 % methanol (v/v)) (pH ~ 8.6) for 5 min. The membranes were transblotted for 1 h (400 mA constant current) at 4 °C. Proteins were initially visualized by reversible staining with 0.1% Ponceau S in 5% acetic acid (v/v) for 2 min, followed by 3to 4, 5 min washes with 5% acetic

acid to removed background staining. The membrane was then rinsed 3 times with distilled water and blocked with blocking buffer (3% skim dry milk in Tris-buffered Saline buffer (TBST) (100 mM Tris-HCl pH 7.5, 150 mM NaCl, 0.3% Tween-20 detergent) for 30 min.

The primary antibody (in blocking buffer) was applied to the membrane which was placed on an orbital shaker to incubate at 4 °C overnight. The primary antibody was removed and the membrane was rinsed with TBST three times, 10 min each rinse. Bound primary antibodies were located using secondary, alkaline-phosphatase conjugated goat anti-rabbit IgG. The secondary antibody (in blocking buffer) was applied to the membrane and incubated for 2 h at room temperature on an orbital shaker. The secondary antibody was removed and the membrane was again rinsed with TBST buffer three times, 10 min each rinse. The membrane was then incubated in activation buffer (100 mM Tris-HCl, pH 9.5, 100 mM NaCl and 10 mM MgCl) for 5 min. Chromogenic detection was then performed by the addition of the color substrate solution (50 µl 5-bromo-4-chloro-3-indolyl phosphate dipotassium salt (BCIP) (35 mg/ml) per 10 ml activation buffer, and 50 µl nitroblue tetrazolium salt (NBT) (70 mg/ml) per 10 ml activation buffer). Color development was stopped with washes of distilled water.

The antibodies used and their respective dilutions are as follows: anti-*Amaranthus viridis* PEPC (1:100,000; Colombo *et al*., 1998), serum against the α-subunit of NAD-ME from *Amaranthus hypochondriacus* (1:2,000; Long *et al*., 1994), anti-*Zea mays* PPDK (1:50,000; courtesy of Dr. T. Sugiyama), anti-spinach (*Spinacia oleracea*) Rubisco LSU (1:10,000; courtesy of Dr. B. McFadden).

The resulting stained membranes were scanned. The intensity of the bands was semi quantified using ImageJ 1.36b (Rasband 1997-2007) image analysis software, and expressed relative to levels in the plants grown without NaCl on a total protein and leaf area basis.

Transmission electron and light microscopy.

Leaves were collected from plants after 6 - 8 weeks of hydroponic growth. Samples were cut into 1mm^2 pieces in 2 % paraformaldehyde, 2% glutaraldehyde, 0.1 M phosphate buffer (pH 7.2), and fixed in the same solution overnight at 4 °C. After three 10 min washes with 0.1 M phosphate buffer, specimens underwent post-fixatation with 1% osmium tetroxide overnight at room temperature. Samples were washed 3 times with buffer then dehydrated stepwise from 30% to 100% ethanol. The leaf tissues were gradually infiltrated with propylene oxide through a series of exchanges, and then infiltrated with increasing concentrations (30%, 50%, 75%, 100%) of Spurr's embedding mixture (#14300, Electron Microscopy Sciences, Hatfield, Pennsylvania, USA). Each resin infiltration step was left overnight. The samples were then left in 100% Spurr's resin for 4 nights, with a fresh exchange of Spurr's each night. After infiltration, samples were finally embedded in fresh Spurr's resin and polymerized in a 40 °C oven (Fisher Scientific, Tustin, CA, USA) overnight.

Ultrathin sections (90 nm) were cut using a glass knife on a Reichert-Jung Ultracut Ultra Microtome (Cambridge Instruments GmbH, West Germany) and then picked up with Formvar (Electron Microscopy Sciences, Ft. Washington, Pennsylvania, USA) coated grids. Sections were stained for 12 min with 4% uranyl acetate and 1% potassium permanganate. The grids were then rinsed with distilled water, dipped in 0.01 N sodium hydroxide, stained for 3 min in Reynolds lead (Reynolds, 1963), rinsed again with 0.01 N sodium hydroxide, and then with distilled water. All staining steps were at room temperature. Sections were observed on a JOEL JEM 1200-EX Transmission Electron Microscope (JOEL USA, Peabody Massachusetts, USA). Images were taken using the MegaView III Digital Camera (Soft Imaging System Corp.,

Lakewood, Colorado, USA) equipped with AnalySIS 3.2 Imaging Software (Soft Imaging System Corp., Lakewood Colorado, USA).

Sections for light microscopy (800 nm) were stained using 1% toluidine blue in 1% borax and mounted on gelatin coated glass slides (Surgipath Medical Ind., Inc., Richmond, IL). Images were captured using an Olympus BH-2 Light Microscope (Olympus Optical Co., Ltd., Tokyo, Japan) and a Jenoptik ProgRes C12plus digital camera (JENOPTIK Laser, Optik, Systeme GmbH, Jena, Germany) with ProgRes Capture Pro software (Jenoptik, Jena, Germany).

Delta ^{13}C Analysis.

Leaf samples used were cut from the plants after 6-8 weeks of growth in hydroponics, or used from gas exchange analysis. Leaves were placed in microfuge tubes and dried at 55 °C for 24 h. Samples were then homogenized to a fine powder using Crescent Wig-L-Bug (Model 3110B, Dentsply Rinn, Elgin, IL, USA). Carbon isotope fractionation values were determined on dried leaves and stems, using a standard procedure relative to PDB (Pee Dee Belemnite) limestone as the carbon isotope standard (Bender *et al*., 1973).

Osmolality determination.

The osmolarity of the samples was measured using a 5500 Vapor Pressure Osmometer (Wescor Inc., Logan, UT, USA). Whole leaf samples were removed from the plants using a razor blade after 6-8 weeks of growth in hydroponics. Leaves (2 to 3) were placed in microfuge tubes and gently macerated using a small plastic pestle. Samples were then centrifuged for 5 min

at 16,000 g. The resulting supernatant was loaded onto the reference disc in the sample holder of the osmometer using 10 µl size samples. The osmometer was calibrated using 290, 100 and 1000 milliosmol standards before each use.

Determination of the total cell count, cell area, and the ratio of the cell area to central cytoplasmic compartment.

Leaf samples were removed from the plants using a razor blade after 6-8 weeks of growth in hydroponics. Individual chlorenchyma cells are readily released from leaves of *B. sinuspersici* by gentle maceration. For the total cell count, leaves were placed whole into a clean microfuge tube and gently macerated using a small, plastic pestle in 1 ml of glycine betaine (GB) buffer (1.25 M glycine betaine, 5 mM 2-(*N*-morpholino)ethanesulfonic acid.(MES), pH = 5.8 with NaOH, and 10 mM $CaCl_2$). The remaining liquid solution was filtered through a 211 µm Nitex nylon mesh (Tetko Inc., Elmsford, NY, USA) into a new microfuge tube to collect chlorenchyma cells. Mesh filtration removes epidermal tissue and vascular stands from the liquid solution. The resulting solution was then diluted with GB buffer into a new microfuge tube until only 1-2 chlorenchyma cells were observed under 10X magnification under a compound light microscope (Ernst Leitz G.m.b.h. Weltzer, Germany). The cell count per leaf was then determined by calculating the total number of cells from the original leaf extract, based on replicate counting of the number of cells observed in a 1 µl aliquote at 10X in one field of view (N = 3; 100 mM and 400 mM N = 1).

For the determination of the ratio of the cell area (CA) to the central cytoplasmic compartment (CCC), leaf samples were removed from the plants using a razor blade after 6-8

weeks of growth in hydroponics. Leaves were gently macerated in 1.25 M, 1.0 M, 0.75 M, or 0.5 M glycine betaine buffer. The cells were viewed and imaged at 10X using a compound light microscope. Quantification of the CA and CA:CCC was done using ImageJ 1.36b (Rasband 1997-2007) image analysis software. Quantification from light microscopy images was also done using ImageJ 1.36b (N = 1).

Data analysis.

Data points from the CO_2 response curves were fitted with a singular rectangular hyperbola equation (Eq. (1) using Sigma Plot (Systat Software, Inc., San Jose, CA, USA). From the fitted curve equation, the Γ value was determined by finding the x value when y = 0. The first derivative of the fitted curve equation was used to calculate the C_E value at x = 0. The coefficients of *a* and *b* were given through the nonlinear regression report given by Sigma Plot.

$$Y = Y_0 + \frac{ax}{(b+x)} \qquad \text{Eq. (1)}$$

The assimilation rates given by the LI-6400 were modified to adjust for low diffusion rates at low intercellular CO_2 (Ci) values (Eq. 2) (LI-COR Biosciences, Version 5, Book 1).

$$A = \frac{F(C_r - C_s)}{100S} - C_s E + \frac{k}{100S}(C_a - C_s) \qquad \text{Eq. (2)}$$

In Eq. 2, A represents the corrected CO_2 assimilation rate (μmol CO_2 m^{-2} s^{-1}), F is the molar flow rate of air entering the leaf chamber (μmol s^{-1}), C_r is the mole fraction of CO_2 in the reference IRGA (μmol CO_2 mol^{-1} air), C_s is the mole fraction of CO_2 in the sample IRGA (μmol CO_2 mol^{-1} air), C_sE is the rate of transpiration (mol H_2O $m^{-2}s^{-1}$), *k* is the diffusion coefficient (0.46), S is the

total incident leaf area in the cuvette chamber (cm^2), and C_a is the reference CO_2 level used (380 μmoles/mol).

Statistical analysis.

For each salt treatment plants were grown in three hydroponic boxes (except the 400 mM treatment where survival was low). Each box contained 3-5 individual plants. Replicate measurements were made within each box by pooling leaves randomly sampled from individual plants. Three independent replicates were measured for each experiment (unless otherwise noted). For gas exchange analysis, 5-10 randomly samples leaves pooled from individual plants were used for each measurement. At least 3 measurements were taken per box. These leaves were subsequently used for protein and chlorophyll content, and western blot analysis. For the leaf fresh and dry weight analysis, at least 10 measurements were made per box, pooling at least 3 leaves randomly samples from individual plants. For the carbon isotope discrimination analysis, at least 12 measurements were made per box; measurements pooled at least 3 leaves randomly sampled from individual plants. The total cell count, cell area, and central cytoplasmic compartment experiments pooled 2 leaves per measurement, and at least 20 measurements were taken per box. Finally, the osmolality experiment pooled at least 2 leaves per sample. At least 10 measurements were taken from this pooled sample. Samples were taken from each individual plant per box.

The statistical analysis of biochemical and phenotypic response variables with respect to the salt treatments was performed using a one-way ANOVA with orthogonal polynomial contrasts. The orthogonal polynomial contrasts were used to assess whether a linear or quadratic relationship existed between the response variables and the salt treatment levels. SAS Proc

Mixed (SAS Version 9.1, SAS Institute, Inc., Cary, North Carolina, USA) was used for all analyses, including cases of non-constant variance. In those instances where the data were heteroscedastic, the analyses were corrected for the non-constant variance using the covariance matrix for unequal variances. P value significance was expressed as noted at the $P < 0.05$ and $P < 0.10$ level.

Results

Anatomy.

The shoot and root morphology of *B. sinuspersici* was documented between 6-8 weeks of growth (Fig. 1, 2). As the NaCl treatment increased from treatment without NaCl to 200 mM, the overall shoot and root biomass was observed to increase. In addition, the overall leaf and shoot morphology demonstrated an observed increase in succulence. The observed root biomass increased with increasing NaCl from treatment without NaCl to 200 mM, but the overall appearance of the root morphology was similar. With the 400 mM NaCl treatment, the shoot and root biomass was observably less than the other treatments. The roots also showed a more 'curly' phenotype and the root mass was a darker color under the 400 mM NaCl, which probably indicates necrosis (Fig. 2).

The leaf morphology also seemed to change with increasing NaCl (Fig. 3), demonstrating larger, more succulent leaves with the appearance of salt crystals. This increase in succulence caused the overall leaf color to change with increasing NaCl. Without salt, leaves had a deeper green color, while leaves had a progressively lighter green color with increasing salinity. The 400 mM treatment had the lightest green color leaves.

Transmission electron micrographs were taken of *B. sinuspersici* at four different NaCl levels (without NaCl, 50, 100 and 200 mM) and at three different locations on the leaf (tip, middle and base) to determine if there was an effect of the salt treatment on chlorenchyma cell and chloroplast anatomy. Under each salt treatment and leaf location (leaf tip, middle and base), the characteristic C_4 type chlorenchyma cell anatomy was observed. A central cytoplasmic compartment was formed, surrounded by peripheral chloroplasts along the plasma membrane of the chlorenchyma cell (not shown).

The anatomy of the individual chloroplasts was also observed (Fig. 4). There were no observed differences between treatments in the overall granality (defined as the ratio of appressed thylakoid membrane length to the length of all nonappressed thylakoid membranes in the chloroplast, Pyankov *et al*., 1997), and starch composition of the central cytoplasmic compartment and peripheral chloroplasts.

Additionally, light microscope images were taken of *B. sinuspersici* under four NaCl treatments (without NaCl, 50, 100 and 200 mM). Views of leaf cross sections revealed the structure of the leaf and chlorenchyma cells (Fig. 5). In all treatments, there were 1-2 chlorenchyma layers with substantial internal air space directly interior to a tightly connected epidermal layer. Internal to the chlorenchyma cells are large water storage cells that surround the vascular bundles located along the central plane. Also, the chlorenchyma cells in all salt treatments have the distinctive central cytoplasmic compartment in addition to a peripheral layer of chloroplasts characteristic of *Bienertia*.

Growth parameters.

Quantitative analyses were made to determine the effects of the NaCl treatments on the overall growth and size of the plant, the incident leaf area, and fresh and dry weights of individual leaves from *B. sinuspersici* (Table S1). There was an increase in the average individual incident leaf area associated with the salt treatment. The lowest individual incident leaf area was without NaCl (0.36 cm^2 ± 0.03), which was significantly lower ($P < 0.05$) than the remaining NaCl treatments. The greatest individual incident leaf area was in 200 and 400 mM, having an average individual incident leaf area of 0.65 ± 0.05 cm^2 and 0.73 cm^2, respectively (Fig. 6).

On a per leaf area basis, the fresh weight seemed to increase with an increase in salinity (Fig. 7). The treatment without NaCl was significantly lower ($P < 0.05$) than the 200 mM treatment, which had the greatest fresh weight per leaf area among the salt treatments. The treatment without NaCl had a fresh weight per leaf area of 107.8 ± 9.1 mg/cm^2, while the 200 mM NaCl treatment had a fresh weight per leaf area of 146.5 ± 7.7 mg/cm^2 (Table S1). Fresh weight per leaf area in the 400 mM NaCl treatment was similar to that without NaCl. The dry weight per leaf area appeared lower when grown under saline conditions (though not significant at $P<0.05$). The 400 and 50 mM NaCl treatment had the lowest dry weight per leaf area (13.1 and 12.9 ± 2.5 mg/cm^2, respectively) while the treatment without NaCl produced the greatest dry weight per leaf area (28.4 ± 6.8 mg/cm^2) (Fig. 7).

On a per leaf basis, the fresh weight (FW) showed a significant increase ($P < 0.05$) with increasing NaCl between the treatment without NaCl compared to the 50, 100, 200 and 400 mM treatments (Fig. 8). The treatment without NaCl, 200 and 400 mM NaCl had a fresh per leaf of

38.2 ± 4.4, 96.0 ± 9.6 and 87.2 mg, respectively (Table S1). The dry weight (DW) per leaf remained relatively constant across all NaCl treatments (Fig. 8). The DW:FW ratio (%) revealed the highest DW:FW per leaf (27.3%) seemed to occur in treatments without salt, as expected with increasing succulence under saline conditions. The remaining treatments (50, 100, 200 and 400 mM) had similar DW:FW ratios (not shown).

The root and shoot fresh and dry weights were measured to determine if the NaCl treatment had an effect on root or shoot growth. Both the root and shoot fresh weights showed strong trends towards increasing with increasing NaCl levels, up to 200 mM NaCl (Table S2). There was a significant difference ($P < 0.05$) in root and shoot fresh weights (FW) between the treatment without NaCl versus 50 mM NaCl (Fig. 9). The 400 mM treatment showed an apparent decrease in root and shoot FW compared to other treatments (Fig. 9). The treatment without NaCl had an average root FW of 8.3 ± 3.0 g, while the 200 mM treatment had an average of 96.4 ± 34.2 g. The treatment without NaCl had an average shoot FW of 13.5 ± 2.7 g, while the 200 mM treatment had an average of 101.9 ± 57.4 g. The root and shoot dry weights also showed a similar trend; there was a significant difference ($P < 0.10$) between the treatment without NaCl and the 50 and 100 mM NaCl treatment root and shoot DW (Fig. 10). The root DW without salt had an average of 0.7 ± 0.1 g, while the 200 mM treatment had an average of 6.1 ± 2.6 g. The shoot DW for the treatment without salt was also lower than the 200 mM shoot DW (1.7 ± 0.1 g and 17.7 ± 15.2 g, respectively) (Table S2).

The DW:FW of shoots showed an interesting trend; it appeared to increase up to the 100 mM NaCl treatment (19.7 ± 3.5 %) and then decreased in the 200 and 400 mM treatments (14.8 ± 2.6 and 14.9%, respectively). The root DW:FW had no apparent trend, but was highest in the

400 mM treatment and the treatment without NaCl (12.4% and 12.3 ± 5.1 %, respectively) (Fig. S1).

Total cell count, cell area and cell area:central cytoplasmic compartment determination

To resolve whether the increase in leaf size and fresh weight is due to an increase in cell number and/or cell size, the total chlorenchyma cell count per leaf, cell area (CA) and ratio of CA:central cytoplasmic compartment (CCC) were determined. Results with measurements from leaf extracts are shown in Fig 11, Fig. 12, Table S3 and Table S4. Although significant differences were not observed at $P<0.05$, some trends based on differences in means are discussed below.

The total chlorenchyma cell count per leaf was highest in the 200 mM NaCl treatment, which was about 2-fold higher than the treatment without NaCl (Table S3). The cell count per leaf was lowest in the treatment without salt; the highest values were obtained between 50 and 200 mM NaCl, while lower values were obtained with 400 mM NaCl (Fig. 11).

The chlorenchyma cell area (CA) and central cytoplasmic compartment (CCC) area were measured and the ratio between the two (CA:CCC) was determined (Table S4, illustrated in Fig. S2). The mean values for CA:CCC at 1.25 M glycine betaine increased with increasing NaCl levels. The CA:CCC ratio in treatment without NaCl was lower than the CA:CCC ratio in all the NaCl treatments (though not significant at $P<0.05$). The largest CA:CCC was in the 200 mM treatment (4.62 ± 1.2), which is 1.75-fold higher than the treatment without NaCl, though not statistically significant (Fig. 12). To determine if the tendency toward an increase in the ratio was due to a change in CA size, the area of the cell was measured (in pixels) using an image

analysis software (Table S4). The mean CA values were larger in the 100 to 400 mM treatments when compared to the 0 and 50 mM treatments (Fig. 12). The largest mean values for CA occured in the 100 mM treatment (49167.1 pixels), which was almost 1.5-fold higher than the treatment without NaCl (34521.7 ± 3060 pixels), (Tabls S4).

The relative change in CA and CCC, and the ratio of CA:CCC were also quantified using light microscopy images of the leaf chlorenchyma cells in the treatment without NaCl to the 200 mM NaCl treatments (illustrated in Fig. 5). There was an apparent increase in the size of the CCC up to 20 to 25% with increasing NaCl (only one replicate was performed, Fig. S3). The lowest area per CCC was in the treatment without NaCl (5291 ± 280 pixels), with the highest CCC area mean values in the 50 and 200 mM treatments (6530 ± 620, and 6025 ± 530 pixels, respectively) (Table S5). The mean values for the CCC in the 50 mM and 200 mM treatments were 1.2- and 1.1-fold higher than in the treatment without NaCl, respectively The lowest mean CA values was in the treatment without NaCl (11882 ± 530 pixels), while the highest CA values were in the 50 and 200 mM treatments (16845 ± 114 and 15325 ± 101 pixels, respectively) (Table S5). The 100 and 200 mM treatments had a 1.2- and 1.3-fold larger mean CA compared to the treatment without NaCl, respectively. The CA:CCC showed a similar trend as the previous quantification, with the lowest CA:CCC in the treatment without NaCl, and an apparent concomitant increase with increasing NaCl (Fig. S3). The highest mean CA:CCC values were in the 100 mM treatment, which was 1.5 fold higher than the treatment without NaCl (Table S5).

Osmolality.

To determine if the NaCl treatment had an effect on the internal solute concentration in *B. sinuspersici* cells, the osmolality was determined using a vapor pressure osmometer. The NaCl level had a significant effect ($P < 0.05$) on the average osmolality (Fig. 13). The osmolality in the treatment without NaCl (1020 ± 54 mmol/kg) was significantly lower ($P < 0.05$) than the osmolality in the 100, 200 and 400 mM NaCl treatments (1473 ± 78, 1731 ± 203, 2306 mmol/kg, respectively) (Table S6). It is also interesting to note the large increase in solute concentration in the leaves compared to the overall increase in solute concentration in the hydroponics solution *B. sinuspersici* was grown in. At 400 mM NaCl, the overall osmolality in the hydroponics solution was approximately 800 mmol/kg, while the leaf osmolality was 2306 mmol/kg (almost a 3-fold increase).

Gas exchange.

To determine if the NaCl treatments had an effect on the ability of *B. sinuspersici* to assimilate CO_2, CO_2 response curves were performed. From these curves (shown as the CO_2 assimilation rate (A) versus the intercellular CO_2 level (Ci, µbars), the CO_2 compensation point (Γ), maximum photosynthetic rate (A_{max}), maximum carboxylation efficiency (C_E) and stomatal conductance (g_s) were derived (Table S7). An illustration of parameters measured from the A/Ci curves is illustrated in Fig. S4. Additionally, the photosynthetic water use efficiency (PWUE), and the ratio of intercellular CO_2 (Ci, µbars) to atmospheric CO_2 (Ca, µbars) (Ci/Ca) were calculated.

The CO_2 assimilation rate (A) was expressed on five different bases and the A/Ci curves from each NaCl treatment were analyzed. A was expressed per leaf area (μmol CO_2 m^{-2} s^{-1}), per leaf (μmol CO_2 $leaf^{-1}$ hr^{-1}), per chlorophyll (μmol CO_2 mg $chlorophyll^{-1}$ min^{-1}), per total protein (μmol CO_2 mg $protein^{-1}$ hr^{-1}) and per dry weight (μmol CO_2 mg dry $weight^{-1}$ hr^{-1}). As mentioned previously, the highest apparent photosynthetic rates were obtained in the treatment without NaCl when expressed on a per leaf area basis, with a decrease in assimilation rates with increasing NaCl (Fig. 14). On a per leaf basis, the highest rates were obtained in the moderate salt treatments (50 mM NaCl, followed by 100, 200, 0 and 400 mM NaCl (though not significant at $P<0.05$, Fig. 14). On a chlorophyll and protein basis, there was no apparent trend based on salt treatment (Fig. S5). On a dry weight basis, the highest assimilation rates were obtained in the moderate salt treatments (100 mM, followed by 200 and 50 mM NaCl treatment), while the treatment without NaCl and 400 mM NaCl were also the lowest overall assimilation rates (Fig. 14). In all treatments, with and without salt, the CO_2 compensation points were either C_4-type or C_4-like, and photosynthesis was nearly saturated at ambient CO_2.

The A_{max} values expressed on a leaf area basis revealed that the NaCl treatment resulted in a decrease in the the maximum photosynthetic rate in *B. sinuspersici* (though not significant at $P<0.05$, Fig. 15). A_{max} mean values without NaCl (18.6 ± 2.9 μbars CO_2 $m^{-2}s^{-1}$), were higher than in the 100, 200 and 400 mM NaCl treatments (12.4 ± 2.9, 12.1 ± 3.2 and 4.5 μbars CO_2 $m^{-2}s^{-1}$, respectively) (Table S7).

The maximum carboxylation efficiency (C_E) represents how efficient the carboxylation reaction occurs with PEP carboxylase in C_4 plants. It is measured using the initial slope of the CO_2 response curve based on A versus Ci. The C_E values derived from the A/Ci curves revealed that increasing salinity had a negative effect on the mean C_E values in *B. sinuspersici* though not

significant at $P<0.05$ (Fig. 16). The highest C_E value derived from A/Ci curves was seen in the treatment without NaCl (0.9 ± 0.8 μmol CO_2 $m^{-2}s^{-1}$/μbar), compared to the lowest value in the 400 mM NaCl treatment (0.02 μmol CO_2 $m^{-2}s^{-1}$ /μbar) (Table S7). Also, C_E values based on A/Ca response curves showed a trend toward decreasing values with increasing salinity (Table S7). Additionally, C_E was expressed on a dry weight basis. While there was an apparent decrease in C_E with increasing salinity on a leaf area basis, on a dry weight basis C_E to the mean CE values without salt treatment was lower than in the 50 to 200 mM NaCl treatments, with the lowest apparent C_E in the 400 mM treatment (results not shown).

To determine if the rate of change in A_{max} was similar to C_E with increasing salinity, the two were graphed against one another (Fig. 17). A plot of A_{max} versus C_E showed a steady decrease from 0 to 100 mM (based on a linear fit to the mean values) in the A_{max} and C_E values (Fig. 19). From 200 to 400 mM however, there was a strong decrease in A_{max} relative to C_E. The results show C_E has a tendency to be more sensitive than A_{max} with increasing salinity from 0 to 200 mM NaCl, whereas at 400 mM there was a dramatic drop in A_{max}.

The lowest Γ values were obtained in treatments without NaCl to 100 mM NaCl (3.7 ± 1.4 to 4.8 ± 0.9 μbar) with values of 200 to 400 mM NaCl having 8.8 ± 3.2 and 7.5 μbars, respectively (Fig. 18, Table S7).

The g_s values were derived from gas exchange measurements after the initial acclimation period, which was approximately 20 minutes. The g_s values expressed on a leaf area basis showed a continual decline in mean g_s values with increasing salinity, which suggests NaCl has a a negative effect on stomatal conductance in *B. sinuspersici* (Fig. 19, Tables S7). The highest g_s value was in the treatment without NaCl (0.17 ± 0.02 mol $m^{-2}s^{-1}$), while the lowest g_s value was

in the 400 mM NaCl treatment (0.06 mol $m^{-2}s^{-1}$). There was a significant difference ($P < 0.10$) between the treatment without NaCl and the 50 mM NaCl treatment, and the 200 mM NaCl treatment (Fig. 19).

The Ci/Ca ratio was determined at the maximum photosynthetic rate (A_{max}) for each NaCl treatment. The Ci/Ca ratio did not significantly change ($P < 0.05$) between each NaCl treatment (Fig. 20). The Ci/Ca ratio was relatively constant between the treatment without NaCl up to the 400 mM NaCl treatment (0.64 ± 0.03, 0.64 ± 0.09, 0.66 ± 0.07, 0.56 ± 0.09, and 0.69 %, respectively) (Table S7).

Finally, the photosynthetic water use efficiency (PWUE) was determined from the CO_2 response curves to see if the NaCl treatment had any effect on the plant's ability to retain water while still taking in CO_2 from the atmosphere. The PWUE did not significantly change ($P < 0.05$ between each NaCl treatment with treatments between 0 and 200 mM NaCl having the highest efficiency (Fig. 21). The lowest PWUE was in 400 mM NaCl (2.2 μmol CO_2 fixed per mmol H_2O lost) (Table S7).

Total protein and chlorophyll content.

The protein and chlorophyll content were determined on a fresh weight (FW), dry weight (DW) (Fig. 22), leaf area and per leaf basis (Fig. 7, 8). There was an apparent decrease in protein content with increasing salt, with the highest content without NaCl treatment (2.0 ± 0.3 μg total protein per mg FW), and the lowest in the 400 mM NaCl treatment (0.7 μg total protein per mg FW) (Table S8). The total protein content per DW and leaf area remained relatively constant (Table S8, S1, respectively).

The chlorophyll content per fresh weight showed a trend toward decreasing with increasing NaCl. The highest chlorophyll content per fresh weight was in the treatment without NaCl (0.51 ± 0.2 µg total chlorophyll per mg FW). The lowest chlorophyll content per fresh weight was found in the 400 mM treatment (0.09 µg total chlorophyll per mg FW) (Fig. 22) (Table S8). There was a significant decrease ($P < 0.10$) between the 50 mM and 100 mM NaCl treatment chlorophyll contents per fresh weight (Fig. 21). On a dry weight basis, the chlorophyll content also seemed to decrease with increasing NaCl (Fig. 22). The highest chlorophyll content per dry weight was observed in the treatment without NaCl (2.9 ± 0.8 µg total chlorophyll per mg DW), while the lowest was observed in the 400 mM treatment (0.9 µg total chlorophyll per mg DW) (Table S8). The chlorophyll content per leaf area was highest in the treatment without NaCl, with the other NaCl treatments measured showing lower, but similar, chlorophyll contents (Table S1).

Western blots.

To determine if the content of certain photosynthetic enzymes were affected by the NaCl treatment, western blots were performed. Proteins were extracted and quantified from each NaCl treatment and a SDS-PAGE analysis was performed (Fig. S6). The membranes were immunblotted for Rubisco large subunit (LSU)(ribulose-1,5 – bisphosphate carboxylase oxygenase), PEPC (phospho*enol*pyruvate carboxylase), PPDK (pyruvate Pi dikinase) and NAD - malic enzyme. The resulting bands were quantified using an image analysis program and the relative intensity on a protein basis (%) compared to the control (treatment without NaCl) was calculated (Fig. 22).

Results from the western blots applying equal amounts of protein, showed an approximate two-fold increase in the C_4 photosynthetic enzymes PEPC, PPDK, and decrease in the C_4 enzyme NAD-ME and the C_3 enzyme Rubisco LSU (Fig. 24). For PEPC, the largest increase was seen between the treatment without NaCl, and the 100 mM and 400 mM NaCl treatment, where there was roughly a ~ 135 and 138% increase in the amount of PEPC. An increase in PPDK was also seen between the treatment without NaCl and the other NaCl treatments. There was a ~ 116 % increase in PPDK between the treatment without NaCl, and the 50 to 200 mM NaCl treatments.

On a leaf area basis, there was a decrease in NAD-ME in the 400 mM NaCl treatment (~ 60% versus without NaCl) (Fig. 24). Compared to the treatment without NaCl, there was a decrease in Rubisco content with increasing salinity (Fig. 24). The largest apparent decrease in Rubisco compared to the treatment without NaCl was in the 400 mM treatment (~84%). PEPC and PPDK also increased when compared to the treatment without NaCl on a per leaf area basis. This increase was smaller however than on a per protein basis (Fig. 24). The largest increase in PEPC was seen in the 50 mM treatment (~53% increase versus without NaCl), while the largest increase in PPDK was seen in the 50 to 200 mM treatments (~ 43% increase versus without NaCl).

$\delta^{13}C$ analysis.

To analyze whether *B. sinuspersici* was functioning as a C_4 plant over a range of salinity levels, the carbon isotope discrimination values ($\delta^{13}C$) of leaf samples were determined (Fig. 25). C_4 plants have more positive $\delta^{13}C$ values compared to C_3 plants, due to less discrimination against

assimilation of $^{13}CO_2$. There was a decrease in the isotope discrimination against $^{13}CO_2$ reflected in more positive mean $\delta^{13}C$ values as the NaCl treatment increased. The values became more positive from the treatment without NaCl (-17.3 ± 0.6 ‰) to 400 mM NaCl (-14.9 ‰). There was a significant decrease (more positive) ($P < 0.10$) between the treatment without NaCl and the 200 mM NaCl treatment (Fig. 25).

Discussion

The single-cell C_4 species *B. sinuspersici* is known to persist in semi-arid deserts with saline soils having varying levels of NaCl (Akhani *et al*., 2005). The goal of this study was to investigate the anatomical nature of the leaf chlorenchyma cell structure, and the photosynthetic and growth response of *B. sinuspersici* under prolonged and continuous exposure to varying levels of salinity. The effect of salinity on the photosynthetic performance, plant development and biochemistry,as well as the optimal salinity level for growth in *B. sinuspersici* was examined.

Shoot and root growth.

The overall shoot fresh weight and dry weight increased from the treatment without NaCl to the 50 mM NaCl treatment. At the 400 mM level the ability of the plant to effectively grow is may be offset by the energy requirements needed to handle such elevated NaCl levels. Since the dry weight per leaf did not significantly change, but the shoot fresh and dry weights increased with increasing NaCl up to 50 mM NaCl, it would follow that the number of leaves also increased with increasing NaCl treatment up to 50 mM NaCl. There was trend of increasing

shoot fresh weight and dry weight from 50 mM to 200 mM NaCl. This suggests that *B. sinuspersici* is able to tolerate NaCl levels up to 200 mM NaCl without a decrease in overall carbon gain (in the form of dry weight).

The overall root biomass also increased from the treatment without NaCl to the 50 mM NaCl treatment. In their native desert habitat in the Irano-Turanian region (Akhani *et al*., 2005), *B. sinuspersici* may be able to grow an extensive root network, which allows it to reach the water table well below the soil surface. It is already documented that desert halophytes in the Chenopodiaceae develop roots that can exploit a relatively large volume of water by reaching great depths when needed (Evenari, 1985). Access to the water table could give this plant a tremendous advantage over other plants in the area. The presence of such a large root biomass in our artificial hydroponics system may mirror what *B. sinuspersici* develops in its natural habitat. The increase in root biomass with increasing salt would be advantageous to the plant in its native habitat, because access to the water table would be even more crucial in increasingly saline soils. Therefore, the increase in root biomass from 0 mM to 50 mM and the apparent increase from 50 to 200 mM NaCl represents a possible mechanism of salt tolerance most likely utilized by *B. sinuspersici* in its natural habitat.

Leaf succulence.

An increase in individual leaf area from the treatment without NaCl to 50 mM, and a tendency for an increase in chlorenchyma cell size, total cell count, and water storage cells all demonstrate the succulent nature of *B. sinuspersici*. Succulence is a common feature of halophytic species, which use the increase in water storage to combat increasingly saline soils.

B. sinuspersici is also a desert species, rang[ing] from the westernmost coasts of Pakistan and extend[ing] westward all along the coastal areas in southern Iran and countries surrounding the Persian Gulf (Ahkani *et al*., 2005). *B. sinuspersici* occurs in areas having a hot climate, and where the humidity of the air is very high (Akhani, *et al*., 2005). With conditions such as this, succulence can protect the plant against drought and dehydration, by giving up water to support photosynthetic tissue, and salinity, by providing for storage of salts in the large vacuoles (Park *et al*., 2009*b*).

The overall leaf fresh weight of *B. sinuspersici* seemed to increase with increasing NaCl, while the overall dry weight did not change significantly ($P < 0.05$) (Table S1). The apparent increase in fresh weight is most likely due to a possible increase in water storage, individual incident leaf area, and corresponding leaf succulence, which would allow the plant to retain water under such saline conditions.

There was a two-fold increase in the individual leaf area between the treatment without NaCl and the 200 NaCl treatment (Table S1). Additionally, there was a significant increase in the leaf area from the treatment without NaCl compared to all of the NaCl treatments. In *B. sinuspersici*, the overall cell count per leaf seemed to increase with increasing NaCl treatments. Additionally, the CA seemed to increase with increasing NaCl level. This apparent increase in the total chlorenchyma cell count and cell size would both contribute to an increase in the overall leaf size. When plants grown without salt were treated with 200 mM NaCl, Park *et al*., (2009*b*) also observed a noticeable increase in succulence and in the size of cells in anatomical studies, including chlorenchyma cells. Earlier work in *S. maritima* has shown enhanced growth in high salt concentrations, which was attributed to increased cell size (Yeo and Flowers, 1980). The

observed accumulation of large amounts of solutes in the cell could potentially increase turgor and promote an increase in cell size in *B. sinuspersici*.

Chlorenchyma development.

Light microscope images typically showed two layers of chlorenchyma cells developed in leaves under all treatments. Observations of the leaf anatomy were similar to those made by Lara *et al*., (2008). Both light and electron microscopy analyses showed that C_4 type single-cell chlorenchyma develop in *B. sinuspersici* without salt and at all salt levels. This includes development of the two cytoplasmic domains: the CCC and the peripheral chloroplasts. A central cytoplasmic compartment was formed, surrounded by peripheral chloroplasts along the plasma membrane of the chlorenchyma cell. Transmission electron micrographs taken of *B. sinuspersici* leaves from treatment without NaCl to the 200 mM NaCl treatments showed no apparent difference in chlorenchyma cell development, formation of a central cytoplasmic compartment, or chloroplast ultrastructure.

A possible increase in leaf succulence also involves an increase in the volume of water storage tissue in *B. sinuspersici* (also, see Park *et al*., 2009*a*). An increased water storage capacity would enable *B. sinuspersici* to take up more solutes, and in turn more water, by lowering its osmotic solute potential. It is also known that *B. sinuspersici* [has] numerous bladder-like glands on both the adaxial and abaxial sides of the leaf (Park et. al., 2009*a*). The presence of salt glands and the increase in water storage are two methods by which *B. sinuspersici* can take up large amounts of NaCl but still remain viable.

Leaf osmolality and salinity tolerance.

A marked increased in the leaf osmolality was seen in *B. sinuspersici* leaves as the NaCl concentration of the hydroponics solution increased (Fig. 13). The presence of such high levels of solutes, again demonstrates the level of salinity tolerance seen in this desert species. There are three means by which *B. sinuspersici* may cope with accumulation of such a large amount of potentially toxic Na^+ and Cl^- ions. One is increased succulence for storage of NaCl in the vacuoles, another is synthesis of the compatible solute glycine betaine, and third is the development of leaf salt glands (Park *et al*., 2009*b*).

Because the osmotic potential of the leaves is becoming more negative with increasing NaCl treatment, the plants overall osmotic potential lowers, which enables it to take up water from saline soils. The synthesis of compatible solutes in the cytoplasm such as glycine betaine, as well as the use of Na^+/H^+ antiporters on the vacuole tonoplast (Nomura *et al*., 1998; Apse *et al*., 1999) are ways in which other halophytic plants achieve a more negative water potential than the surrounding soil while still protecting its cellular proteins from toxic Na^+ and Cl^- levels. Recent work on *Suaeda salsa*, also in tribe Suaedeae (Chenopodiaceae), demonstrated a compartmentalization of the toxic Na^+ ions into the vacuole, which was facilitated by V-H^+-ATPase (Han, *et al*., 2005). Tonoplast Na^+/H^+ antiporters are dependent on the activity of V-H^+-ATPase (EC 3.6.1.35) and V-H^+-PPase (EC 3.6.1.1), which establish electrochemical H^+-gradients across the tonoplast that energize the transport of Na^+ against the concentration gradient (Han *et al*., 2005). Therefore, membrane-bound translocating proteins regulating cytosolic ion homeostasis (Na^+, K^+ and Ca^{2+}) and ion accumulation in the vacuole could be of crucial importance for adaptation to saline conditions (Han *et al* ., 2005). Future work on these

transporters is needed to confirm if this is the means by which *B. sinuspersici* lowers cytosolic levels of Na^+ and Cl^-.

Total protein and chlorophyll content.

To further understand the halophytic response of *B. sinuspersici*, changes in the protein and chlorophyll content with increasing leaf succulence under saline conditions was analyzed. The protein and chlorophyll content did not change significantly ($P < 0.05$) on a dry weight basis. The apparent decrease in protein and chlorophyll content per fresh weight and per leaf area with increasing NaCl coincides with an apparent increase in the fresh weight and area per leaf. This indicates the overall chlorophyll and protein production is not being inhibited or enhanced by NaCl. The ability of this plant to maintain stable levels of protein and chlorophyll production under such elevated NaCl levels demonstrates its extreme halophytic nature. It does not however, indicate *B. sinuspersici* is an obligate halophyte, since the protein and chlorophyll levels on a dry weight basis without NaCl treatment were not significantly different from saline treatments.

Gas exchange.

Measurements of gas exchange (e.g. CO_2 saturated rates of CO_2 assimilation, maximum carboxylation efficiency, CO_2 compensation point, and water use efficiency) can be taken to assess how effectively a plant's carbon metabolism is working. Rates can be expressed in various ways (e.g. on a leaf area, individual leaf, dry weight, chlorophyll and protein basis). In

B. sinuspersici, there was a decrease in the mean A_{max} values on a per leaf area basis with increasing NaCl (though not significant at $P<0.05$), which coincided with an increase in area per leaf due to an increase in succulence. The dramatic drop in photosynthesis in the 400 mM NaCl treatment, along with reduced growth, indicates salinity toxicity, or elevated rates of respiration. This apparent drop in photosynthesis on a per leaf area basis between nonsaline and saline conditions coincides with an increased succulence, and a tendency towards a decrease in protein, chlorophyll, and dry weight on a leaf area basis.

To account for the fact that the leaf area increases with increasing NaCl, the assimilation rates were analyzed on a per leaf basis. This revealed the highest assimilation rates to be in the 50 mM NaCl treatment and next highest in the 100 mM NaCl treatment. On a dry weight, chlorophyll, and protein basis, the CO_2 assimilation rate was highest in the 100 mM NaCl treated plants, with the lowest rates in the treatment without NaCl and the 400 mM NaCl treatment. Taking all of this into account, it suggests 100 mM is the optimal level of salinity for *B. sinuspersici* based on CO_2 assimilation rates. Under moderate salinity levels, *B. sinuspersici* may achieve higher rates of photosynthesis by increased succulence and distributing the photosynthetic apparatus over a larger surface area. At these levels, one can speculate that the energy needed for the production of compatible solutes does not offset the energy required for carbon metabolism. Further investigation into the investment of energy, carbon and nitrogen sources for the production of glycine betaine would be necessary to prove this.

With increasing salinity, and an apparent decrease in A_{max}, there seemed to be a decrease in C_E (on a leaf area basis/ μbar CO_2). However, plots of A_{max} versus C_E indicated that C_E seemed to be more sensitive to increasing salinity up to 200 mM NaCl, whereas NaCl levels up to 400 mM caused a large drop in A_{max} which coincides with a large drop in Rubisco content.

This suggests that increasing salinity has differential effects on the biochemistry. If A_{max} and C_E were regulated the same, the plot of A_{max} versus C_E would have a linear slope.

The Γ values measured from treatments without NaCl up to 100 mM NaCl were typical of C_4 plants. For a C_3 plant, at 25 °C based on Rubisco kinetic properties, Γ is 43 μbars (Bernacchi *et al*., 2001). Experimental values will be higher depending on the contribution from dark type mitochondrial respiration. C_4 plants typically have Γ values of 0 to 5 μbars. The values of *B. sinuspersici* when grown without NaCl and 50 and 100 mM NaCl are C_4 type. The somewhat higher, but not significant, values under 200 and 400 mM NaCl might reflect higher levels of mitochondrial respiration.

By calculating the Γ values one can determine at what intercellular CO_2 level (Ci) there is no net gain or loss of CO_2. This indicates how well CO_2 is concentrated around Rubisco; the lower the Γ value, the more effective the concentrating mechanism. The CO_2 concentrating mechanism can also be assessed by measuring the leakiness of the system. Carbon isotope discrimination ($\delta^{13}C$) values can indirectly measure the leakiness of the CO_2 concentrating mechanism. The $\delta^{13}C$ biomass, with more positive values under higher salt, suggests minimum leakage of CO_2, and high efficiency of captures of CO_2 from the C_4 cycle by Rubisco.

Similar to A_{max} and the rate of CO_2 fixation, g_s seemed to decrease with increasing NaCl on a leaf area basis. Stomatal conductance could decrease with increasing salinity because there is an internal biochemical limitation on photosynthesis, which causes a higher intercellular level of CO_2 (Ci). With increasing intercellular levels of CO_2, the stomata tend to close, which reduces water loss (without affecting assimilation) (Farquhar and Sharkey, 1982). Stomatal conductance could also decrease with salinity because of a direct effect of salinity on stomata

due to things such as water stress and abscisic acid (ABA) signaling. Most of the ABA in nonstressed leaves is in the chloroplast, and since the chloroplast envelope becomes leaky when water stressed, ABA may be partially responsible for the rapid responses of stomatal conductance to reduced water status and for the longer term correlation between declining conductance and assimilation rate (Farquhar and Sharkey, 1982). Since water use efficiency is not influenced by salinity level (Fig. 21), it suggests a coordinated change in the rate of CO_2 assimilation and stomatal conductance at elevated NaCl levels.

The relatively constant ratio of Ci/Ca with increasing NaCl demonstrates that the level of intracellular CO_2 is not decreasing with increasing salinity. Since Ci/Ca is relatively constant across all NaCl levels, we can conclude that A_{max} is not decreasing because of the lowered g_s. Thus, the decrease in A_{max} could occur, either due to a decrease in g_m (mesophyll conductance for diffusion of CO_2 from intercellular air to PEPC in the peripheral cytoplasm) or due to decreased biochemical capacity to support photosynthesis). As previously mentioned, if there was some rise in Ci with increasing salinity because of a biochemical limitation on photosynthesis, then the stomates could close, which would decrease g_s. Alternatively, there could be a decrease in the stomatal frequency with increasing leaf size, along with some biochemical limitation (e.g. decreased Rubisco on a leaf area basis) which in turn would lower stomatal conductance but maintain a constant Ci/Ca while decreasing photosynthetic rate per leaf area.

Photosynthetic water use efficiency (PWUE).

An important factor to consider when examining rates of CO_2 assimilation is stomatal conductance and transpiration. If under high NaCl conditions the plant decreases stomatal conductance to reduce water loss, then CO_2 uptake will be decreased and in turn, CO_2 fixation becomes limited. The determination of PWUE is an indicator of the H_2O lost per CO_2 fixed. The PWUE was not significantly ($P < 0.05$) different between the different NaCl treatments up to 200 mM NaCl (Fig. 21). This indicates a balance is maintained between stomatal conductance and the biochemical capacity for CO_2 assimilation across salinity treatments. The apparent severe drop in PWUE in the 400 mM NaCl treatment indicates high salinity is having a toxic effect on the biochemistry of CO_2 assimilation, resulting in more water loss per CO_2 fixed. However, averages for 400 mM NaCl are based on one replicate, so the experiment needs to be repeated.

Levels of photosynthetic enzymes.

The photosynthetic components examined (A_{max}, C_E and Γ) are affected by the relative activity of the C_3 and C_4 enzymes. If we examine the affect of NaCl on these enzymes, one must first consider the spatial separation of salt from cytoplasmic components by sequestration in the vacuole, which argues for low cytoplasmic sodium content (Hall and Flowers, 1973). In turn, high levels of cytoplasmic NaCl can inhibit many enzymes, even in halophytic species (Flowers, 1972). It has been documented that PEPC isolated from leaves of C_4 plants is extremely sensitive to inorganic salts, while Rubisco is less salt-sensitive than PEPC (Greenway and Osmond, 1972). The increase in PEPC and PPDK content with increasing NaCl on a protein and

leaf area basis observed in *B. sinuspersici* indicates the plant may be increasing the amount of PEPC and PPDK to compensate for the decreased catalytic activity of these enzymes in the carboxylation phase of the C_4 cycle. With respect to the decarboxylation phase of the C_4 cycle, NAD-ME content decreased under the higher salinity levels.

Additionally, western blot data indicates Rubisco levels on a leaf area basis decreased with increasing salinity (Fig. 24), which may account for the decrease in Amax on a leaf area basis with increasing salinity. A concomitant decline of ATPase activity and the ability to activate decarbamylated Rubisco has been observed for Rubisco activase in response to salt treatments (Salvucci and Klein, 1994). Work on salinity stress in tomato came up with similar findings, stating it seem[ed] likely that the residual ATPase activity was insufficient to support Rubisco activation. These interactions could probably explain the down-regulation of ATPase and Rubisco after salt stress (Chen *et al*., 2009). Therefore, the decrease in Rubisco may be compounded by the limiting ability of the plant to activate Rubisco. However, work on the ATPase activity in *B. sinuspersici* needs to be done in order to determine the effects of NaCl on this enzyme and its downstream effects on Rubisco activity and content.

Different maximal PEP carboxylase activities are considered to affect primarily the initial slope of CO_2 response curves (C_E). However, when PEP carboxylase activity is very low there is also a reduction in the saturated rate of CO_2 assimilation, due to the fact that the Rubisco is not completely saturated with CO_2 (von Caemmerer, 2000). If the amount of Rubisco is constant, then the amount and/or catalytic capacity of PEPC would have a strong affect on C_E. CO_2 response curve data from *B. sinuspersici* under varying NaCl levels indicate C_E is decreasing with increasing NaCl (Fig. 16). Therefore, one could postulate that the observed reduction in C_E with increasing NaCl in *B. sinuspersici* suggests a reduction in PEPC activity in vivo. The

apparent increase in PEPC content seen in the western data might indicate a compensating effect; in response to in vivo inhibition of PEPC by NaCl.

Additionally, Γ showed a tendency to increase with under the highest levels of NaCl. This indicates the CO_2 concentrating mechanism is may not be as effective at concentrating CO_2 around Rubisco, or there is an increase in dark type mitochondrial respiration. It has been reported that an 80% reduction in PEPC activity results in a substantial increase in the compensation point (von Caemmerer, 2000). As with CE, the increase in PEPC in response to salinity may be ameliorate against the loss of PEPC due to inhibition by NaCl.

The apparent decrease seen in the maximum photosynthetic rate (A_{max}) under saturating CO_2 may be related to the observed trend of a reduction in Rubisco and NAD-ME on a leaf area basis. Modeling predicts that maximal Rubisco activity affects the CO_2 saturated of photosynthesis, which is measured by A_{max}. Gas exchange measurements on transgenic *Flaveria bidentis* with reduced amounts of Rubisco confirm this (von Caemmerer, 2000). Limitations on the rate of PEP regeneration could also affect the CO_2-saturated rate of CO_2 assimilation in a similar way to Rubisco activity (von Caemmerer, 2000), although the levels PPDK increased with increasing salinity.

The change in CO_2 assimilatory rates might also be related to more upstream enzyme activities not quantified in this study. C_4 PEPC is subjected to *in vivo* regulatory phosphorylation by a light up-regulated, calcium independent protein kinase, phosphoenolpyruvate carboxylase-kinase (PEPC kinase) (Garcia-Mauriño *et al*., 2003). Additionally, when the activity states of PEPC kinase and, thus, its target enzyme (PEPC) were downregulated *in vivo* by short-term pretreatment with cytosolic protein-synthesis inhibitors in the light, net leaf CO_2 uptake was

diminished markedly (Chollet *et al*., 1996). In contrast, no effects were observed on the activation states of other nuclear-encoded, photosynthesis-related enzymes, stomatal conductance, or CO_2 uptake by a C_3 leaf (Chollet *et al*., 1996).

Salt stress greatly enhanced PEPC kinase activity in leaves of Sorghum (C_4) (Garcia-Mauriño *et al*., 2003). The rise in PEPCase kinase activity resulted primarily from the ionic stress and was not attributable to a water deficit (Garcia- Mauriño *et al*., 2003). Therefore, there is a potential that the ionic stress related to an increase in the NaCl concentration in the hydroponics solution may have led to a change in PEC kinase activity (as seen through the apparent decrease in C_E). While an upregulation of PEPC kinase should ultimately activate more PEPC, toxic levels of Na^+/Cl^- may affect phosphorylated PEPC in ways which decreases its catalytic capacity. Furture work on PEPC kinase and PEPC activity could be valuable in further elucidating any biochemical changes in *B. sinuspersici* due to elevated NaCl levels.

Furthermore, biochemical changes due to salinity which result in an increase in the resistance of the mesophyll to CO_2 uptake may be the immediate cause of the drop in net photosynthesis in some species (Nieva *et al*., 1999). Variations in net photosynthesis may also be related to biochemical changes that affect carboxylase activity of the ribulose-1,5-bisphosphate carboxylase/oxygenase and the size of the phosphate triose pool (Nieva *et al* ., 1999). While the tendency for an increase in PEPC and PPDK in *B. sinuspersici* is larger than apparent decrease in NAD-ME and Rubisco, differences in the in vivo effects of NaCl on the capacity of these enzymes may affect photosynthetic rates.

Further investigation is needed to fully understand the role of PEPC and PEPC kinase under salinity stress. While the A_{max} is decreasing with increasing NaCl, there may be other

mechanisms that prevent the CO_2 assimilation rates from dropping even further. The possible gain in PEPC kinase activity and PEPC phosphorylation state might allow the enzyme to carboxylate PEP during the night (Garcia- Mauriño *et al*., 2003). Previous studies have shown an increase in malate accumulation in the dark during NaCl treatment in *Sorghum* (Garcia-Mauriño *et al*., 2003), and an increase in PEPC phosphorylation was also detected in darkened leaves treated with salt (Echevarria *et al.,* 2001). While this increase in dark period malate synthesis is not mainly from the fixation of atmospheric CO_2 during the night, the use of respiratory CO_2 would allow the preservation of a positive carbon balance in conditions of severely reduced photosynthesis (Garcia- Mauriño *et al*., 2003). This salt-induced atypical functioning of C_4 plants is reminiscent of the CAM mode of CO_2 fixation in salt induced CAM species like the facultative halophyte *M. crystallinum* (Garcia-Mauriño *et al*., 2003).

$\delta^{13}C$ values.

The $\delta^{13}C$ measurement is an indicator of how much Rubisco discriminates between the two different isotopes of carbon (^{13}C and ^{12}C) found in atmospheric CO_2. The atmosphere is composed of 98.9% ^{12}C and 1.1% ^{13}C (Farquhar *et al*., 1989). Rubisco reacts more readily with the lighter isotope, ^{12}C and discriminates against ^{13}C. Mass spectrometry is used to analyze the $^{12/13}C$ composition of the sample. In C_4 plants, atmospheric CO_2 is fixed by PEPC, which only slightly discriminate between the two carbon isotopes. C_4 plants therefore have a less negative $\delta^{13}C$ value than C_3 plants. *B. sinuspersici* exhibits C_4-type $\delta^{13}C$ values (Akhani *et al*., 2005). The more positive values with NaCl treatments suggests less CO_2 leakage which could be due to increased diffusive resistance from the CCC to the intercellular space (due to the increased ratio of the CA:CCC). Also, the apparent decrease in C_E with increasing salinity suggests a decrease in

the strength of the CO_2 pump, which could prevent overcycling of the C_4 cycle (compared to the C_3 cycle). This could lead to less CO_2 leakage and more positive $\delta^{13}C$.

The $\delta^{13}C$ values were examined to assess whether salinity influences the isotopic signature. The $\delta^{13}C$ values for C_4 plants are approximately between -10‰ and -15‰; whereas, values for C_3 plants are typically between -24‰ and -30‰ (Akhani *et al*., 2009). The most positive values in *B. sinuspersici* grown under different levels of salinity were in the 200 and 400 mM NaCl treatments (-14.5‰ and -14.9‰, respectively). The most negative value was grown in the absence of NaCl (-17.3‰). The results indicate a C_4 system is forming under all conditions. However, under low or no salt, the more negative values suggest there may be more leakage of fixed CO_2 delivered from the C_4 cycle to the CCC (perhaps due to a reduced length of the diffusion path from the CCC to the intercellular airspace in the smaller chlorenchyma cell). More negative values in biomass can also occur for non-photosynthetic reasons, which include fractionation occurring during respiration and during biosynthesis (e.g., synthesis of lignin and lipids) (Akhani *et al*., 2009).

Conclusions

Overall, salinity had a number of possible positive effects on *B. sinuspersici*. NaCl levels up to 200 mM lead to an observed increase in overall biomass production. This was seen in the trend towards production of more shoot and root biomass. Also, the leaf size increased over a range of salinity levels. With regards to the photosynthetic parameters, NaCl treatments up to 200 mM caused an apparent increase the maximum photosynthetic rate on a dry weight basis. The carbon isotope date showed more positive $\delta^{13}C$ values with increasing NaCl, indicating less discrimination against $^{13}CO_2$. This indicates the efficient function of C_4 photosynthesis in plants

grown under increasing salinity. However, there is an apparent decrease in the maximum C_E with increasing salinity, which is measured under limiting CO_2. The increase in Γ with increasing salinity may also be linked to a decrease in C_E. This decrease in C_E due to elevated cytosolic levels of Na^+ or Cl^- may lead to increased production of certain photosynthetic enzymes (mainly PEPC and PPDK) to ameliorate the effects of salt. While the data shows strong trends with regards to the parameters measured, there was lack of statistical significance in some cases, due to large standard errors.

The results indicate the optimal NaCl level is 50 to 200 mM, which allows for an increase in CO_2 fixation per unit dry weight and biomass production. Also, the development of the single-cell C_4 chloroplast and chlorenchyma cell anatomy, and C_4 physiological response without NaCl, leads us to conclude that NaCl is not a requirement for the development of single-cell C_4 photosynthesis. While there are a number of means of providing tolerance to salinity in halophytic Chenopods, C_4 photosynthesis, including single-cell C_4, can be a contributing factor by enabling photosynthesis to function under conditions where CO_2 would otherwise be limiting.

With the advent of soil salinization and aridization, understanding tolerance mechanisms in species like *B. sinuspersici* is critical to understanding what our future global ecosystem will look like. Furthermore, with the prospect of converting C_3 species into C_4 species, information on the other tolerance mechanisms that could be associated with different C_4 anatomies might allow us to one day confer these tolerances to our world's crop species.

References

Akhnai H, Lara MV, Ghasemkhani M, Ziegler H, and Edwards GE (2009) Does *Bienertia cycloptera* with the single-cell system of C_4 photosynthesis exhibit a seasonal pattern of $\delta^{13}C$ values in nature similar to co-existing C_4 Chenopodiaceae having the dual-cell (Kranz) system? Photosynth Res. 99: 23-36.

Akhani H, Barroca J, Koteeva N, Vonesenskaya E, Franceschi V, Edwards GE, Ghaffari SM, and Ziegler H (2005) *Bienertia sinuspersici* (Chenopodiaceae): A new species from southwest Asia and discovery of a third terrestrial C_4 plant without Kranz anatomy. Sys. Bot. 30: 290-301.

Akhani H, Ghobadnejhad M, and Hashemi SMH (2003) Ecology, biogeography and pollen morphology of *Bienertia cycloptera* ex. Bioss (Chenopodiaceae), an enigmatic C_4 plant without Kranz anatomy. Plant Boil. 5:167-178.

Apse MP, Aharon GS, Snedden WA, Blumwald E (1999) Salt tolerance conferred by overexpression of a vacuolar Na^+/H^+ antiport in *Arabidopsis*. Science 285: 1256–1258.

Bender MM, Rouhani I, Vines HM and Black CC Jr (1973) $^{13}C/^{12}C$ ratio in Crassulacean acid metabolism. Plant Physiol. 52: 427-430.

Bernacchi CJ, Singsaas EL, Pimentel C, Portis Jr. AR, and Long SP (2001) Improved temperature response functions for models of Rubisco-limited photosynthesis. Plant Cell Env. 24: 253-259.

Chen S, Gollop N, and Heuer B (2009) Proteomic analysis of salt-stressed tomato (*Solanum lycopersicum*) seedlings: effect of genotype and exogenous application of glycinebetaine. J. of Expt. Bot. 60: 2005-1019.

Chollet R, Vidal J, and O'Leary MH (1996) Phospho*enol*pyruvate carboxylase: A ubiquitous, highly regulated enzyme in plants. Annu. Rev. Plant Physiol. Plant Mol. Biol. 47: 273-298.

Colombo SL, Andrea CS, Chollet R (1998) The interaction of shikimic acid and protein phosphorylation with PEP carboxylase from the C_4 dicot *Amaranthus viridis*. Phytochemistry 48: 55-59.

Echevarria C, Garcia- Maurino S, Alvarez R, Soler A, and Vidal J (2001) Salt stress increases the Ca^{2+}-independent phospho*enol*pyruvate carboxylase kinase activity in *Sorghum* leaves. Planta 214: 283-287.

Edwards GE, Franceschi VR, and Voznesenskaya EV (2004) Single-cell C_4 photosynthesis versus the dual-cell (Kranz) paradigm. Annu. Rev. Plant Biol. 55:173-196.

Evenari M (1985) Adaptations of plants and animals to the desert environment. *in* M. Evenari, I. Noy-Meir, and D. W. Goodall, editors. Ecosystems of the world: hot deserts and arid shrublands, A. Elsevier Science Publishers B.V., New York, New York, USA. pp. 79-92.

Evans JR and von Caemmerer S (2000) Would C_4 rice produce more biomass than C_3 rice? *in* Sheey, JE and B Hardy, editors. Redesigning Rice Photosynthesis to Increase Yield. Elsevier, The Netherlands. pp 53-71.

Farquhar GD, Ehleringer JR, Hubik KT (1989) Carbon isotope discrimination and photosynthesis. Annu. Rev. Plant Physiol. Mol. Biol. 40: 503-537.

Farquhar GD, and Sharkey TD (1982) Stomatal conductance and photosynthesis. Annu. Rev. Plant Physiol. 33: 317-345.

Flowers TJ (1972) Salt Tolerance in *Suaeda maritima* (L.) Dum, The effect of sodium chloride on growth, respiration, and soluble enzymes in a comparative study with *Pisum sativum* L. J. Exp. Bot. 23: 310-321.

Garcia-Mauriño S, Monreal JA, Alvarez R, Vidal J, and Echevarría C (2003) Characterization of salt stress-enhanced phosphoenolpyruvate carboxylase kinase activity in leaves of *Sorghum vulgare*: independence from osmotic stress, involvement of ion toxicity and significance of dark phosphorylation. Planta 216: 648-655.

Greenway H, and Osmond CB (1972) Salt responses of carboxylation enzymes from species differing in salt tolerance. Plant Physiol. 49: 260-263.

Hall JL and Flowers TJ (1973) The effect of salt on protein synthesis in the halophyte *Suaeda maritima*. Planta 110: 361-368.

Han N, Shao Q, Lu C, and Wang B (2005) The leaf tonoplast V-H^+-ATPase activity of a C_3 halophyte *Suaeda salsa* is enhanced by salt stress in a Ca-dependent mode. J. Plant Physiol. 162: 267-274.

Kanai R and Edwards GE (1999) The Biochemistry of C_4 Photosynthesis . *in* Sage, R. and R. Monson, editors. C_4 Plant Biology. Academic Press, San Diego, CA, USA. pg 49-80.

Lara MV, Offermann S, Smith M, Okita TW, Andrea CS, and Edwards GE (2008) Leaf development in the single-cell C_4 system in *Bienertia sinuspersici*: expression of genes and peptide levels for C_4 metabolism in relation to chlorenchyma structure under different light conditions. Plant Physiol. 148: 593-610.

Long, JJ, Wang JL, and Berry JO (1994) Cloning and analysis of the C_4 NAD-dependent malic enzyme of amaranth mitochondria. Plant Physiol. 112: 473-482.

Nieva FJJ, Castellanos EM, Figueroa ME, and Gil F (1999) Gas exchange and chlorophyll fluorescence of C_3 and C_4 saltmarsh species. Photosynthetica 36: 397-406.

Nomura M, Hibino T, Takabe T, Sugiyama T, Yokota A, and Miyake H (1998) Transgenically produced glycine betaine protects ribulose 1,5-bisphosphate carboxylase/oxygenase from inactivation in Synechococcus sp. PCC7942 under salt stress. Plant Cell Physiol. 39: 425–432.

Park J, Knoblauch M, Okita TW, Edwards GE (2009*a*) Structural changes in the vacuole and cytoskeleton are key to development of the two cytoplasmic domains supporting single-cell C_4 photosynthesis in *Bienertia sinuspersici*. Planta 229: 369-382.

Park J, Okita TW, Edwards TW (2009*b*) Salt tolerant mechanisms in single-cell C_4 species *Bienertia sinuspersici* and *Suaeda aralocaspica* (Chenopodiaceae). Plant Sci. 176: 616-626.

Porra RJ, Thompson WA, Kriedemann PE (1989) Determination of accurate extinction coefficients and simultaneous equations for assaying chlorophylls a and b extracted with four different solvents: verification of the concentration of chlorophyll standards by atomic absorption spectroscopy. Biochimica et Biophysica Acta 975: 384-394.

Pyankov VI, Voznesenskaya EV, Kondratschuk AV, and Black, CC Jr (1997) A comparative anatomical and biochemical analysis in *Salsola* (Chenopodiaceae) species with and without a Kranz type leaf anatomy: a possible reversion of C_4 to C_3 photosynthesis. Am. J. of Bot. 84: 597-606.

Reynolds ES (1963) The use of lead citrate at high pH as an electron-opaque stain in electron microscopy. J. Cell Biol. 17: 208–212.

Sage, R (1999) Why C_4 Photosynthesis? *in* R. F. Sage and R. K. Monson, editors. C_4 Plant Biology, Academic Press, San Diego, California, USA. pg. 3-16.

Salvucci ME, and Klein RR (1994) Site-directed mutagenesis of a reactive lysyl residue (Lys-247) of Rubisco activase. Arch. Biochem. Biophys. 314: 178-185.

Toqcuin P, Corbesier L, Havelange A, Pieltain A, Kurtem E, Bernier G, and Périlleux C (2003) A novel high efficiency, low maintenance hydroponic system for synchronous growth and flowering of *Arabidopsis thaliana*. BMC Plant Biol. 3: 2-12.

Von Caemmerer S (2000) Biochemical models of leaf photosynthesis. Pages 91-122. CSIRO Publishing, Australia.

Voznesenskaya EV, Franceschi VR, Kiirats O, Artyusheva EG, Freitag H, and Edwards GE (2002) Proof of C_4 photosynthesis without Kranz anatomy in *Bienertia cycloptera* (Chenopodiaceae). The Plant J. 31:649-662.

Voznesenskaya EV, Franceschi VR, Kiirats O, Artyusheva EG, Freitag H, and Edwards GE (2001) Kranz anatomy is not essential for terrestrial C_4 photosynthesis. Nature 414:543-546.

Yeo AR, and Flowers TJ (1980) Salt tolerance in the halophyte *Suaeda maritima* L. Dum.: Evaluation of the effect of salinity upon growth. J. Expt. Bot. 31(4):1171-1181.

Figure 1. Shoots of *B. sinuspersici* grown in hydroponics under varying NaCl levels. Propagated cuttings of *B. sinuspersici* were placed in hydroponics with varying NaCl concentrations (0, 50, 100, 200 and 400 mM). Pictures were taken between 6-8 weeks of growth. Scale bar = 1 cm.

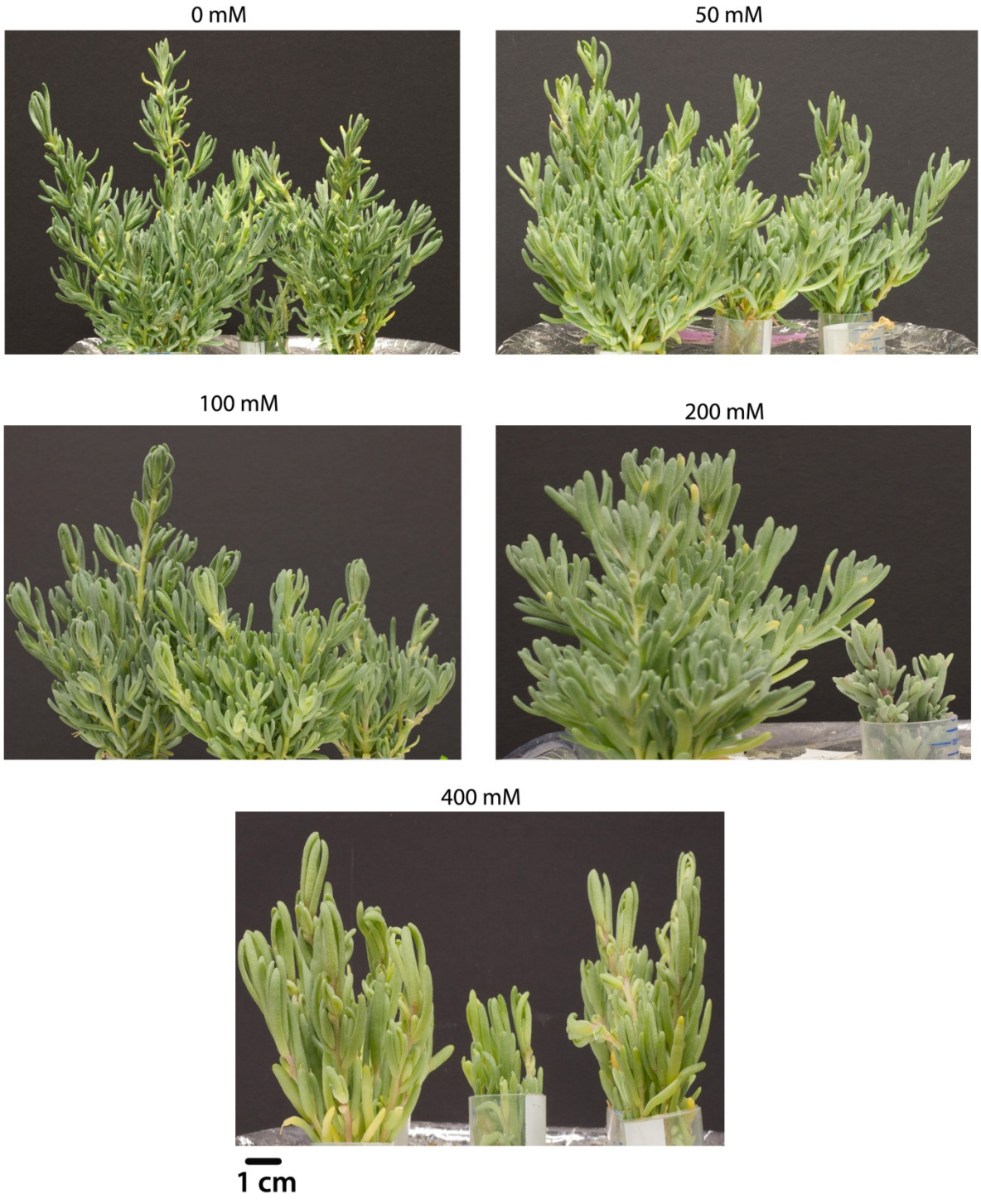
0 mM
50 mM
100 mM
200 mM
400 mM
1 cm

Figure 2. Roots of *B. sinuspersici* grown in hydroponics under varying NaCl levels. Propagated cuttings of *B. sinuspersici* were placed in hydroponics with varying NaCl concentrations (0, 50, 100, 200 and 400 mM). Pictures were taken between 6-8 weeks of growth. Scale bar = 1 cm.

0 mM

50 mM

100 mM

200 mM

1 cm

400 mM

Figure 3. *B. sinuspersici* leaf images from salt treated plants. Images of *B. sinuspersici* grown under different NaCl concentrations (0, 50, 100, 200 and 400 mM). Pictures were taken between 6-8 weeks of growth. The scale bar = 1cm.

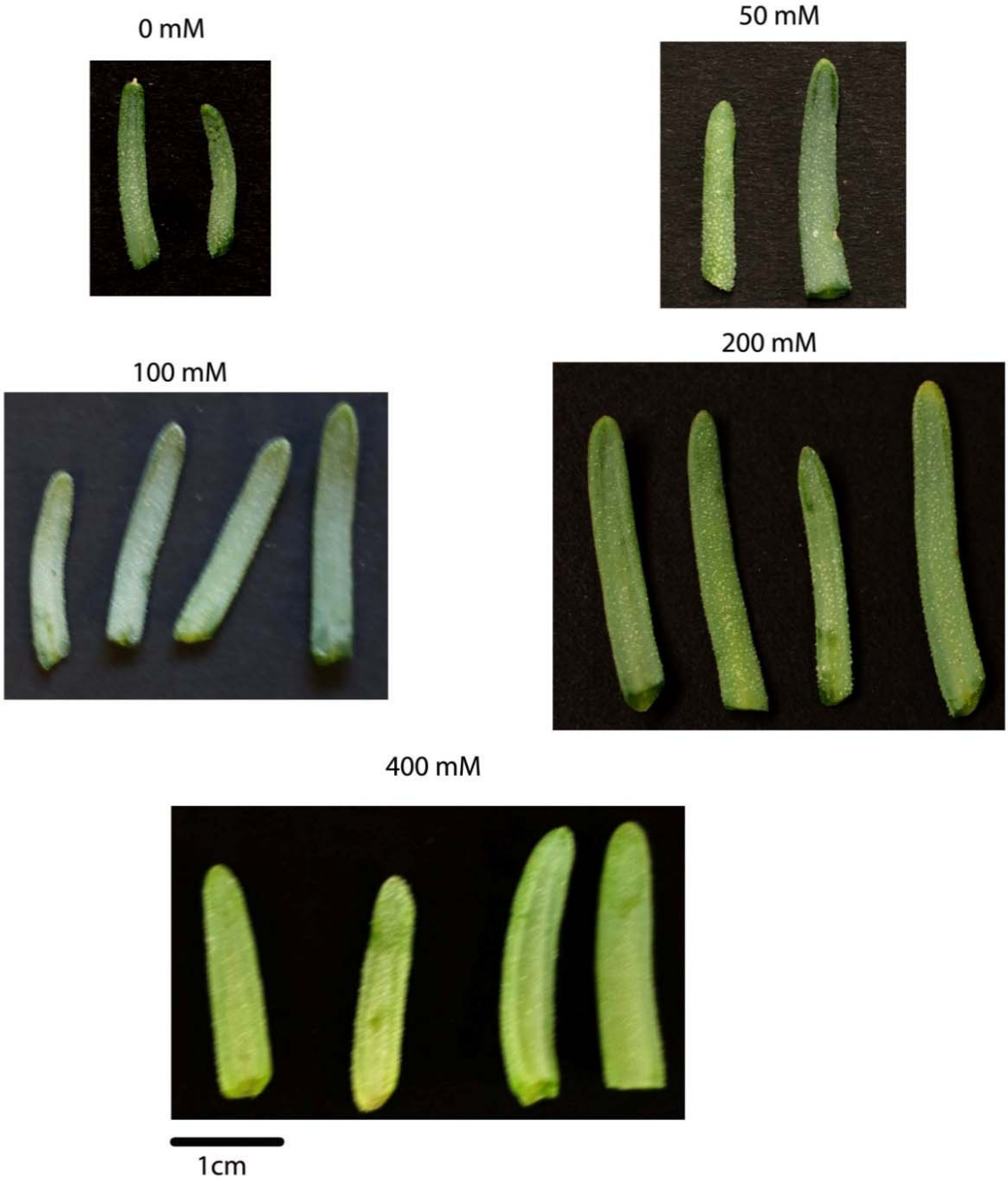
0 mM
50 mM
100 mM
200 mM
400 mM
1cm

Figure 4. Transmission electron micrographs of chlorenchyma cell structure in salt treated *B. sinuspersici.* Leaf samples were removed from the plant at 6 weeks and fixed in 2% paraformaldehyde, 2% gluteraldehyde, and 0.1M phosphate buffer. After a post-fix with 1% osmium tetroxide samples were infiltrated with Spurr's and propylene oxide, and embedded. Leaf cross sections. A) 0 mM NaCl treated plant grown in hydroponics (40,000X, scale bar = 1 μm), B) 50 mM NaCl treated plant grown in hydroponics (30,000X, Scale bar = 1 μm), C)100 mM NaCl treated plant grown in hydroponics (30,000X, Scale bar = 1 μm), and D) 200 mM NaCl treated plant grown in hydroponics (30,000x, Scale bar = 1 μm). S = Starch granules, L = Lipid bodies, M = Mitochondria.

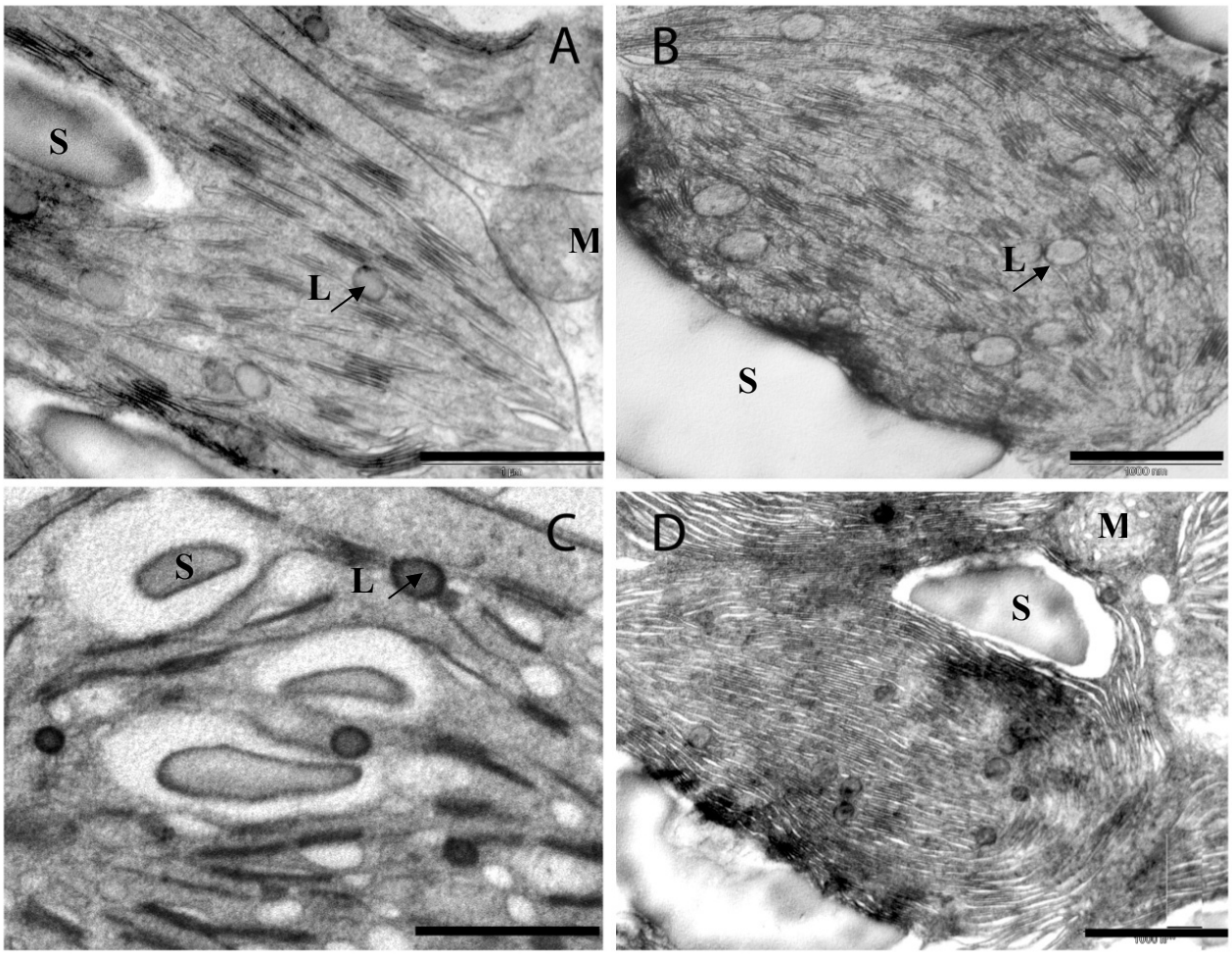
A
S
M
L
B
L
S
C
S
L
D
M
S

Figure 5. Light microscopy images of *B. sinuspersici* anatomy from salt treated plants. Sections (800 nm) were stained using 1% toluidine blue in 1% borax and mounted on gelatin coated glass slides (Surgipath Medical Ind., Inc., Richmond, IL). Images were captured using an Olympus BH-2 Light Microscope (Olympus Optical Co., Ltd., Tokyo, Japan) and a Jenoptik ProgRes C12plus digital camera (JENOPTIK Laser, Optik, Systeme GmbH, Jena, Germany) with ProgRes Capture Pro software (Jenoptik, Jena, Germany). Longitudinal view of leaf cross sections. A) 0 mM NaCl treated plant grown in hydroponics (10x), B) 50 mM NaCl treated plant grown in hydroponics (10x), C) 100 mM NaCl treated plant grown in hydroponics (10x), and D) 200 mM NaCl treated plant grown in hydroponics (10x). M = Mesophyll cells, WS = Water storage cells. Scale bar = 0.10 mm.

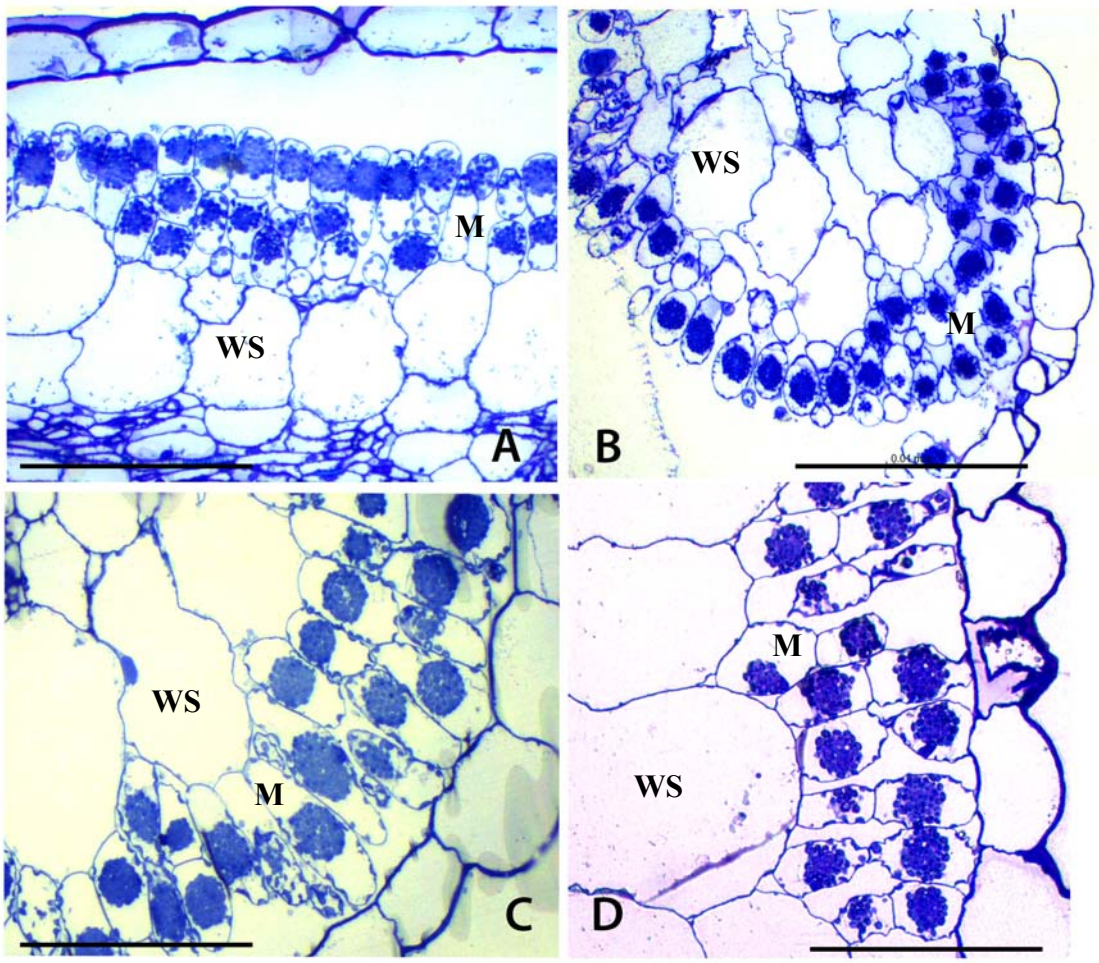

Scale bar = 0.1mm

Figure 6. Individual incident leaf area in *B. sinuspersici* under varying NaCl treatments. The individual incident leaf area was measured for leaves under each NaCl treatment. Error bars represent the standard error of the mean. One-way ANOVA tests with orthogonal polynomial contrasts were done to determine the significance. Different letters represent a significant difference; the same letter indicates no significant difference based on $P < 0.05$. N= 3, 400 mM N = 1

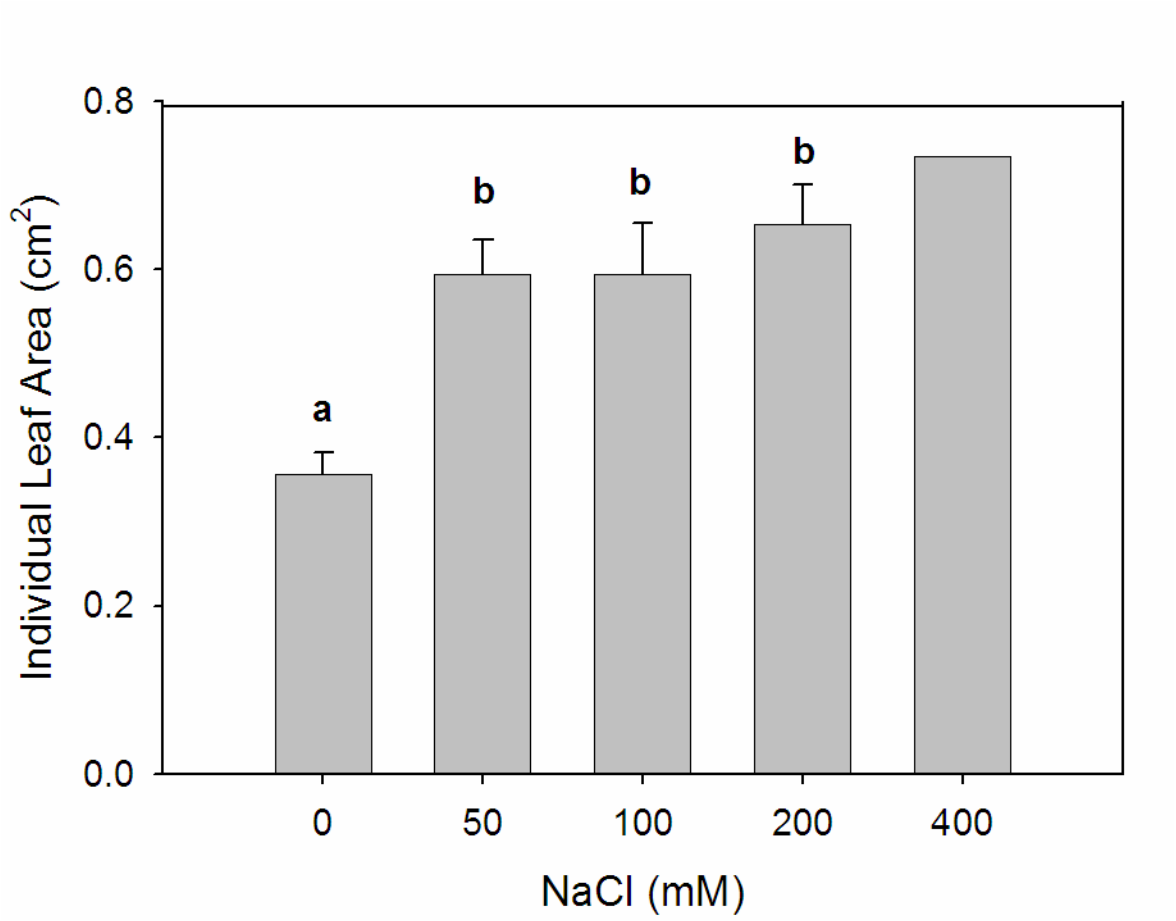

Figure 7. Effects of salt treatment on protein, chlorophyll, fresh weight, and dry weight on a per leaf area basis. The protein and chlorophyll were extracted and quantified on a per leaf area basis. The fresh weights were measured after removal from the plant and expressed on a per leaf area basis. The dry weights were measured after leaves were placed in a 55 °C oven for 24 hours, and expressed on a per leaf area basis. A) fresh weight per leaf area (mg/cm^2), B) dry weight per leaf area (mg/cm^2), C) total protein per leaf area (mg/cm^2), and D) total chlorophyll per leaf area (mg/cm^2). Error bars represent the standard error of the mean. One-way ANOVA tests with orthogonal polynomial contrasts were done to determine the significance. Different letters represent a significant difference; the same letter indicates no significant difference based on $P < 0.05$. N= 3, 400 mM N = 1

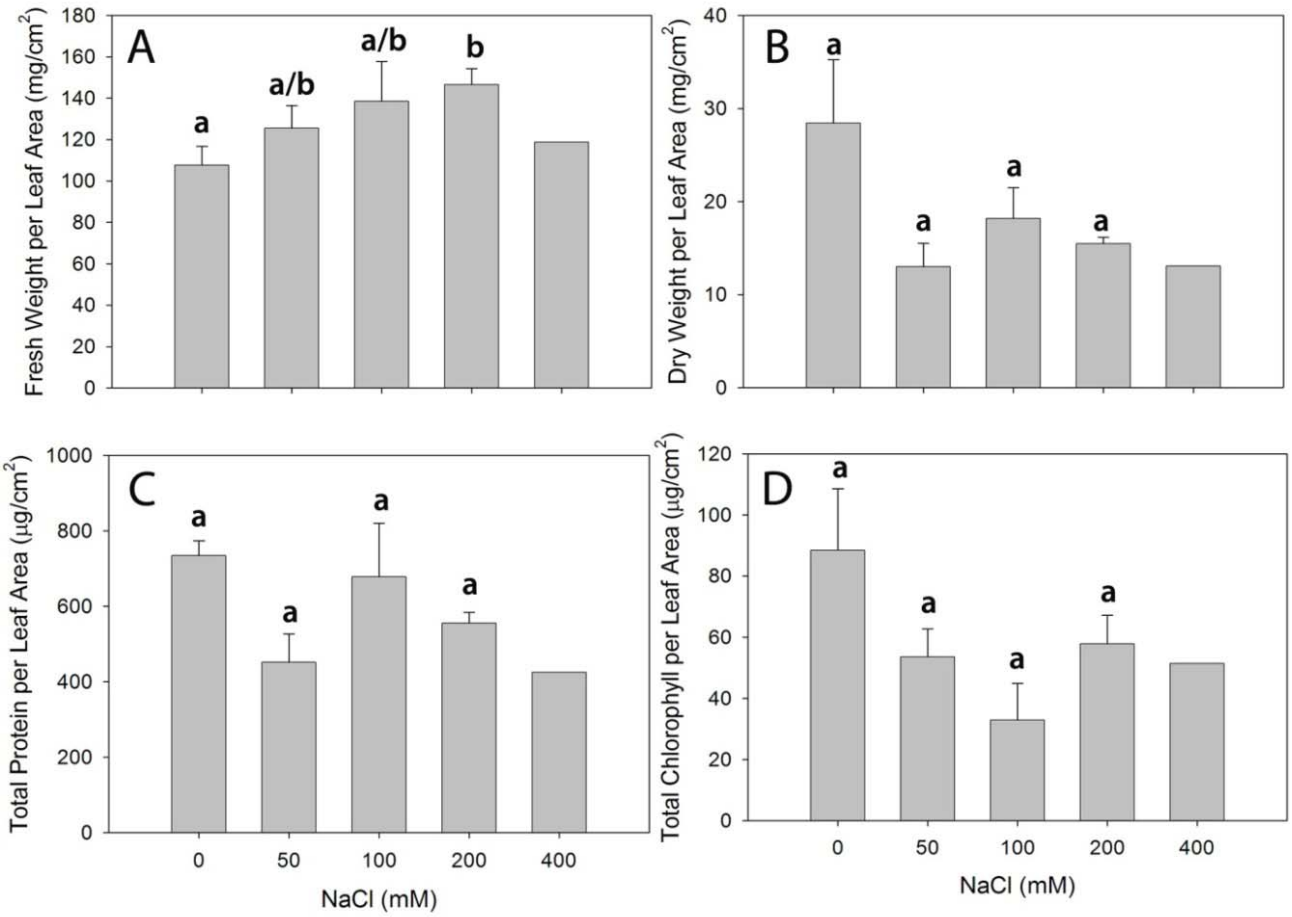
A
Fresh Weight per Leaf Area (mg/cm2)
180
160
140
120
100
80
60
40
20
0
a
a/b
a/b
b
B
Dry Weight per Leaf Area (mg/cm2)
40
30
20
10
0
a
a
a
a
C
Total Protein per Leaf Area (μg/cm2)
1000
800
600
400
200
0
a
a
a
a
0
50
100
200
400
NaCl (mM)
D
Total Chlorophyll per Leaf Area (μg/cm2)
120
100
80
60
40
20
0
a
a
a
a
0
50
100
200
400
NaCl (mM)

Figure 8. Effects of salt treatment on protein, chlorophyll, fresh weight and dry weight on a per leaf basis. The protein and chlorophyll were extracted and quantified on a per leaf basis. The fresh weights were measured after removal from the plant and expressed on a per leaf basis. The dry weights were obtained after leaves were placed in a 55 °C oven for 24 hours, and expressed on a per leaf basis. A) fresh weight per leaf (mg), B) dry weight per leaf (mg), C) total protein per leaf (μg), and D) total chlorophyll per leaf (μg). Error bars represent the standard error of the mean. One-way ANOVA tests with orthogonal polynomial contrasts were done to determine the significance. Different letters represent a significant difference; the same letter indicates no significant difference based on $P < 0.05$. N= 3, 400 mM N = 1

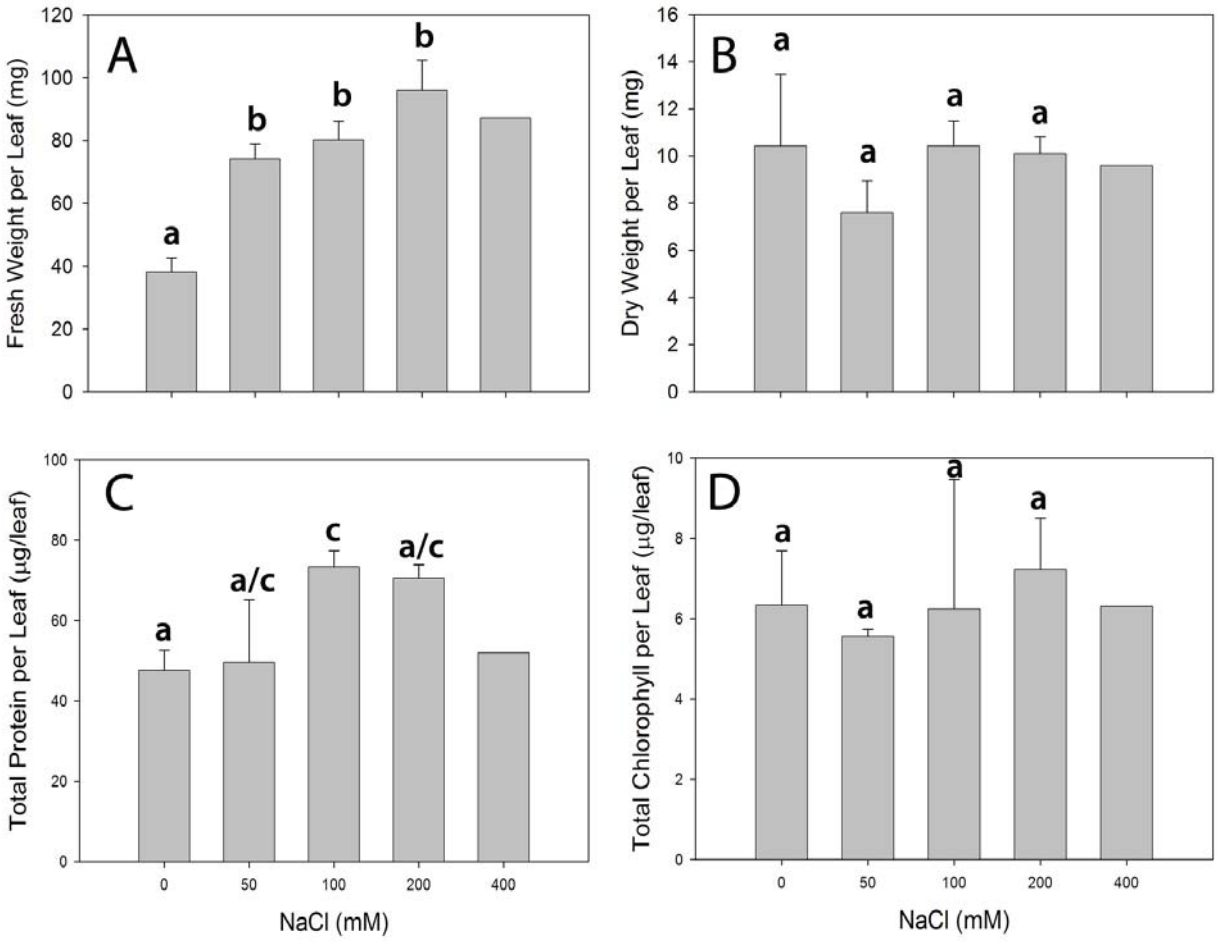
A
Fresh Weight per Leaf (mg)
120
100
80
60
40
20
0
a
b
b
b
B
Dry Weight per Leaf (mg)
16
14
12
10
8
6
4
2
0
a
a
a
a
C
Total Protein per Leaf (µg/leaf)
100
80
60
40
20
0
a
a/c
c
a/c
0
50
100
200
400
NaCl (mM)
D
Total Chlorophyll per Leaf (µg/leaf)
10
8
6
4
2
0
a
a
a
a
0
50
100
200
400
NaCl (mM)

Figure 9. Root and shoot fresh weight in *B. sinuspersici* under varying NaCl levels. The root and shoot fresh weights were measured in *B. sinuspersici* between 6-8 weeks of growth. The entire plant was removed from the hydroponics system. The shoot and root sections were separated and the fresh weights were measured. A) root fresh weight (g), and B) shoot fresh weight (g). Error bars represent the standard error of the mean. One-way ANOVA tests with orthogonal polynomial contrasts were performed to determine the significance. Different letters represent a significant difference; the same letter indicates no significant difference based on $P < 0.05$. N= 3, 400 mM N = 1

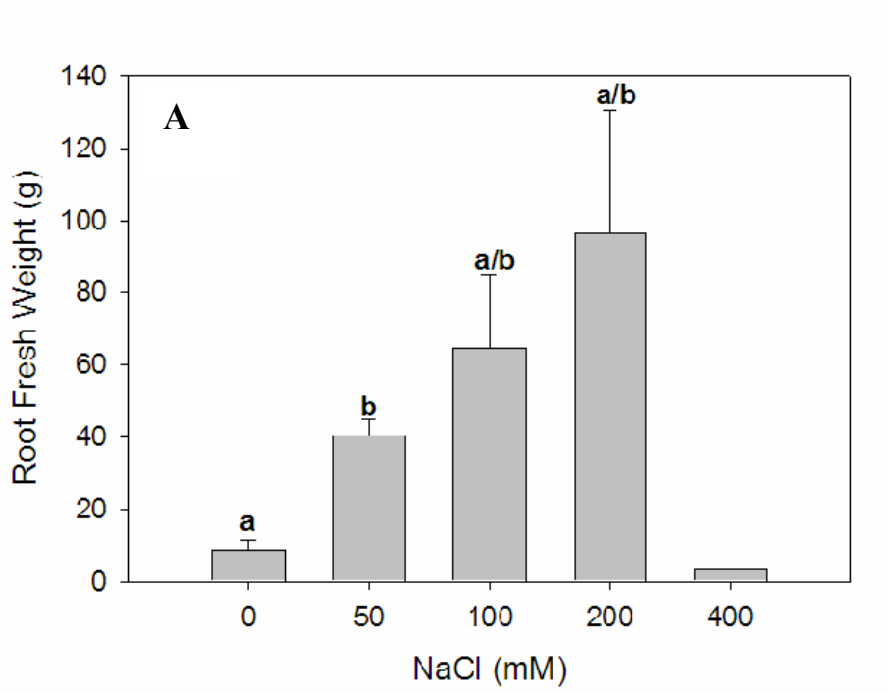
A
Root Fresh Weight (g)
140
120
100
80
60
40
20
0
a
b
a/b
a/b
0
50
100
200
400
NaCl (mM)

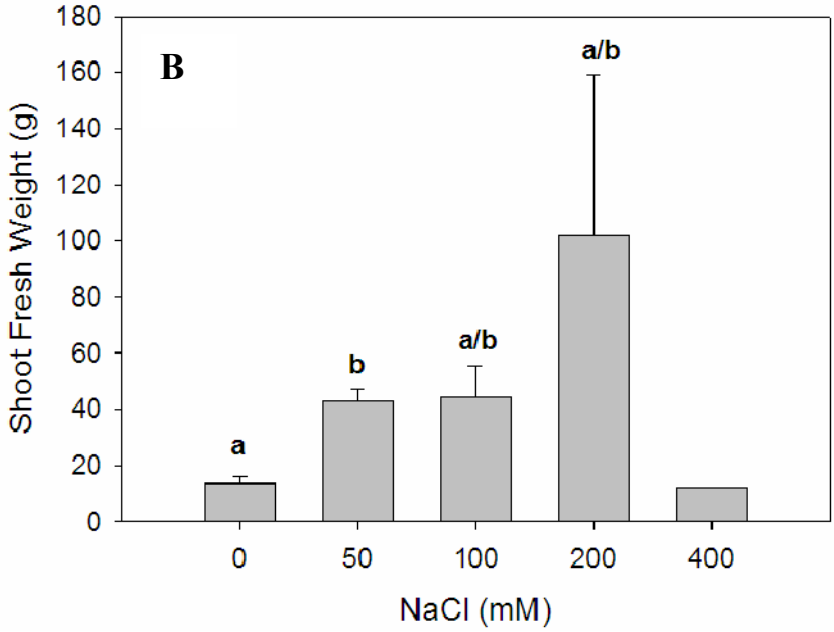
B
Shoot Fresh Weight (g)
180
160
140
120
100
80
60
40
20
0
a
b
a/b
a/b
0
50
100
200
400
NaCl (mM)

Figure 10. Root and shoot dry weight in *B. sinuspersici* under varying NaCl levels. The root and shoot dry weights were measured in *B. sinuspersici* between 6-8 weeks of growth. The entire plant was removed from the hydroponics system. The shoot and root sections were separated and the dry weights were measured. The dry weights were obtained after the shoots and roots were placed in a 55 °C oven for several days. A) root dry weight (g), and B) shoot dry weight (g). Error bars represent the standard error of the mean. One-way ANOVA tests with orthogonal polynomial contrasts were performed to determine the significance. Different letters represent a significant difference; the same letter indicates no significant difference based on $P < 0.10$. N= 3, 400 mM N = 1

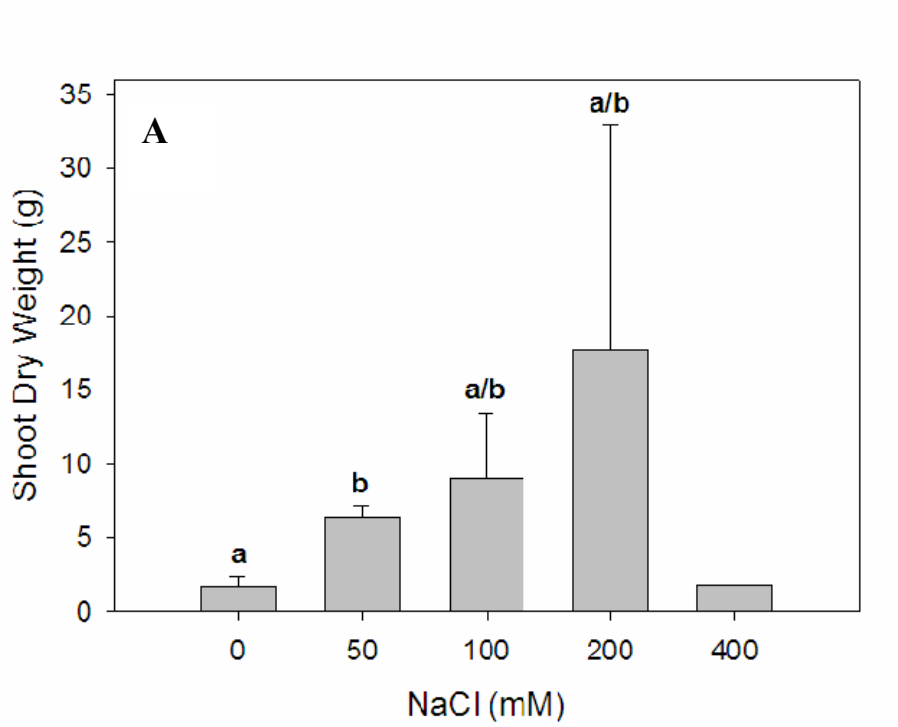
A
Shoot Dry Weight (g)
35
30
25
20
15
10
5
0
a
b
a/b
a/b
0
50
100
200
400
NaCl (mM)

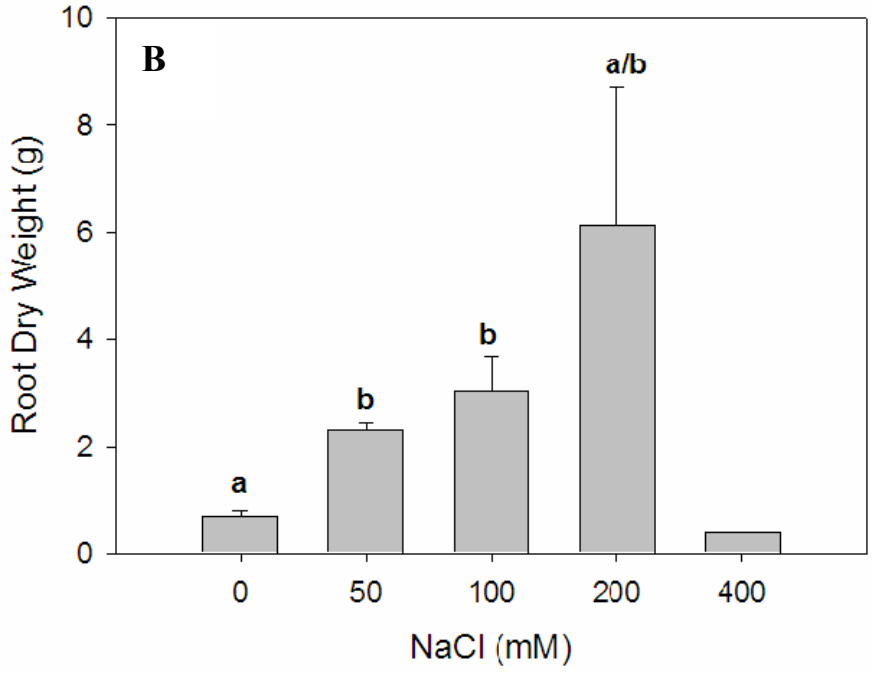
B
Root Dry Weight (g)
10
8
6
4
2
0
a
b
b
a/b
0
50
100
200
400
NaCl (mM)

Figure 11. Total chlorenchyma cell count per leaf under varying NaCl levels in *B. sinuspersici*. The total chlorenchyma cell count per leaf was made on *B. sinuspersici* at each NaCl level. Cells were extracted from leaf material through maceration and placement in a 1.25 M glycine betaine solution. Cells were diluted and viewed under a light microscope at 10X. Error bars represent the standard error of the mean. One-way ANOVA tests with orthogonal polynomial contrasts were done to determine the significance. Different letters represent a significant difference; the same letter indicates no significant difference based on $P < 0.05$. N= 3; 100 mM N = 2, 400 mM N = 1

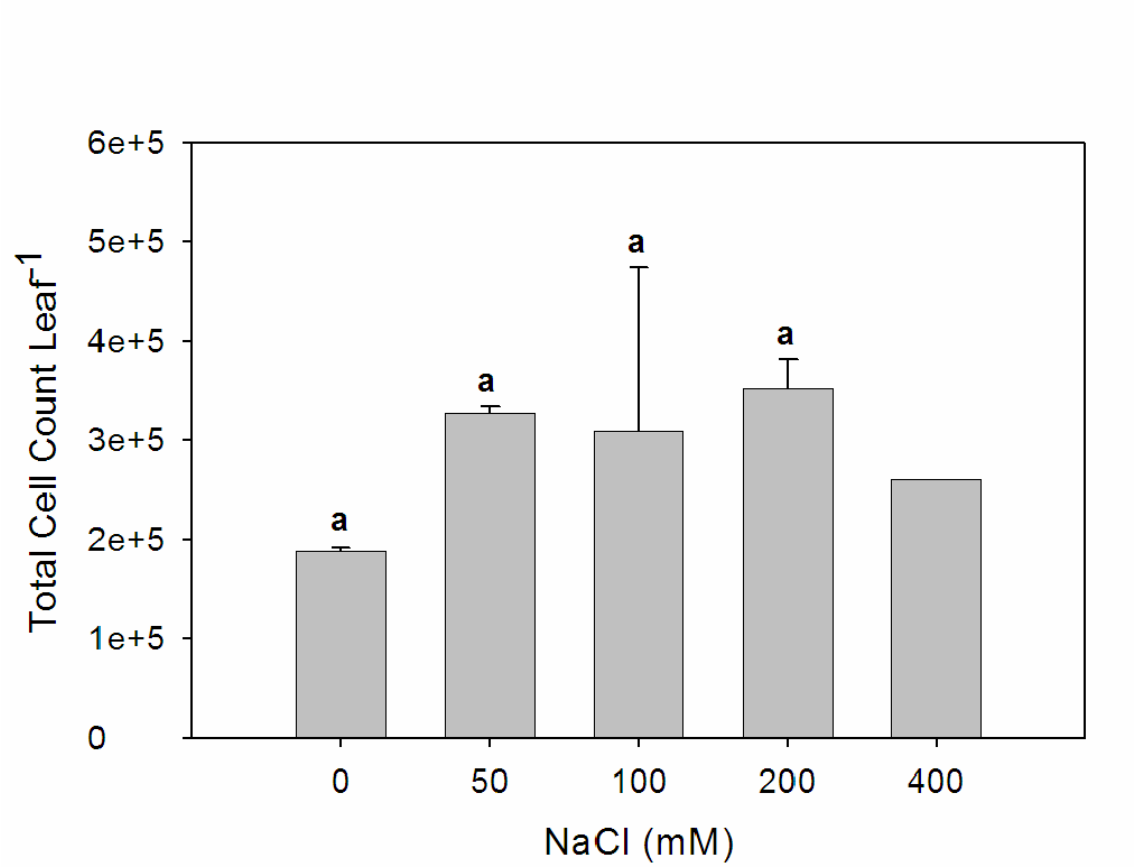

Figure 12. Cell area:central cytoplasmic compartment at 1.25 M glycine betaine and cell area under varying NaCl levels in *B. sinuspersici*. The cell area (CA) and central cytoplasmic compartment (CCC) were measured using ImageJ analysis software. Leaf maceration with a plastic pestle produced a cell suspension. This was diluted in 1.25 M glycine betaine and viewed at 10X in a light microscope. A) CA:CCC in 1.25 M glycine betaine solution, B) relative cell area in 1.25 M glycine betaine solution. Error bars represent the standard error of the mean. One-way ANOVA tests with orthogonal polynomial contrast were done to determine the significance. Different letters represent a significant difference; the same letter indicates no significant difference based on $P < 0.05$. N= 3; 100 mM and 400 mM N = 1

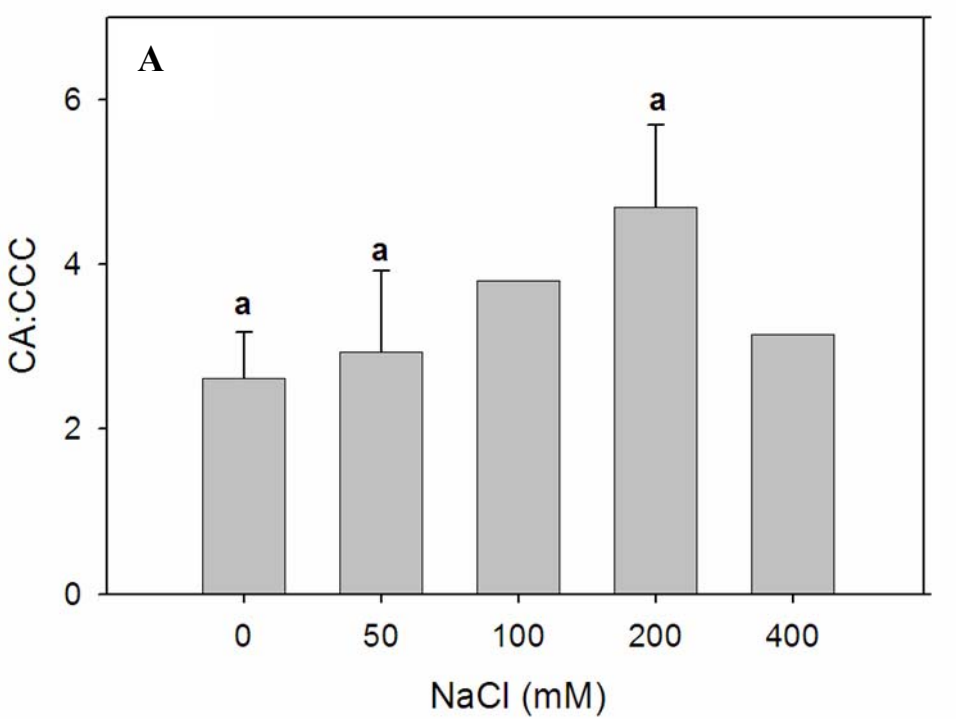
A
CA:CCC
6
4
2
0
a
a
a
0
50
100
200
400
NaCl (mM)

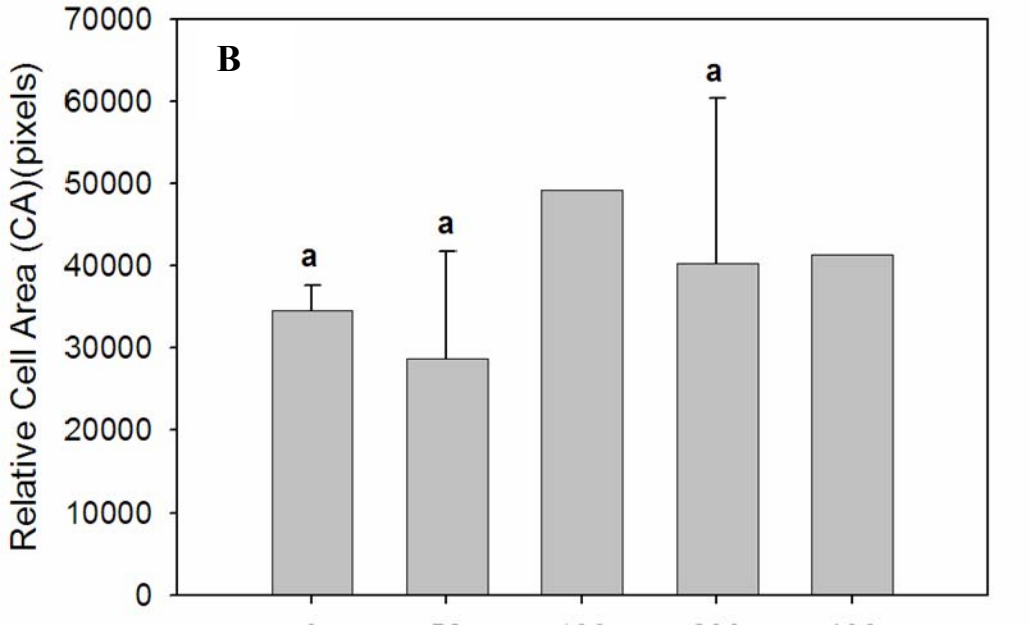
B
Relative Cell Area (CA)(pixels)
70000
60000
50000
40000
30000
20000
10000
0
a
a
a

Figure 13. Leaf osmolality under varying NaCl levels in *B. sinuspersici*. The leaf osmolality was measured in *B. sinuspersici* using a vapor pressure osmometer at each NaCl level. The solution osmolality was calculated from known solute concentrations of each NaCl solution and Hoagland's solution. Error bars represent the standard error of the mean. One-way ANOVA tests with polynomial contrasts were done to determine the significance. Different letters represent a significant difference; the same letter indicates no significant difference based on $P < 0.05$. N= 3, 400 mM N = 1

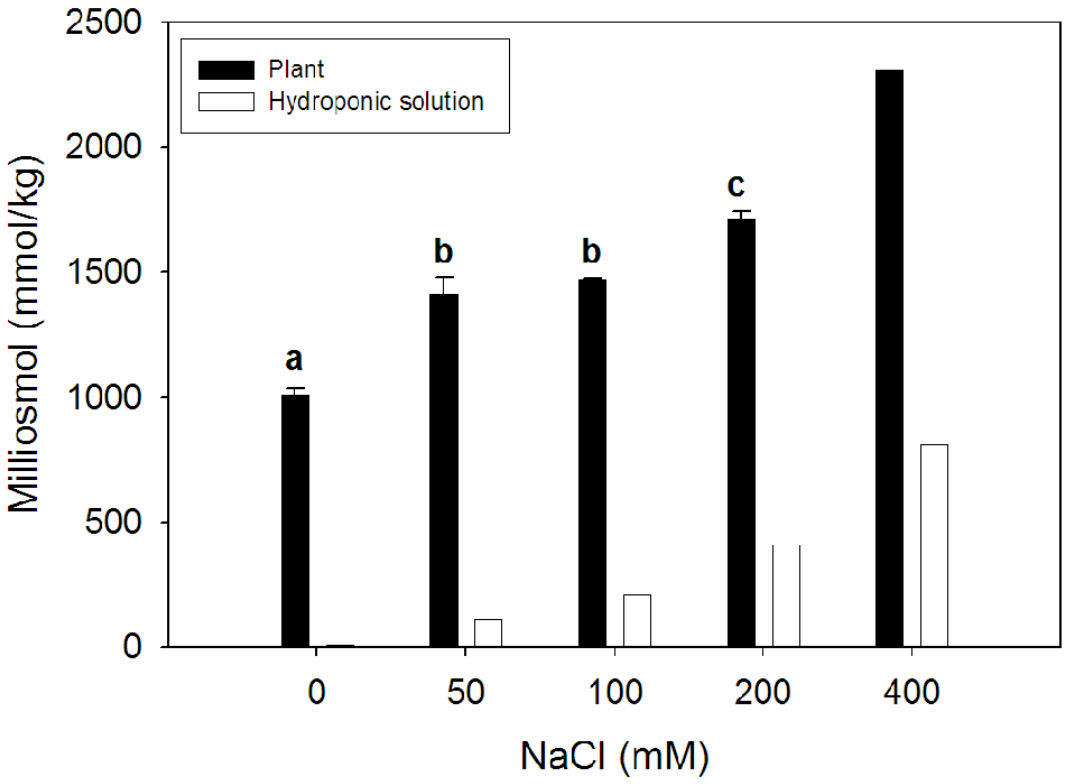

Figure 14. CO_2 response curves for *B. sinuspersici* under varying NaCl levels. CO_2 response curves were performed on *B. sinuspersici* at each NaCl level. 0 mM NaCl ● , 50 mM NaCl ▽ , 100 mM NaCl ■ , 200 mM NaCl ◇ , and 400 mM NaCl ▲ . The photosynthetic rates are expressed in A) µmol CO_2 per leaf area, B) µmol CO_2 per leaf, and C) µmol CO_2 per milligram dry weight. A represents CO_2 assimilation, Ci represents the intercellular CO_2 level. N = 2, 400 mM N = 1

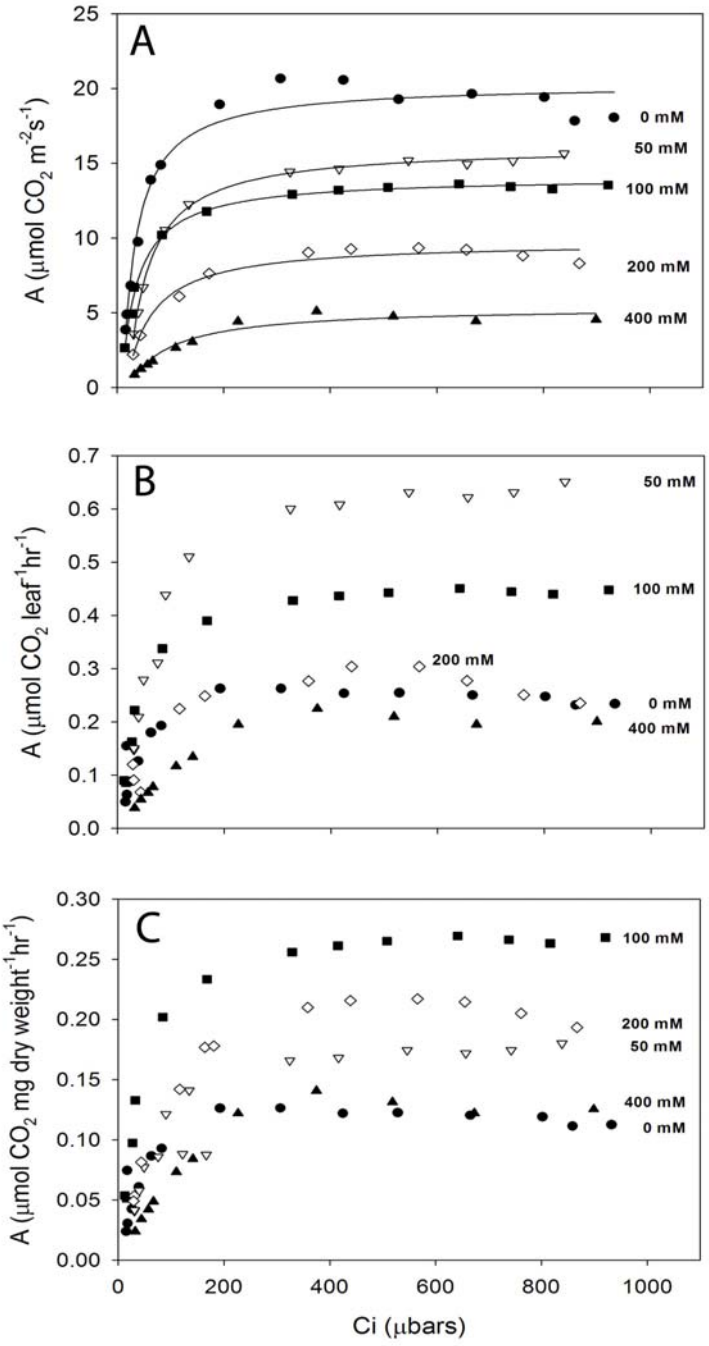
A
A (μmol CO2 m-2s-1)
0 mM
50 mM
100 mM
200 mM
400 mM
B
A (μmol CO2 leaf-1hr-1)
50 mM
100 mM
200 mM
0 mM
400 mM
C
A (μmol CO2 mg dry weight-1hr-1)
100 mM
200 mM
50 mM
400 mM
0 mM
Ci (μbars)

Figure 15. The maximum photosynthetic rate under saturating CO_2 (A_{max}) measured under each NaCl treatment in *B. sinuspersici*. Error bars represent the standard error of the mean. One-way ANOVA tests with orthogonal polynomial contrasts were done to determine the significance. Different letters represent a significant difference; the same letter indicates no significant difference based on $P < 0.05$. N= 3, 400 mM N = 1

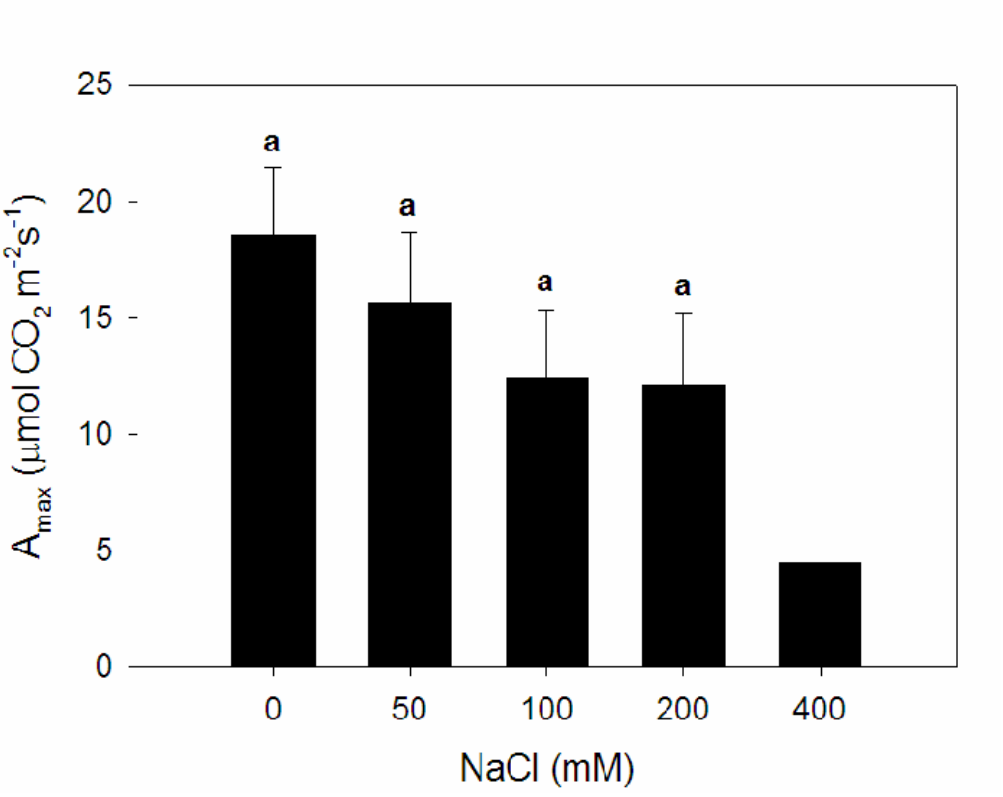

Figure 16. The carboxylation efficiency (C_E) measured under each NaCl treatment in *B. sinuspersici*. Ci is the intercellular CO_2. Ca is the atmospheric CO_2. Error bars represent the standard error of the mean. One-way ANOVA tests with orthogonal polynomial contrasts were done to determine the significance. Different letters represent a significant difference; the same letter indicates no significant difference based on $P < 0.05$. N= 3, 400 mM N = 1

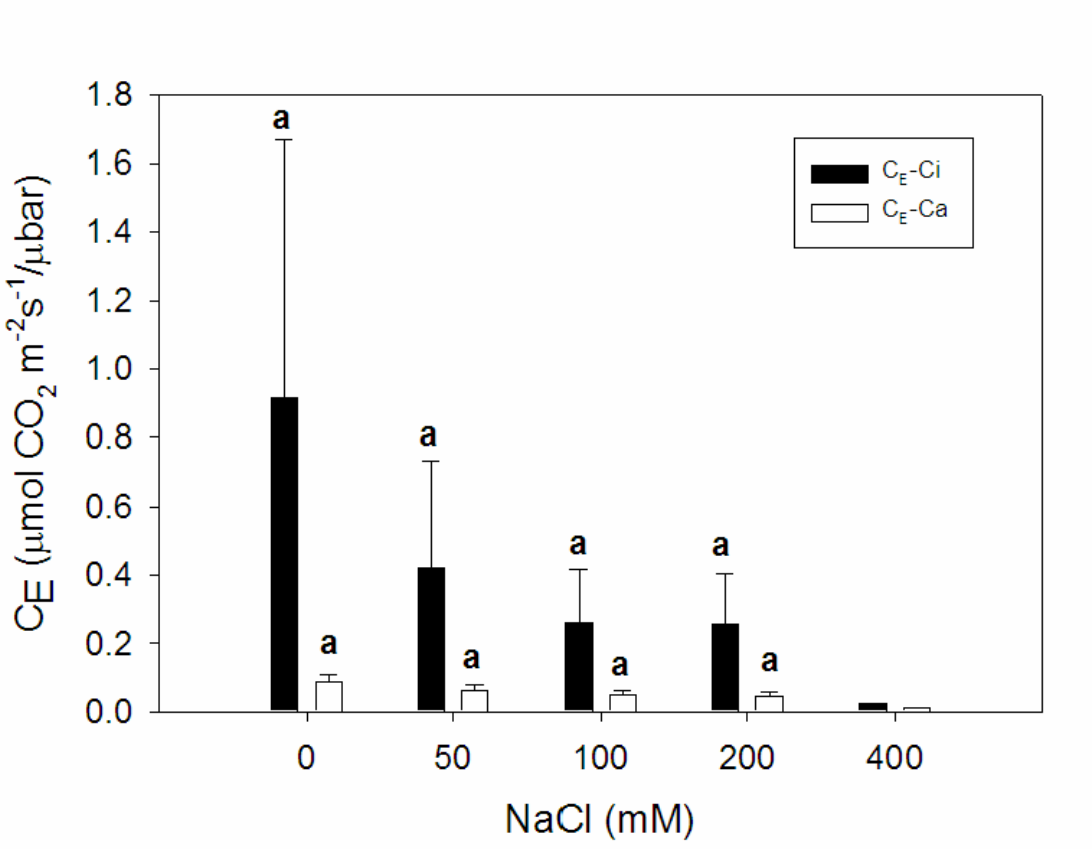

Figure 17. A_{max} versus C_E under varying NaCl levels in *B. sinuspersici*. The A_{max} values were plotted against the C_E-Ci values to determine if the rate of change was similar for both parameters. The data labels represent the points for each range of NaCl treatments. The trendline represents a linear regression. N = 3, 400 mM N = 1

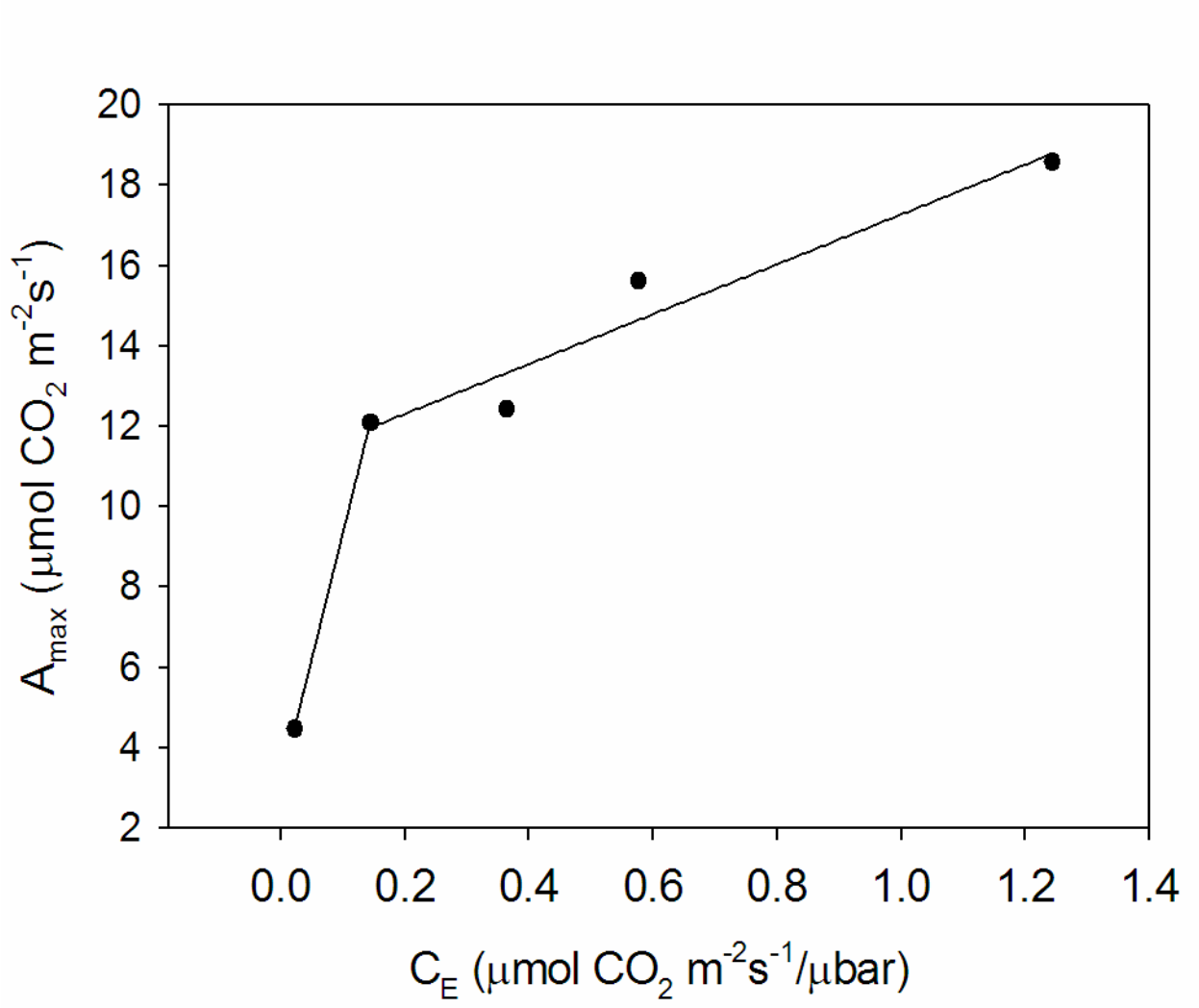

Figure 18. The CO_2 compensation point (Γ) measured under each NaCl treatment in *B. sinuspersici*. Error bars represent the standard error of the mean. One-way ANOVA tests with orthogonal polynomial contrasts were done to determine the significance. Different letters represent a significant difference; the same letter indicates no significant difference based on $P < 0.05$. N= 3, 400 mM N = 1

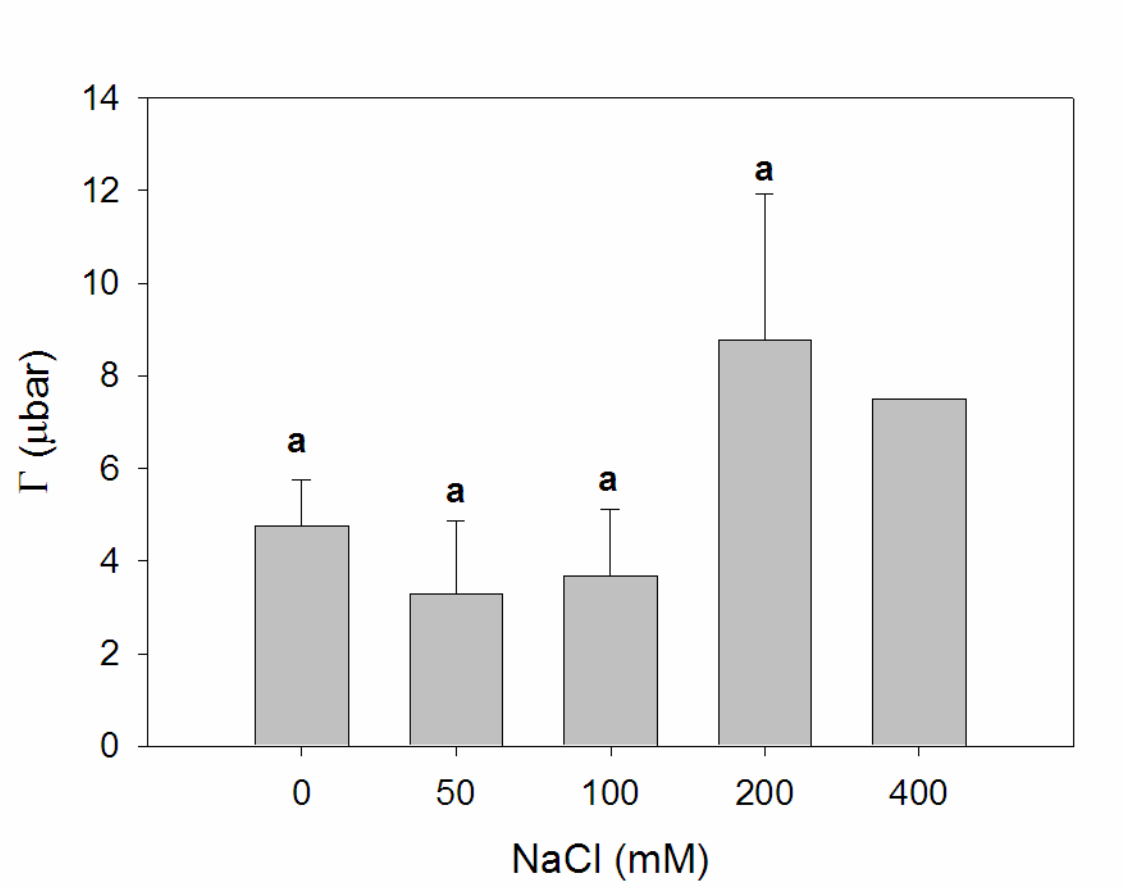

Figure 19. The stomatal conductance (g_s) measured under each NaCl treatment in *B. sinuspersici*. The stomatal conductance was measured during gas exchange analysis after the initial acclimation period. Error bars represent the standard error of the mean. One-way ANOVA tests with orthogonal polynomial contrasts were done to determine the significance. Different letters represent a significant difference; the same letter indicates no significant difference based on $P < 0.10$. N= 3, 400 mM N = 1

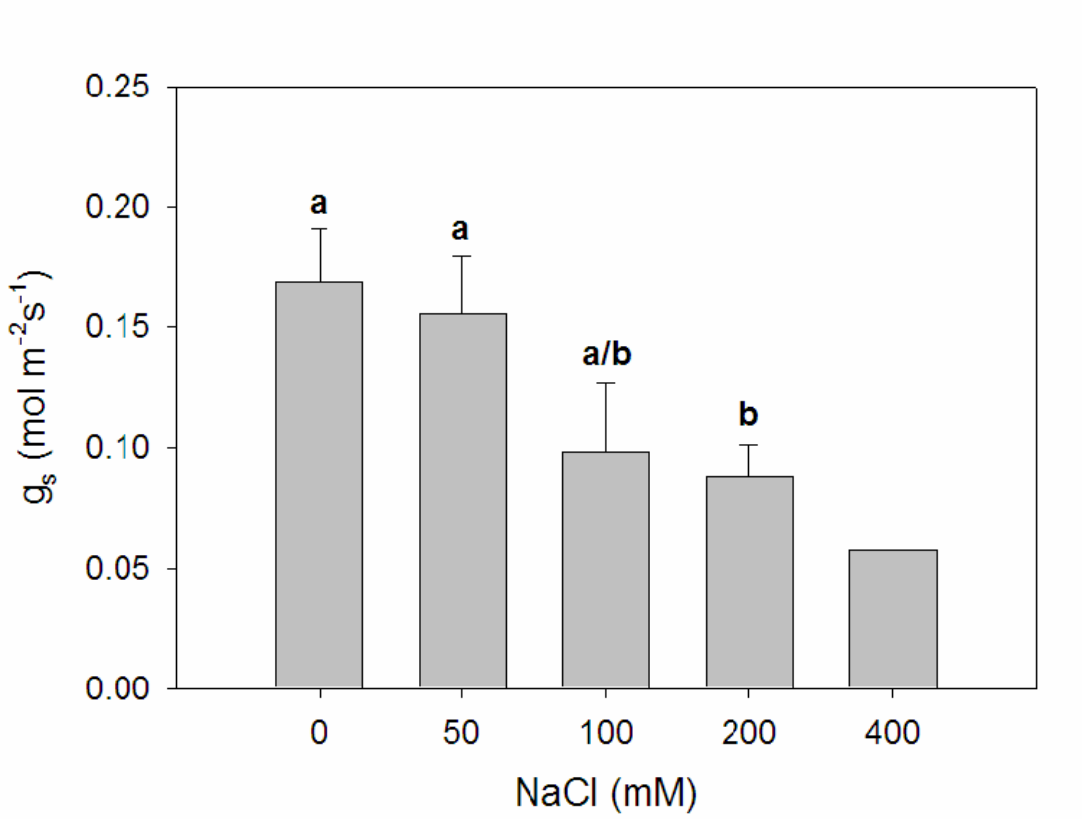

Figure 20. The Ci/Ca measured under each NaCl treatment in *B. sinuspersici*. The Ci/Ca ratio was determined from the Ci and Ca values at the maximum photosynthetic rate under saturating CO_2 (A_{max}). Error bars represent the standard error of the mean. One-way ANOVA tests with orthogonal polynomial contrasts were done to determine the significance. Different letters represent a significant difference; the same letter indicates no significant difference based on $P < 0.05$. N= 3, 400 mM N = 1

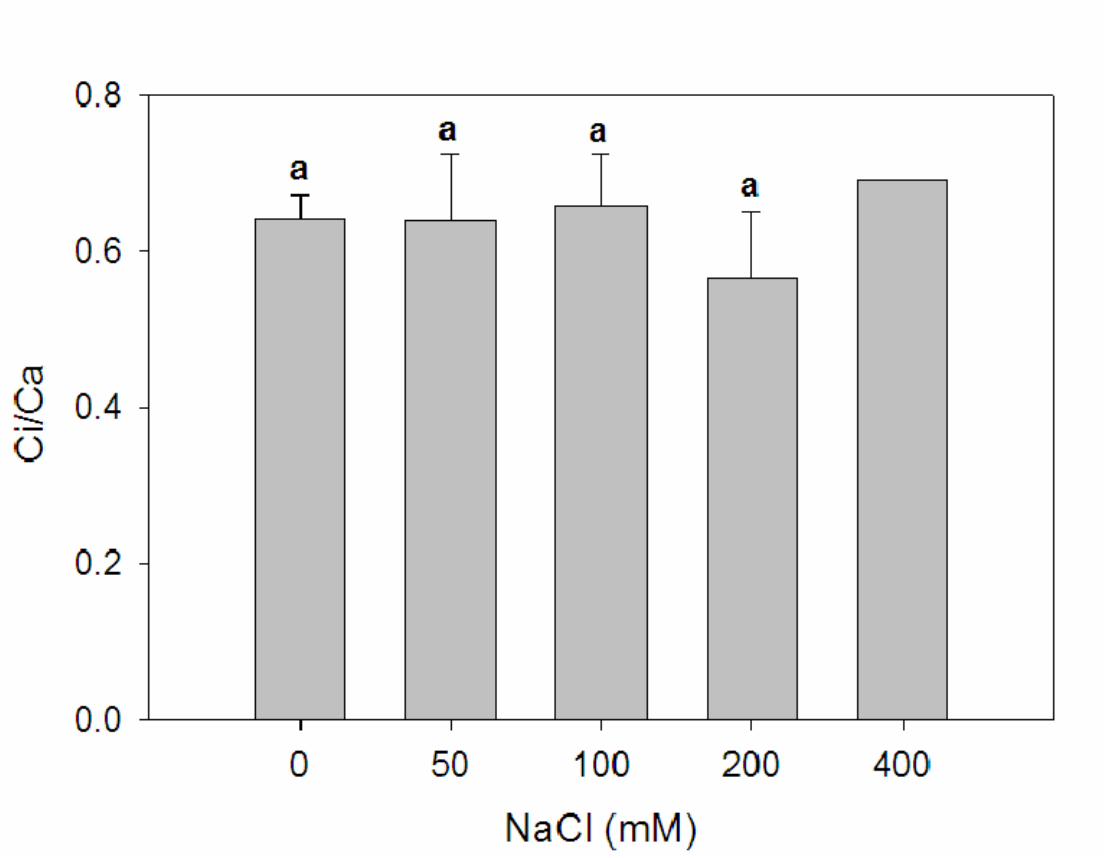

Figure 21. The photosynthetic water use efficiency (PWUE) measured under each NaCl treatment in *B. sinuspersici*. The PWUE was calculated by dividing the transpiration rate by the assimilation rate. These rate values were generated from gas exchange measurements. Error bars represent the standard error of the mean. One-way ANOVA tests with orthogonal polynomial contrasts were done to determine the significance. Different letters represent a significant difference; the same letter indicates no significant difference based on $P < 0.05$. N= 3, 400 mM N = 1

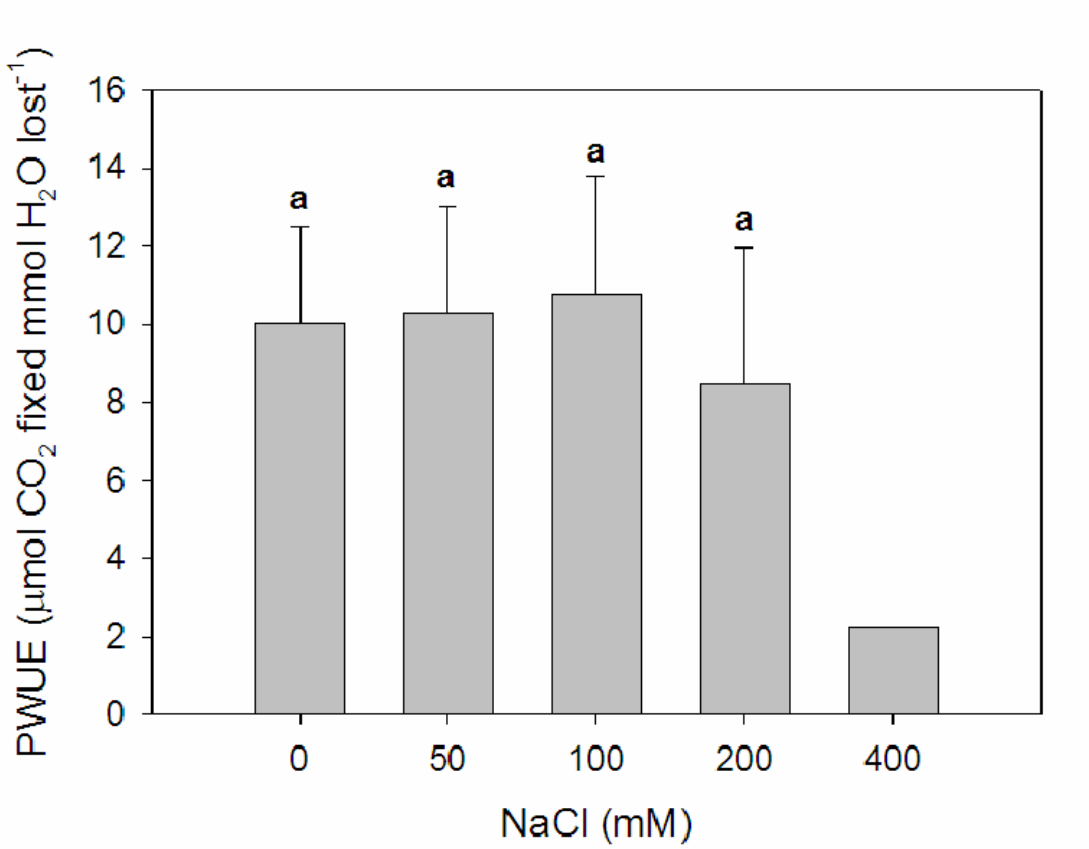

Figure 22. The effect of salt on the total chlorophyll and protein on a fresh weight and dry weight basis in *B. sinuspersici*. After extraction and quantification, the total chlorophyll and protein were expressed on a fresh and dry weight basis. A) total protein and chlorophyll on a fresh weight basis (µg/mg), and B) total protein and chlorophyll on a dry weight basis (µg/mg). Error bars represent the standard error of the mean. One-way ANOVA tests with orthogonal polynomial contrasts were done to determine the significance. Different letters represent a significant difference; the same letter indicates no significant difference based on $P < 0.10$. N= 3, 400 mM N = 1

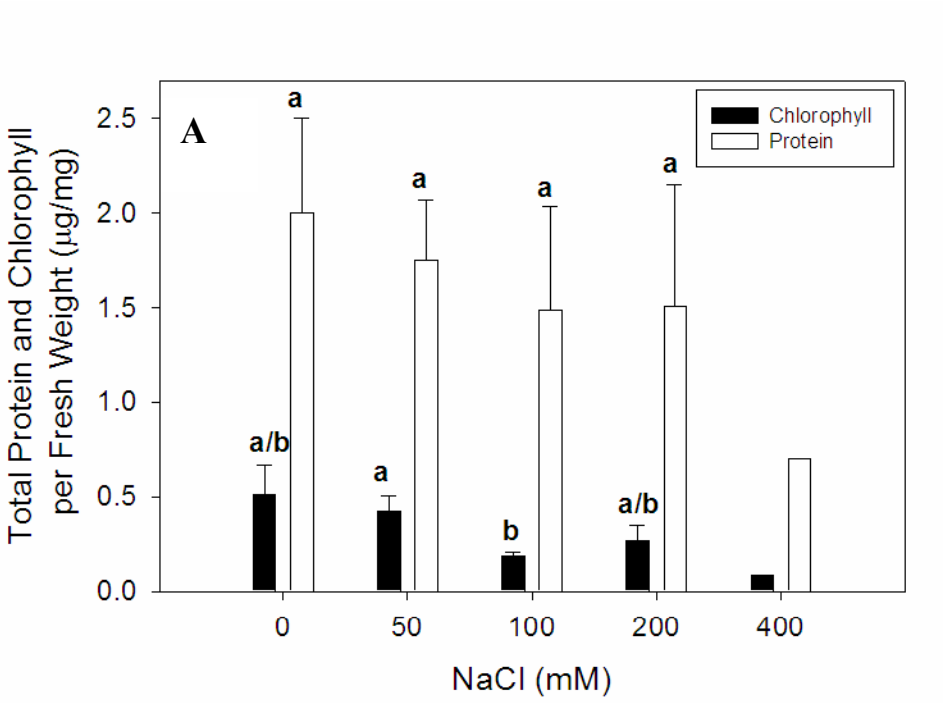
A
Chlorophyll
Protein
Total Protein and Chlorophyll per Fresh Weight (µg/mg)
2.5
2.0
1.5
1.0
0.5
0.0
a
a
a
a
a
a/b
a
b
a/b
0
50
100
200
400
NaCl (mM)

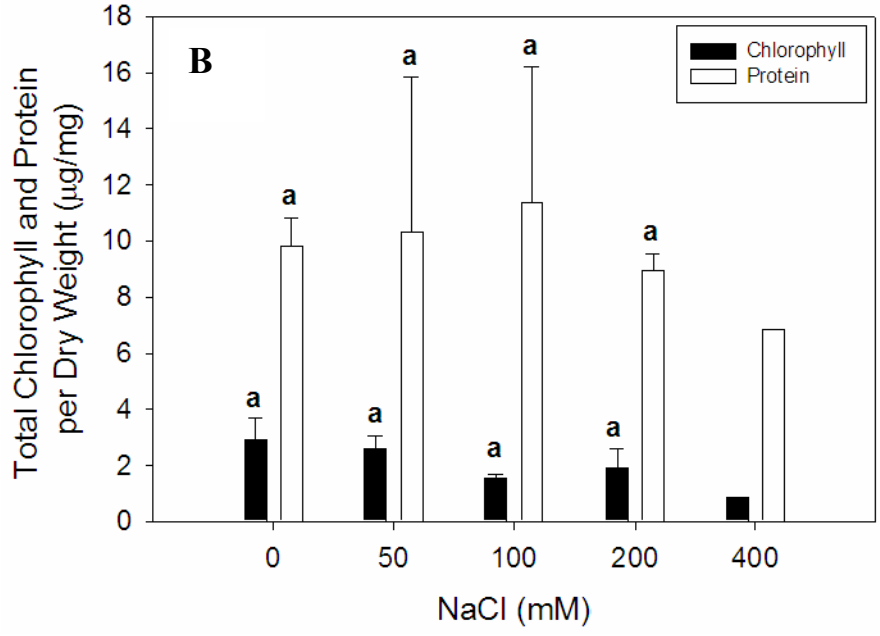
B
Chlorophyll
Protein
Total Chlorophyll and Protein per Dry Weight (µg/mg)
18
16
14
12
10
8
6
4
2
0
a
a
a
a
a
a
a
a
a
0
50
100
200
400
NaCl (mM)

Figure 23. Western blot quantification under varying NaCl levels in *B. sinuspersici* on a total protein basis. The relative intensity of each band was quantified using ImageJ analysis program. The relative intensity was compared to the treatment without NaCl, which represented 100%. Error bars represent the standard error of the mean. One-way ANOVA tests with orthogonal polynomial contrasts were done to determine the significance. Different letters represent a significant difference; the same letter indicates no significant difference based on $P < 0.05$. N= 3, 400 mM N = 1

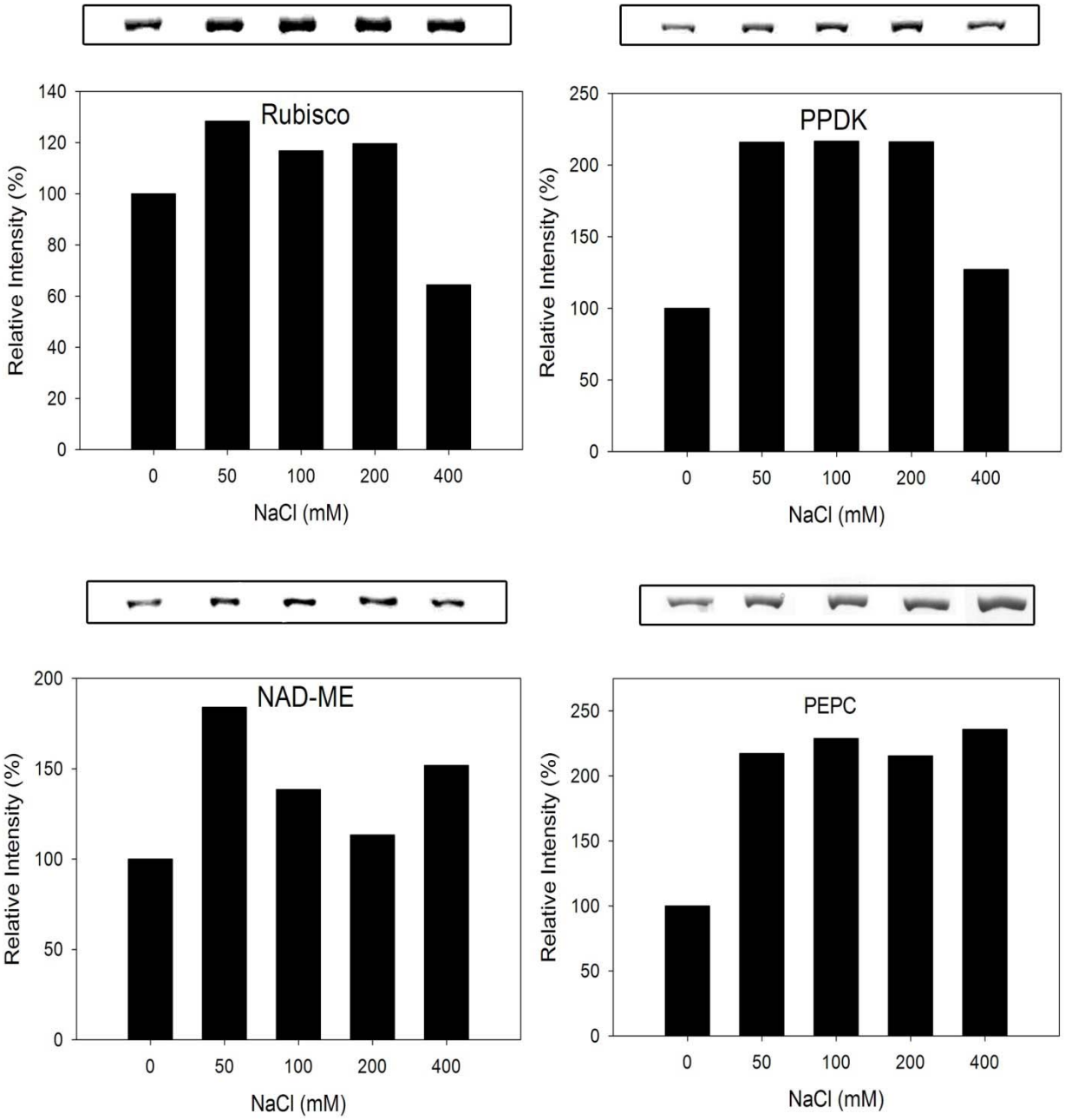
Rubisco
Relative Intensity (%)
0
20
40
60
80
100
120
140
0
50
100
200
400
NaCl (mM)
PPDK
Relative Intensity (%)
0
50
100
150
200
250
0
50
100
200
400
NaCl (mM)
NAD-ME
Relative Intensity (%)
0
50
100
150
200
0
50
100
200
400
NaCl (mM)
PEPC
Relative Intensity (%)
0
50
100
150
200
250
0
50
100
200
400
NaCl (mM)

Figure 24. Western blot comparison among NaCl treatments in *B. sinuspersici* on a total protein and leaf area basis. The relative intensities for each enzyme were expressed on a protein and leaf area basis. The relative intensity was compared to the treatment without NaCl, which represented 100%. A) relative intensity on a protein basis (%), and B) relative intensity on a leaf area basis (%). Error bars represent the standard error of the mean. One-way ANOVA tests with orthogonal polynomial contrasts were done to determine the significance. Different letters represent a significant difference; the same letter indicates no significant difference based on $P < 0.05$. Error bars represent the standard error. N= 3, 400 mM N = 1

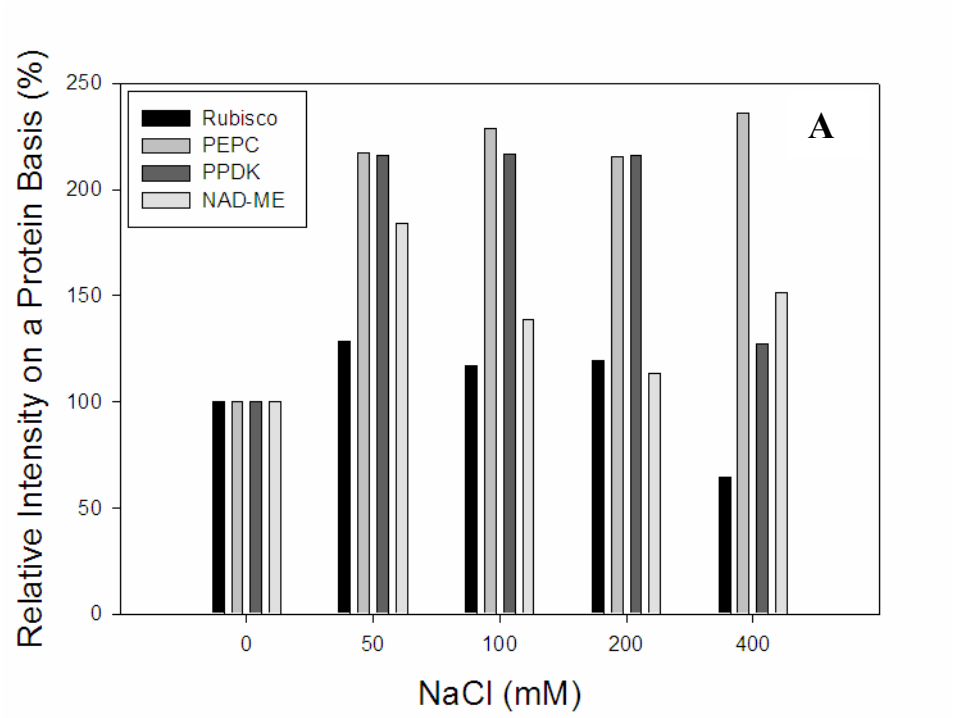
Relative Intensity on a Protein Basis (%)
250
200
150
100
50
0
Rubisco
PEPC
PPDK
NAD-ME
A
0
50
100
200
400
NaCl (mM)

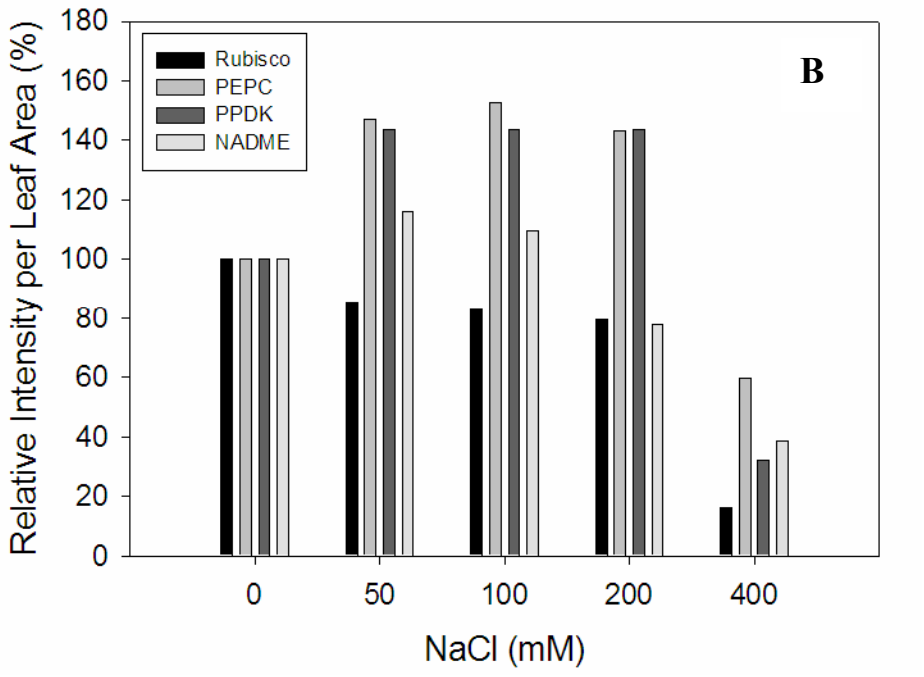
Relative Intensity per Leaf Area (%)
180
160
140
120
100
80
60
40
20
0
Rubisco
PEPC
PPDK
NADME
B
0
50
100
200
400
NaCl (mM)

Figure 25. Carbon isotope discrimination ($\delta^{13}C$) analysis under varying NaCl levels in *B. sinuspersici*. The carbon isotope discrimination was measured under each NaCl treatment in *B. sinuspersici*. The isotope discrimination is measured in parts per thousand. Error bars represent the standard error of the mean. One-way ANOVA tests with orthogonal polynomial contrasts were done to determine the significance. Different letters represent a significant difference; the same letter indicates no significant difference based on $P < 0.10$. N= 3, 400 mM N = 1

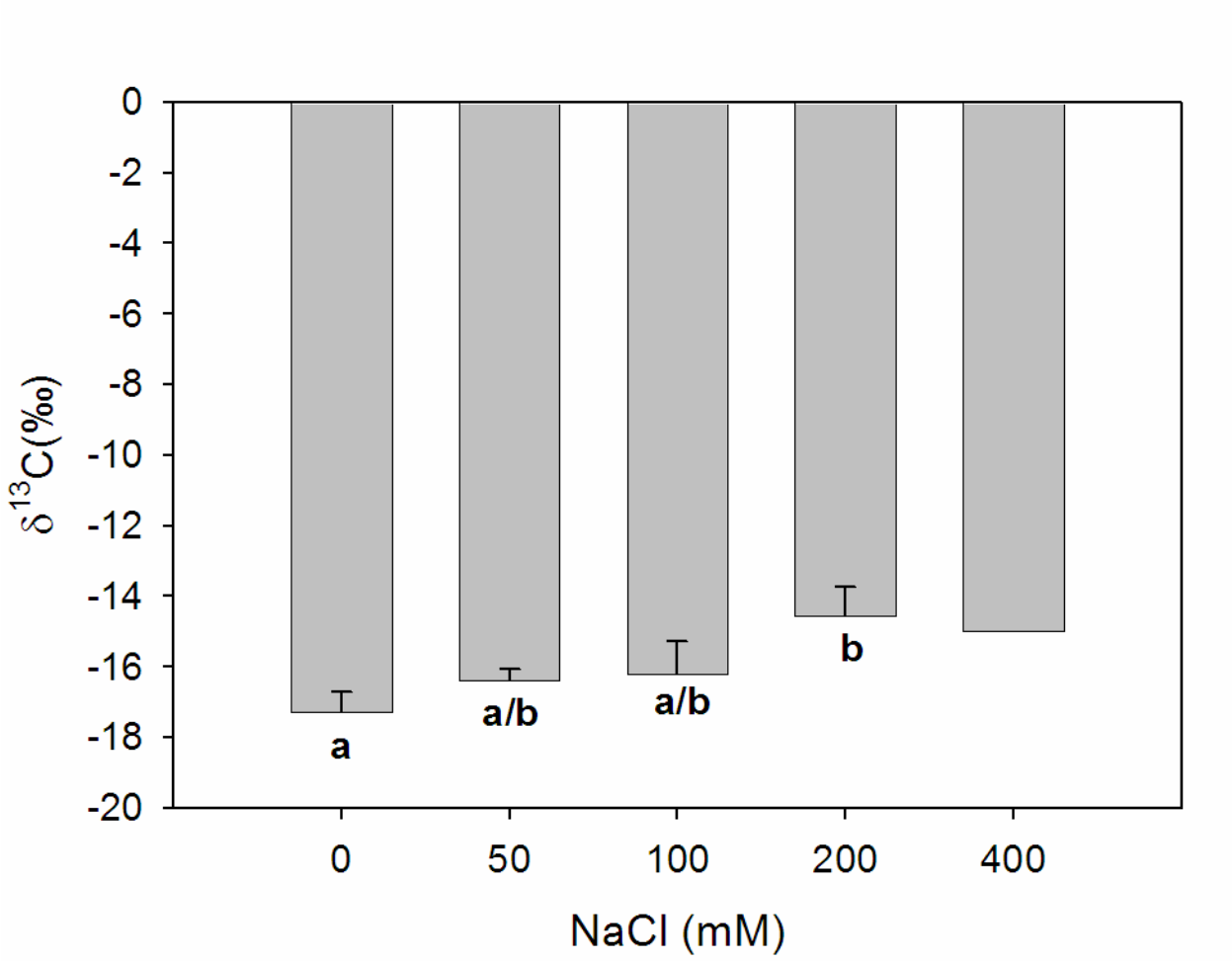

SUPPLEMENTAL TABLES: CHAPTER TWO

Table S1. Growth parameters in *B. sinuspersici* under varying NaCl treatments.

The individual incident leaf area was measured for each NaCl treatment. The chlorophyll, protein, fresh and dry weights were then quantified on a per leaf and per leaf area basis for each NaCl treatement. The mean values are in bold ± the standard error of the mean. N = 3, 400 mM N = 1

		Per leaf area (cm^2)				**Per leaf**			
NaCl (mM)	**Individual Incident Leaf Area**	**Total protein (µg)**	**Total chlorophyll (µg)**	**Dry weight (mg)**	**Fresh weight (mg)**	**Total protein (µg)**	**Total chlorophyll (µg)**	**Dry weight (mg)**	**Fresh weight (mg)**
0	**0.36** ± 0.03	**88.5** ± 20.1	**734.1** ± 27.1	**28.4** ± 6.8	**107.8** ± 9.1	**47.6** ± 5.0	**6.3** ± 1.3	**10.4** ± 3.0	**38.2** ± 4.4
50	**0.59** ± 0.04	**53.6** ± 9.1	**451.3** ± 53.3	**12.9** ± 2.5	**125.6** ± 10.9	**49.6** ± 15.4	**5.5** ± 0.2	**7.6** ± 1.3	**74.1** ± 4.8
100	**0.59** ± 0.06	**32.9** ± 12.0	**817.5** ± 38.9	**18.2** ± 3.3	**138.5** ± 19.2	**73.4** ± 4.0	**6.2** ± 3.2	**10.4** ± 1.0	**80.2** ± 5.9
200	**0.65** ± 0.05	**57.9** ± 9.3	**555.5** ± 19.8	**15.5** ± 0.7	**146.5** ± 7.7	**70.5** ± 3.3	**7.2** ± 1.3	**10.1** ± 0.7	**96.0** ± 9.6
400	**0.73**	**51.5**	**424.7**	**13.1**	**118.8**	**51.9**	**6.3**	**9.6**	**87.2**

Table S2. Root fresh and dry weights, and shoot fresh and dry weights in *B. sinuspersici* under varying NaCl treatments. Individual plants were removed from the hydroponics system and the roots and shoots were separated. Dry weight measurements were taken after roots and shoots were dried in a 55 °C oven for several days. The mean values are in bold ± the standard error of the mean. N = 3, 400 mM N = 1

Root	**0 mM**	**50 mM**	**100 mM**	**200 mM**	**400 mM**
Fresh Weight (g)	**8.3** ± 3.0	**40.2** ± 4.6	**64.5** ± 20.5	**96.4** ± 34.2	**3.2**
Dry Weight (g)	**0.7** ± 0.1	**2.3** ± 0.1	**3.0** ± 0.6	**6.1** ± 2.6	**0.39**
DW:FW (%)	**12.3** ± 5.1	**5.9** ± 0.9	**5.7** ± 1.7	**7.0** ± 1.4	**12.4**

Shoot	**0 mM**	**50 mM**	**100 mM**	**200 mM**	**400 mM**
Fresh Weight (g)	**13.5** ± 2.7	**43.1** ± 3.9	**44.3** ± 11.2	**101.9** ± 57.4	**12.1**
Dry Weight (g)	**1.7** ± 0.7	**6.4** ± 0.7	**9.1** ± 4.4	**17.7** ± 15.2	**1.8**
DW:FW (%)	**12.8** ± 3.9	**15.4** ± 2.7	**19.7** ± 3.5	**14.8** ± 2.6	**14.9**

Table S3. Total chlorenchyma cell count per leaf under varying NaCl levels in *B. sinuspersici*. The total cell count per leaf was counted after extraction from leaf material. The total cell count per leaf is expressed x 10^3. The mean values are in bold ± the standard error of the mean. N = 3; 100 mM and 400 mM N = 2

NaCl (mM)	**0**	**50**	**100**	**200**	**400**
Total Cell Count per leaf (x 10^3)	**188.7** ± 2.4	**328.0** ± 6.1	**308.9** ± 164.4	**351.4** ± 29.9	**260**

Table S4. Cell area and cell area:central cytoplasmic compartment at 1.25 M glycine betaine under varying NaCl levels in *B. sinuspersici*. The cell area (CA) and cell area:central cytoplasmic compartment (CA:CCC) were measured at each NaCl level in a 1.25 M glycine betaine solution. The mean values are in bold ± the standard error of the mean. N = 3; 100 mM and 400 mM N = 1

NaCl (mM)	Average CA:CCC at 1.25 M glycine betaine	CA (pixels) (x 10^2)
0	**2.6** ± 0.7	**345.2** ± 30.6
50	**2.7** ± 1.4	**285.9 ± 131.7**
100	**3.7**	**491.7**
200	**4.6** ± 1.2	**402.7** ± 201.1
400	**2.86**	**413.1**

Table S5. Cell area and central cytoplasmic compartment from light microscopy quantifications under varying NaCl levels in *B. sinuspersici*. The cell area (CA) and central cytoplasmic compartment (CCC) were measured from light microscopy sections (illustrated in Fig. 5). The CA:CCC and CA were quantified using ImageJ software. The mean values are in bold ± the standard error of the mean within one replicate. N = 1

NaCl (mM)	CCC (pixels) (x 10^2)	CA (pixels) (x 10^2)	CA:CCC
0	**52.9** ± 2.8	**118.8** ± 5.3	**2.48** ± 0.16
50	**65.3** ± 6.2	**168.5** ± 11.4	**2.86** ± 0.18
100	**47.2** ± 2.9	**147.9** ± 6.7	**3.82** ± 0.31
200	**60.3** ± 5.3	**153.3** ± 10.1	**2.99** ± 0.35

Table S6. Leaf osmolality under varying NaCl levels in *B. sinuspersici*. The osmolality was measured with a vapor pressure osmomter in *B. sinuspersici* at each NaCl level. Whole leaf samples were removed from the plants after 6-8 weeks of growth in hydroponics. After gentle maceration samples were centrifuged for 5 minutes at 16,000 g. The resulting supernatant was loaded onto the reference disc in the sample holder of the osmometer using 10 µl size samples. The osmometer was calibrated using 100, 290 and 1000 milliosmol standards before each use. The mean values are in bold ± the standard error of the mean. N = 3, 400 mM N = 1

NaCl (mM)	**0**	**50**	**100**	**200**	**400**
Milliosmol (mmol/kg)	**1020** ± 54	**1463** ± 79	**1473** ± 78	**1731** ± 103	**2306**

Table S7. Summary of photosynthetic components under varying NaCl levels in *B. sinuspersici*. Γ is the CO_2 compensation point. C_E is the carboxylation efficiency. A_{max} is the maximum photosynthetic rate under saturating CO_2. PWUE is the photosynthetic water use efficiency. Photosynthetic parameters were measured at 1000 PPFD and 25 °C. The mean values are in bold ± the standard error of the mean. N = 3, 400 mM N = 1

NaCl (mM)	0	50	100	200	400
Γ(µbar)	**4.8** ± 0.9	**3.3** ± 1.6	**3.7** ± 1.4	**8.8** ± 3.2	**7.5**
C_E (µmol CO_2 $m^{-2}s^{-1}$/µbar) (Ci)	**0.9** ± 0.8	**0.42** ± 0.3	**0.26** ± 0.2	**0.26** ± 0.1	**0.02**
C_E(µmol CO_2 $m^{-2}s^{-1}$/µbar) (Ca)	**0.09** ± 0.02	**0.08** ± 0.02	**0.05** ± 0.01	**0.05** ± 0.01	**0.01**
A_{max} (µmol CO_2 $m^{-2}s^{-1}$)	**18.6** ± 2.5	**15.6** ± 3.0	**12.4** ± 2.9	**12.1** ± 3.2	**4.5**
g_s (mol $m^{-2}s^{-1}$)	**0.17** ± 0.02	**0.16** ± 0.02	**0.10** ± 0.03	**0.09** ± 0.01	**0.06**
Ci/Ca (%)	**0.64** ± 0.03	**0.64** ± 0.09	**0.66** ± 0.07	**0.56** ± 0.09	**0.69**
PWUE (µmol CO_2 fixed per mmol H_20 lost)	**10.0** ± 2.4	**10.3** ± 2.7	**10.8** ± 3.0	**8.4** ± 3.5	**2.2**

Table S8. Chlorophyll and protein on a per fresh and dry weight basis under varying NaCl levels in *B. sinuspersici*. After extraction and quantification, the total chlorophyll and protein were expressed on a fresh and dry weight basis. The mean values are in bold ± the standard error of the mean. N = 3, 400 mM N = 1

NaCl (mM)	Total protein per fresh weight (µg/mg)	Total protein per dry weight (µg/mg)	Total chlorophyll per fresh weight (µg/mg)	Total chlorophyll per dry weight (µg/mg)
0	**2.0** ± 0.3.	**13.6** ± 3.8	**0.51** ± 0.2	**2.9** ± 0.8
50	**1.75** ± 0.2	**13.5** ± 3.2	**0.242** ± 0.08	**2.6** ± 0.5
100	**1. 90** ± 0.5	**15.7** ± 4.8	**0.19** ± 0.02	**1.6** ± 0.1
200	**1. 5** ± 0.4	**12.6** ± 3.6	**0.27** ± 0.08	**1.9** ± 0.7
400	**0.7**	**6.9**	**0.09**	**0.9**

Table S9. $\delta^{13}C$ analysis under varying NaCl levels for *B. sinuspersici*. The carbon isotope discrimination was measured under each NaCl treatment in *B. sinuspersici*. The isotope discrimination is measured in parts per thousand. The mean values are in bold ± the standard error of the mean. N = 3, 400 mM N = 1

NaCl (mM)	**$\delta^{13}C$ (‰)**
0	**-17.3** ± 0.6
50	**-16.4** ± 0.3
100	**-16.2** ± 0.9
200	**-14.5** ± 0.8
400	**-14.9**

SUPPLEMENTAL FIGURES: CHAPTER TWO

Figure S1. Root DW:FW and shoot DW:FW in *B. sinuspersici* under varying NaCl levels. The root and shoot DW:FW was quantified after the root and shoot dry weight and fresh weights were measured. The dry weights were obtained after the root and shoots had been dried in a 55 °C oven for several days. A) root DW:FW (%) and B) shoot DW:FW (5). Error bars represent the standard error of the mean. One-way ANOVA tests with orthogonal polynomial contrasts were done to determine the significance. Different letters represent a significant difference; the same letter indicates no significant difference based on $P < 0.05$. N= 3, 400 mM N = 1

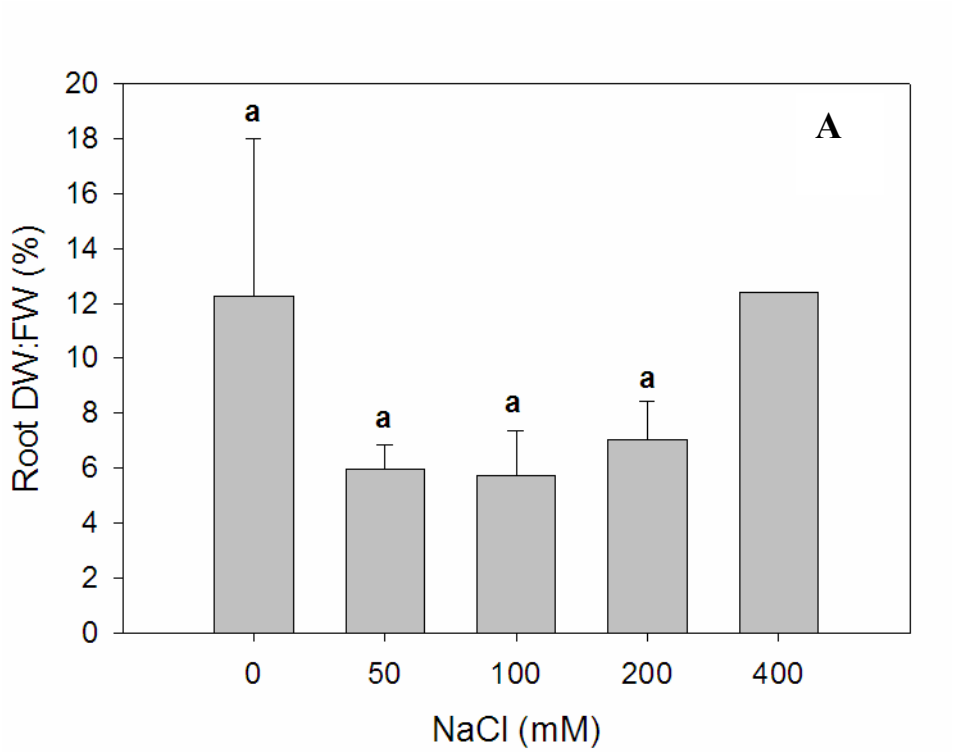
A
Root DW:FW (%)
20
18
16
14
12
10
8
6
4
2
0
a
a
a
a
0
50
100
200
400
NaCl (mM)

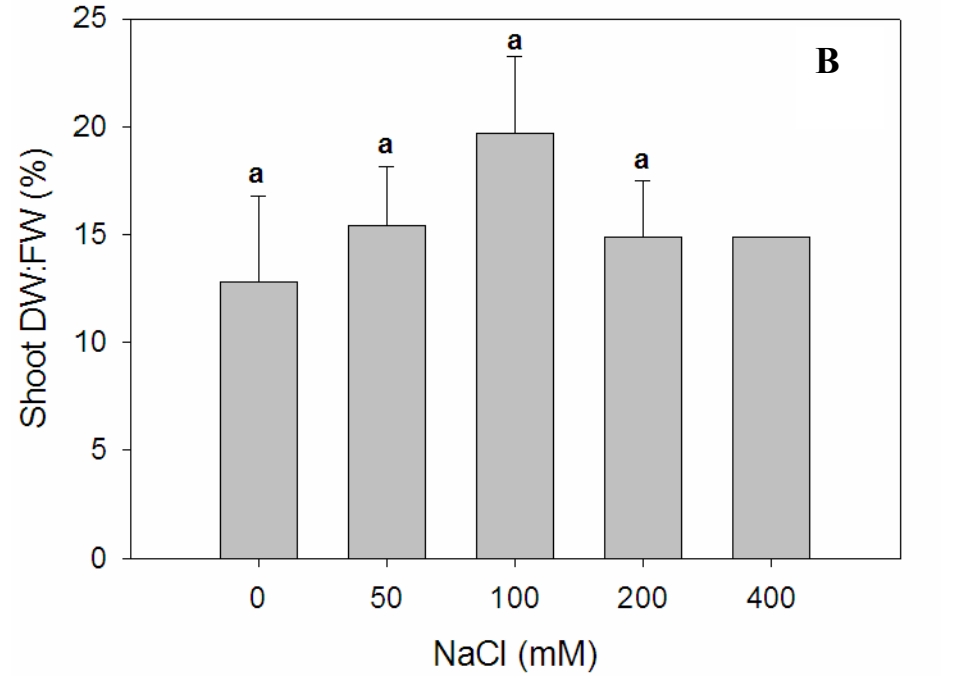
B
Shoot DW:FW (%)
25
20
15
10
5
0
a
a
a
a
0
50
100
200
400
NaCl (mM)

Figure S2. Light microscopy images (10x) of chlorenchyma cells of *B. sinuspersici* in different osmotic conditions. Glycine betaine is a compatible solute produced by *B. sinuspersici* and was therefore used to adjust the osmotic concentration of each solution. When the osmotic concentration of the solution is adjusted to match the osmotic concentration of the cells, then the true difference between the overall cell area and area of the central cytoplasmic compartment can be seen. As the salt level increases, the overall ratio of the cell area to central cytoplasmic compartment increases.

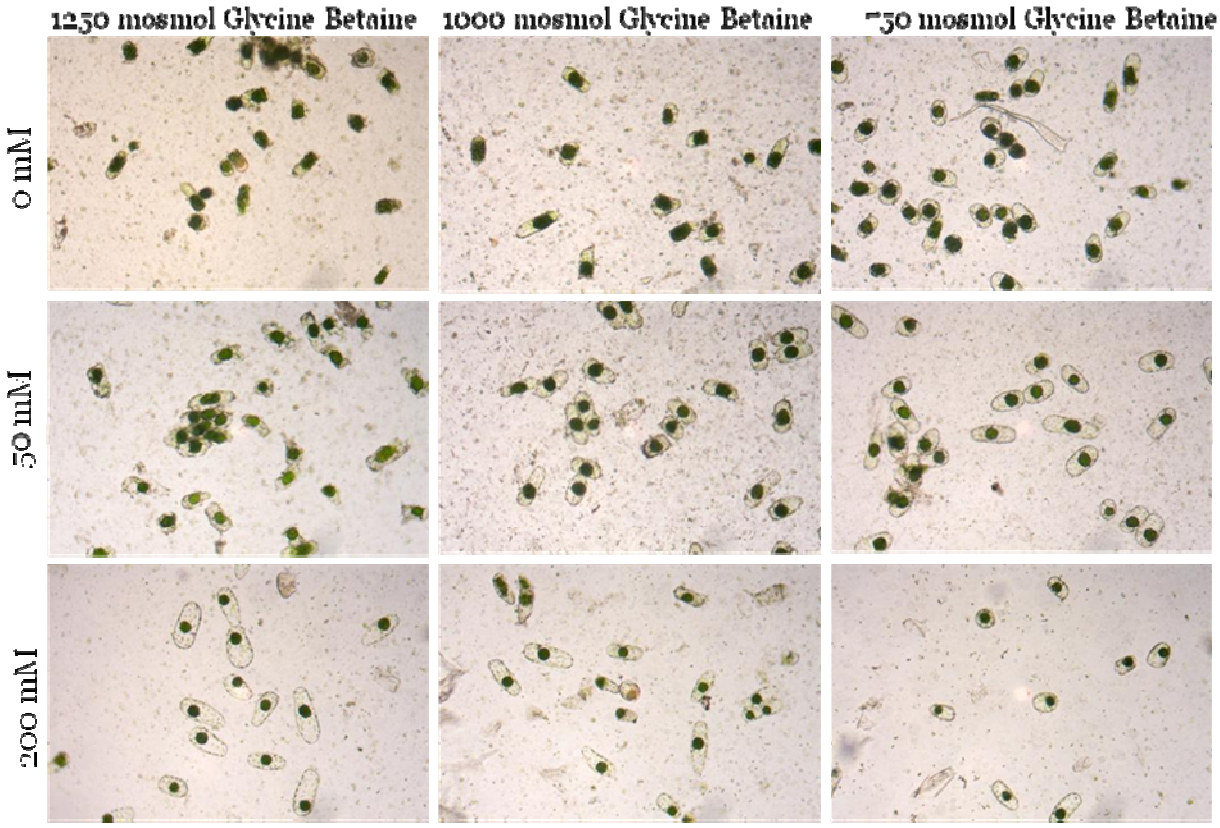

Figure S3. Cell area, central cytoplasmic compartment and the cell area:central cytoplasmic compartment quantification from light microscope images in *B. sinuspersici* under varying NaCl levels. The cell area (CA) and central cytoplasmic compartment (CCC) were measured from light microscopy sections (illustrated in Fig. 5). The CA:CCC and CA were quantified using ImageJ software. Error bars represent the standard error of the mean from one replicate. N= 1

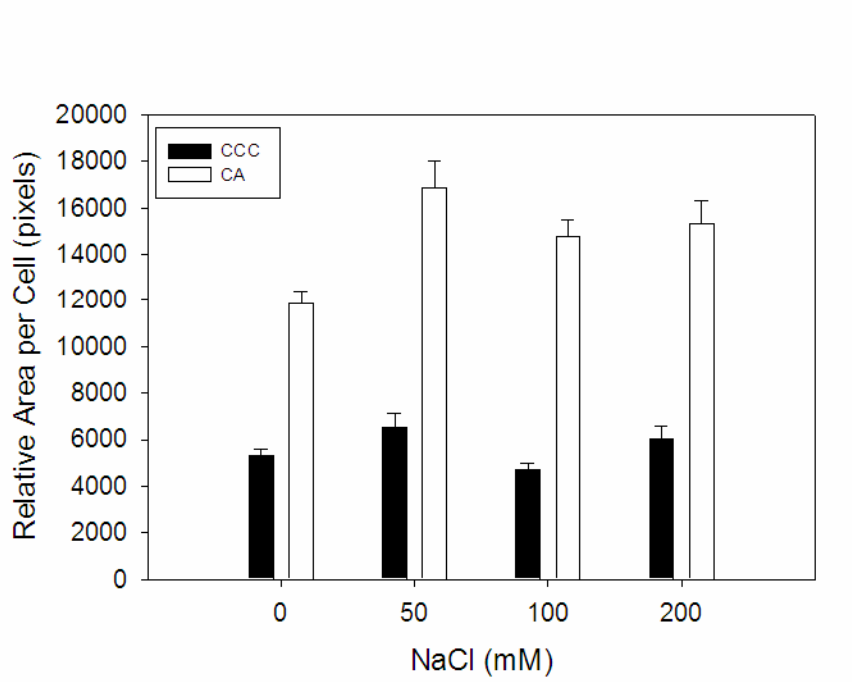
Relative Area per Cell (pixels)
20000
18000
16000
14000
12000
10000
8000
6000
4000
2000
0
CCC
CA
0
50
100
200
NaCl (mM)

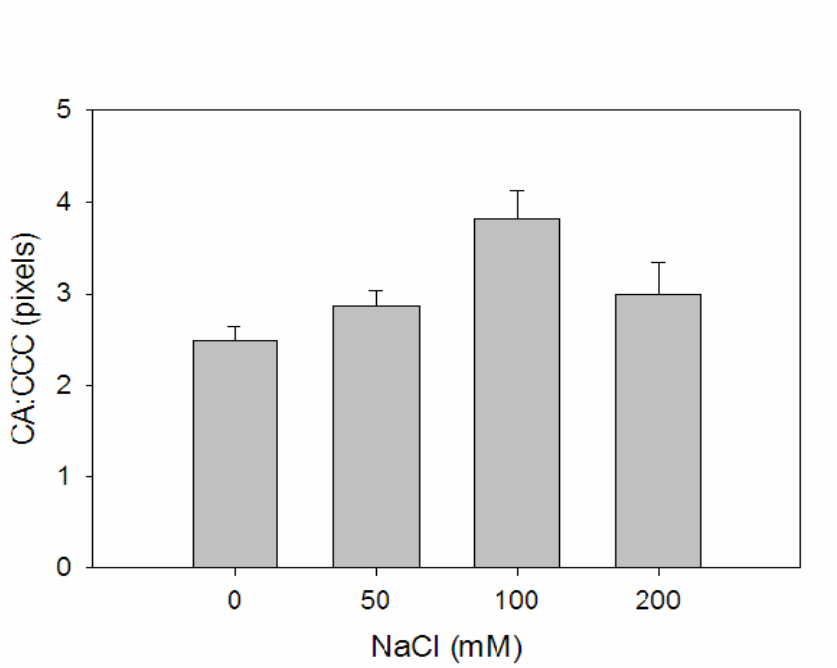
CA:CCC (pixels)
5
4
3
2
1
0
0
50
100
200
NaCl (mM)

Figure S4. Example CO_2 response curve with defined variables. An example CO_2 response curve has been drawn to define the photosynthetic variables and parameters investigated. A represents the CO_2 assimilation rate, Ci represents the intercellular CO_2 levels, and A_{max} represents the maximum photosynthetic rate under saturating CO_2.

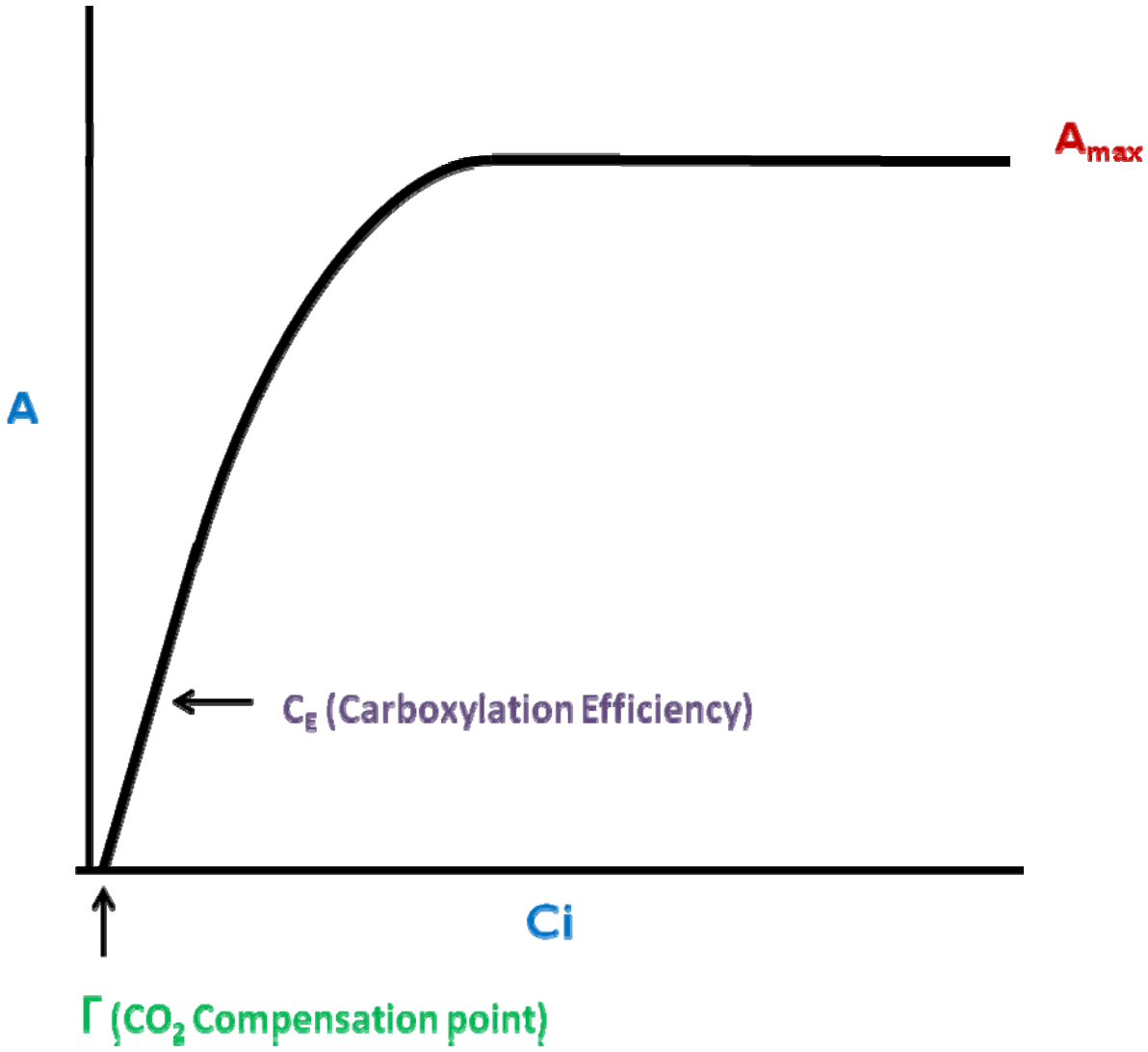

Figure S5. CO_2 response curves for *B. sinuspersici* under varying NaCl levels. CO_2 response curves for *B. sinuspersici* were performed on *B. sinuspersici* at each NaCl level. 0 mM NaCl ● , 50 mM NaCl ▽ , 100 mM NaCl ■ , 200 mM NaCl ◇ , and 400 mM NaCl ▲ . The photosynthetic rates were expressed in A) µmol CO_2 µg protein^{-1}hr^{-1}, and B) µmol CO_2 µg chlorophyll^{-1} min^{-1} basis. A represents CO_2 assimilation, Ci represents the intercellularCO_2 level. N = 2, 400 mM N = 1

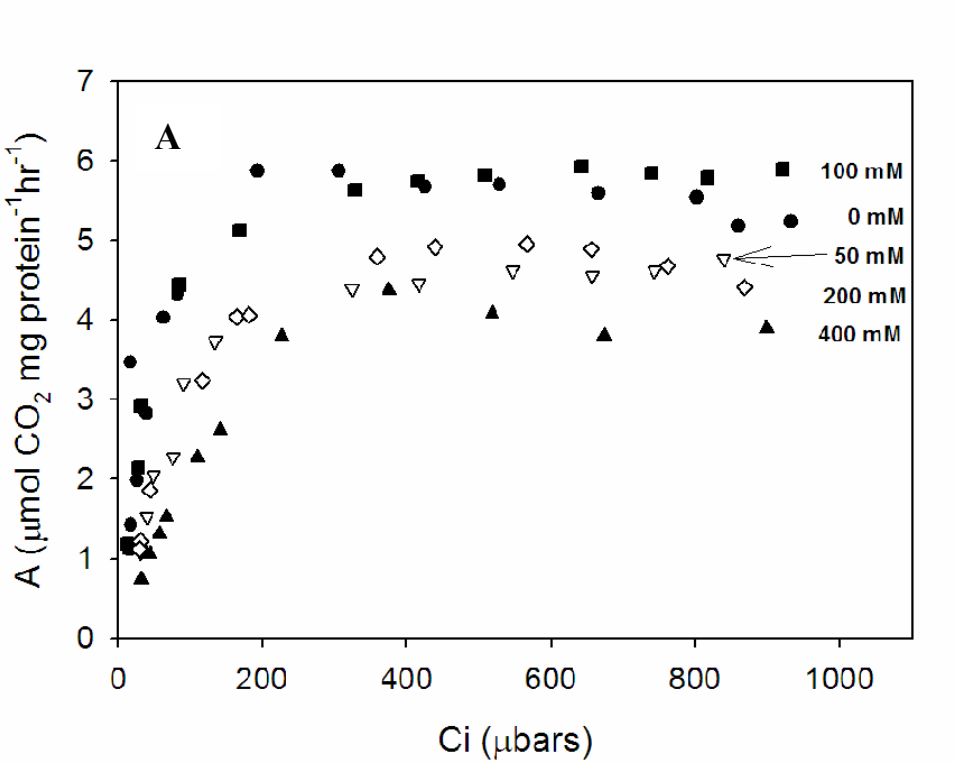
A
A (μmol CO2 mg protein-1hr-1)
Ci (μbars)
100 mM
0 mM
50 mM
200 mM
400 mM
0
1
2
3
4
5
6
7
0
200
400
600
800
1000

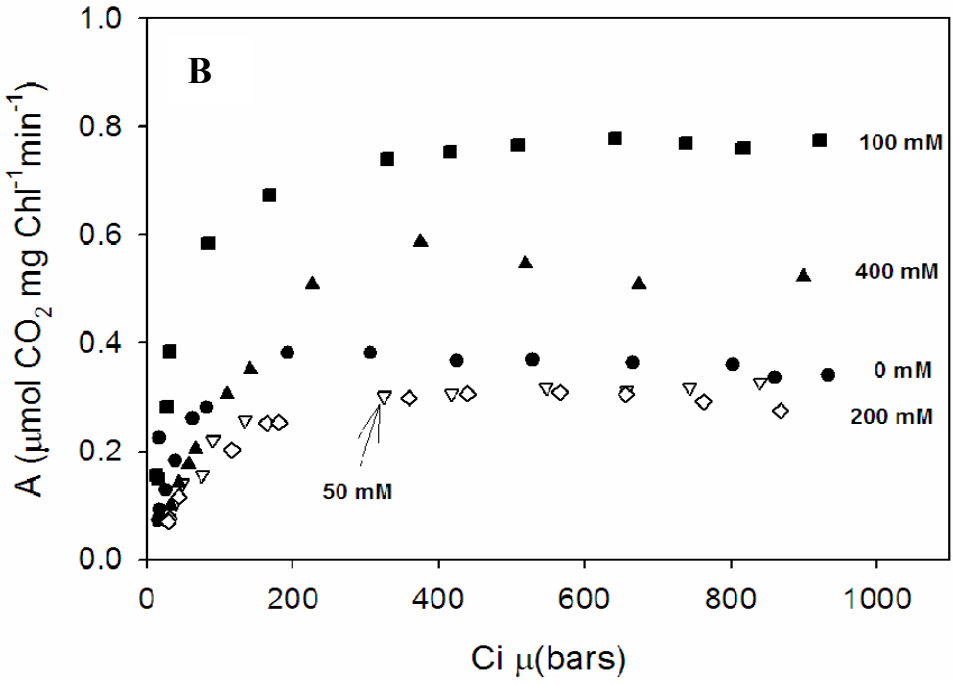
B
A (μmol CO2 mg Chl-1min-1)
Ci μ(bars)
100 mM
400 mM
0 mM
200 mM
50 mM
0.0
0.2
0.4
0.6
0.8
1.0
0
200
400
600
800
1000

Figure S6. Western blot at different NaCl levels in *B. sinuspersici*: Ponceau S stain. The fractionated proteins from *B. sinuspersici* are shown in the gel below. The molecular weights are shown beside the protein ladder. Samples were loaded onto the gel with the same amount of total protein. Two different amounts of protein were loaded to prevent over staining of high abundance proteins.

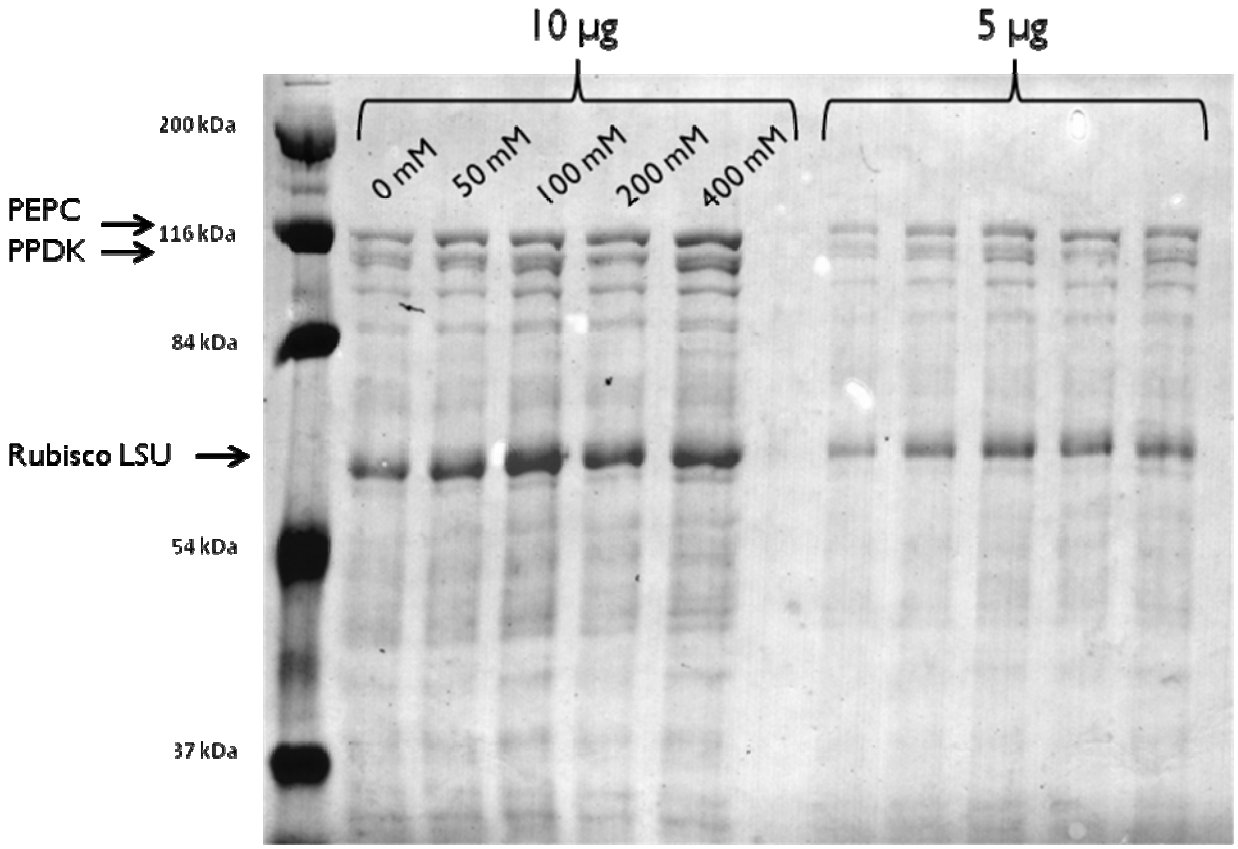

APPENDIX

SALINITY TOLERANCE IN THE KRANZ-TYPE C_4 SPECIES *SUAEDA ELTONICA* (CHENOPODIACEAE)

Introduction

Suaeda eltonica is a Kranz-type C_4 species in the Chenopodiaceae. It is in the subfamily Suaedoideae, which also contains the single-cell C_4 species *Bienertia sinuspersici* (Kapralov *et al*., 2006). *S. eltonica* is an endemic species around Lake Elton, a highly saline lake near the Russian border with Kazakhstan (Komarov, 1936). *S. eltonica* has adapted to living in highly saline soils, which has given it some level of salinity tolerance.

As mentioned in Chapter 2, Kranz-type C_4 photosynthesis requires spatial separation of the fixation of atmospheric CO_2 and the carboxylation of CO_2 by Rubisco in the mesophyll and bundle sheath cells, respectively. In single-cell C_4 photosynthesis, the same spatial separation is achieved, but through dimorphic chloroplasts, as opposed to a dual-cell system. With its known halophytic properties and phylogenetic relationship with *B. sinuspersici*, *S. eltonica* was chosen as the model Kranz-type species to examine salinity tolerance.

Research aim.

The aim of this experiment was to examine salinity tolerance in *S. eltonica* compared to the single-cell C_4 *B. sinuspersici*. This will allow comparisons in how salinity affects the mode of photosynthesis and in what capacity, between a single-cell versus Kranz type C_4.

The overall growth rate and morphology was measured. Gas exchange measurements were performed to assess maximum photosynthetic rates, compensation point, carboxylation

efficiency, and photosynthetic water use efficiency. Total protein and chlorophyll content were measured and the enzyme content of four photosynthetic enzymes in C_4 photosynthesis was determined from western blot analysis. All of these measurements were made on plants grown in hydroponics without NaCl versus with 200 mM NaCl.

Materials and Methods

Plant Material.

Suaeda eltonica was propagated from cuttings grown in 2MS Media. This consisted of 8.6 g/L complete MS salt (Plant Media),10 ml/L 100X MS vitamin stock, 20 g/L sucrose, 1.95 g/L MES buffer (10 mM MES free acid), 10 mM NaCl, pH 5.8, and 0.4 % gelrite. Once roots were formed, the cuttings were placed into the hydroponics system. Cuttings were placed in modified sterile plastic test tubes (50 ml) (#227261, Cell Star, Greiner Bio-One North America Inc., Monroe, NC, USA) which had the top half removed and three 1-inch long slits, 1mm wide, cut in the narrow bottom of the tube. The tubes (with rooted cuttings) were placed in 3 liter plastic containers (GladWare, Glad Products Co., Oakland, CA, USA) that were spray painted black and covered with aluminum foil to prevent algal growth. Each 3 liter container held 5 tubes. In addition, the containers were fitted with an air hose and aquarium bubbler (MillionAire MA300, Commodity Axis, Inc., Camarillo, CA, USA) to oxygenate the water. The hydroponics solution used was a modified 1/4X Hoagland's solution, as described for growth of *Arabidopsis* (Toqcuin *et al*., 2003). Plants were grown in a growth chamber (model GC-16l Econair Ecological Chambers Inc., Wiinipeg, Canada) under a maximum photosynthetic flux density of 500 µmole quanta m^{-2} s^{-1} (PPFD) during a 14/10 hr, 25/18 °C, day/night cycle. Atmospheric

CO_2 was used and the relative humidity was 40%. The lights in the chamber were programmed to come on and off in a stepwise increase and decrease over a 3 hour period at the beginning and the end of the photoperiod, respectively.

Gas exchange.

Rates of photosynthesis under varying ambient CO_2 concentrations were measured using a LI-6400 portable photosynthesis system from LI-COR Biosciences (Lincoln, NE, USA). Mature leaves were removed from the plant and the leaf area was measured. Detached leaves were placed in the 6400-02B LED Light Source chamber (maximum leaf area 6 cm^2). A modified leaf chamber cuvette was used; detached leaves were placed on a mesh screen that was glued to the cuvette gasket with silicon epoxy. A slit was made in the center of the mesh screen to allow for the thermocouple to have contact with the detached leaves. Once in the chamber, the detached leaves were allowed to acclimate under 1000 PPFD, a leaf temperature of 25 °C, and 353 µbars CO_2 for 20 min until steady state photosynthesis was achieved. Preliminary tests showed that photosynthesis of the succulent detached leaves was stable for approximately 1 hour. After this acclimation period, CO_2 response measurements were made in decreasing intervals from 353 µbars to 46 µbars and then increasing intervals to 1578 µbars atmospheric CO_2. Rates of photosynthesis were measured on a leaf area, µg chlorophyll, mg of soluble protein and mg dry weight basis.

From these response curves, the CO_2 compensation point (Γ), maximum carboxylation efficiency from the initial slope (C_E), and A_{max} values (level of CO_2 needed for saturating photosynthesis) was determined. Additionally, the intercellular CO_2 concentration (Ci) was

calculated. After the CO_2 response curve was completed, the detached leaves were removed and partitioned for $\delta^{13}C$, chlorophyll and western blot analysis. At least 2 leaves were partitioned for $\delta^{13}C$ analysis. These leaves were put a 55 °C oven and dried for 24 hours. The remaining leaves were placed whole into liquid nitrogen and stored in microfuge tubes at -80 °C for chlorophyll and western blot analysis.

Chlorophyll and soluble protein determination.

Total chlorophyll and soluble protein were determined from crude extracts of material used in gas exchange analyzes that was frozen in liquid nitrogen and stored at -80 °C. Leaf material was homogenized with a mortar and pestle in liquid nitrogen and then equally aliquoted into separate microfuge tubes for chlorophyll and protein extraction. For chlorophyll extraction, 1 ml of 80% (v/v) acetone was added. Material was kept in the dark to prevent chlorophyll degradation. Leaf material was incubated for 3 days in 80% (v/v) acetone, with a removal and renewal of the acetone each day following centrifugation at 16,000 g for 5 minutes. The removed acetone was stored at room temperature in the dark until the chlorophyll content was determined. After the incubation period the supernatants of all three acetone extractions were combined and an aliquot was used for the total chlorophyll measurement. Measurements were made at 663.2 and 646.8 nm in a Shimadzu UV-240 Spectrophotometer (Shimadzu Scientific Instruments, Columbia, MD, USA) using constants from Porra *et al*., (1989).

Total protein was measured from the remaining frozen leaf material previously aliquoted. The pellet was resuspended in 200 µl of the total protein extraction buffer (TBEB) (2% SDS, 10% glycerol, 5% 2-mercaptoethanol, 0.0625M Tris-HCl, pH = 6.8) and immediately boiled for

5 minutes. The extract was then centrifuged for 5 minutes at 16,000 g, the supernatant removed, placed in a new microfuge tube and assayed for total protein using the RD DC Bio-Rad Protein Assay (#500-0121, Bio-Rad Laboratories, Hercules, CA, USA) according to the manufacturer's protocol. A standard curve of bovine serum albumin (BSA) (F. Hoffman La-Roche Ltd., Basel, Switzerland) was used for calibration.

For western blots, supernatant fractions from the crude extracts from different salt treatments were adjusted to the same protein concentration, and 10 and 5 μg of protein were loaded per lane. The samples were loaded onto a 10% polyacrylamide-SDS gel and separated through gel electrophoresis (10 V/cm for 1 h in a Bio-Rad Mini-PROTEAN Tetra Electrophoresis System (Bio-Rad Laboratories, Hercules, CA, USA)). After electrophoresis, the gel was transblotted onto a nitrocellulose membrane (Bio-Rad Laboratories, Hercules, CA, USA) that was presoaked in 1X transblotting buffer (20 mM Tris base, 150 mM Glycine, 0.025% SDS, and 20 % methanol (v/v)) for 5 min. The membranes were transblotted for 1 h (400 mA constant current) at 4 °C. Proteins were initially visualized by reversible staining with 0.1% Ponceau S in 5% acetic acid (v/v) for 2 min, followed by 3-4, 5 min washes with 5% acetic acid to removed background staining. The membrane was then rinsed 3 times with distilled water and blocked with blocking buffer (3% skim dry milk in Tris-buffered Saline buffer (TBST) (100 mM Tris-HCl pH 7.5, 150 mM NaCl, 0.3% Tween-20 detergent) for 30 min.

The primary antibody (in blocking buffer) was applied to the membrane which was placed on an orbital shaker to incubate at 4 °C overnight. The primary antibody was removed and the membrane was rinsed with TBST three times, 10 min each rinse. Bound primary antibodies were located using secondary, alkaline-phosphatase conjugated goat anti-rabbit IgG. The secondary antibody (in blocking buffer) was applied to the membrane and incubated for 2 h

at room temperature on an orbital shaker. The secondary antibody was removed and the membrane was again rinsed with TBST buffer three times, 10 min each rinse. The membrane was then incubated in activation buffer (100 mM Tris-HCl, pH 9.5, 100 mM NaCl and 10 mM MgCl) for 5 min. Chromogenic detection was then performed by the addition of the color substrate solution (50 µl 5-bromo-4-chloro-3-indolyl phosphate dipotassium salt (BCIP) (35 mg/ml) per 10 ml activation buffer, and 50 µl nitroblue tetrazolium salt (NBT) (70 mg/ml) per 10 ml activation buffer). Color development was stopped with washes of distilled water.

The antibodies used and their respective dilutions are as follows: anti-*Amaranthus viridis* PEPC (1:100,000; Colombo *et al*., 1998), serum against the α-subunit of NAD-ME from *Amaranthus hypochondriacus* (1:2,000; Long *et al*., 1994), anti-*Zea mays* PPDK (1:50,000; courtesy of Dr. T. Sugiyama), anti-spinach (*Spinacia oleracea*) Rubisco LSU (1:10,000; courtesy of Dr. B. McFadden).

The resulting stained membranes were scanned. The intensity of the bands was semi quantified using ImageJ 1.36b (Rasband 1997-2007)) image analysis software, and expressed relative to levels in the plants grown without NaCl.

Delta ^{13}C Analysis.

Leaf samples used were cut from the plants after 6-8 weeks of growth in hydroponics, or used from gas exchange analysis. Leaves were placed in microfuge tubes and dried at 55 °C for 24 h. Samples were then homogenized to a fine powder using Crescent Wig-L-Bug (Model 3110B, Dentsply Rinn, Elgin, IL, USA). Carbon isotope fractionation values were determined on dried leaves and stems, using a standard procedure relative to PDB (Pee Dee Belemnite) limestone as the carbon isotope standard (Bender *et al*., 1973).

Data analysis.

Data points from the CO_2 response curves were fitted with a singular rectangular hyperbola equation (Eq, (1) using Sigma Plot (Systat Software, Inc., San Jose, CA, USA). From the fitted curve equation, the Γ value was determined by finding the x value when y = 0. The first derivative of the fitted curve equation was used to calculate the C_E value at x = 0. The coefficients of *a* and *b* were given through the nonlinear regression report given by Sigma Plot.

$$Y = Y_0 + \frac{ax}{(b+x)} \qquad \text{Eq. (1)}$$

The assimilation rates given by the LI-6400 were modified to adjust for low diffusion rates at low intercellular CO_2 (Ci) values (Eq. 2) (LI-COR Biosciences, Version 5, Book 1).

$$A = \frac{F(C_r - C_s)}{100S} - C_s E + \frac{k}{100S}(C_a - C_s) \qquad \text{Eq. (2)}$$

In Eq. 2, A represents the corrected CO_2 assimilation rate (μmol CO_2 m^{-2} s^{-1}), F is the molar flow rate of air entering the leaf chamber (μmol s^{-1}), C_r is the mole fraction of CO_2 in the reference IRGA (μmol CO_2 mol^{-1} air), C_s is the mole fraction of CO_2 in the sample IRGA (μmol CO_2 mol^{-1} air), C_sE is the rate of transpiration (mol H_2O $m^{-2}s^{-1}$), *k* is the diffusion coefficient (0.46), S is the total leaf area in the cuvette chamber (cm^2), and C_a is reference CO_2 level used (380 μmoles/mol).

Statistical analysis.

For the treatment without NaCl and 200 mM NaCl plants were grown in two hydroponic boxes. Each box contained 3-5 individual plants. Replicate measurements were made within

each box by pooling leaves randomly sampled from individual plants. Two independent replicates were measured for each experiment (unless otherwise noted). For gas exchange analysis, 5-10 randomly samples leaves pooled from individual plants were used for each measurement. At least 3 measurements were taken per box. These leaves were subsequently used for protein and chlorophyll content, and western blot analysis. For the leaf fresh and dry weight analysis, at least 10 measurements were made per box, pooling at least 3 leaves per plant. For the carbon isotope discrimination analysis, at least 12 measurements were made per box; measurements pooled at least 4 leaves randomly sampled from individual plants. The standard error of the mean was determined for each experiment. N = 2.

Preliminary Results

Results represent measurements based on only two replicates at two different NaCl concentrations. Preliminary results show *S. eltonica* has a similar growth response to 200 mM NaCl versus without NaCl as *B. sinuspersici* (Ch. 2), although the magnitude of the response was lower. The overall shoot production seemed to increase with increasing NaCl (Fig. 1). The overall shoot and leaf coloration had a darker green color in the 200 mM treatment than treatment without NaCl (Fig. 1, 3), which is opposite to the trend seen in *B. sinuspersici*. The root biomass also seemed to increase with increasing NaCl (Fig. 2). An apparent increase in the individual incident leaf area from 0.25 cm^2 to 0.3 cm^2 was seen from 0 to 200 mM NaCl (Fig. 4, Table 1).

On a per leaf area basis, the fresh weight seemed to increase from 47.7 ± 18.4 mg/cm^2 to 50.9 ± 2.9 mg/cm^2 with increasing NaCl (Table 1). The dry weight showed the reverse trend

(Fig. 5). The dry weight for the treatment without NaCl was of 13.0 ± 1.2 mg/cm^2, while it was 8.9 ± 0.1 mg/cm^2 for the 200 mM NaCl treated plant (Table 1). On a per leaf basis, the fresh weight seemed to increase from 10.4 ± 1.0 mg to 15.5 ± 7.5 mg (Fig. 6), while the dry weight seemed to remain relatively the same from treatment without NaCl to 200 mM NaCl (2.4 ± 0.2 to 2.1 ± 0.9 mg per leaf, respectively (Table 2).

A tendency toward an increase in the root and shoot fresh weight and dry weight were seen with salinity treatment (Fig. 7). The shoot fresh weight seemed to increase from 22.8 ± 6.7 g to 37.6 ± 2.2 g, while the dry weight seemed to increase from 4.7 ± 0.3 g to 7.7 ± 1.0 g with increasing NaCl (Table 3). The root fresh weight seemed to increase from 14.3 ± 1.7 g to 17.9 ± 1.4 g, while the root dry weight seemed to increase slightly from 1.2 ± 0.02 g to 1.5 ± 0.2 g with increasing NaCl (Table 3). The overall shoot DW:FW seemed higher than the root DW:FW, but the shoot and root DW:FW did not seem to change with increasing NaCl (Fig. 8).

The gas exchange measurements showed a tendency toward the maximum photosynthetic rates under the treatment without NaCl on a per leaf area basis (Fig. 9). A_{max} for the treatment without NaCl was 7.5 ± 3.0 μmol CO_2 $m^{-2}s^{-1}$, while A_{max} for 200 mM was 5.4 ± 2.4 μmol CO_2 $m^{-2}s^{-1}$ (Table 4). An apparent increase in the carboxylation efficiency from the treatment without NaCl to 200 mM NaCl was also seen (Fig.10). C_E seemed to increase from 0.03 ± 0.02 μmol CO_2 $m^{-2}s^{-}1$ per μbar to 0.06 ± 0.03 μmol CO_2 $m^{-2}s^{-}1$ per μbar with increasing NaCl (Table 4). Also, the Γ values seemed to increase with increasing NaCl (Fig. 10). Γ seemed to increase from 3.41 ± 1.8 μbars to 8.4 ± 0.9 μbars from the treatment without NaCl to the 200 mM NaCl treatment. In addition, the PWUE seemed to remain relatively constant across the two NaCl treatments (Fig. 10), only changing from 5.6 ± 0.8 μmol CO_2 fixed per mmol H_2O lost to 5.2 ± 2.7 μmol CO_2 fixed per mmol H_2O lost with increasing NaCl (Table 4).

Total protein content seemed to increase with increasing NaCl, but there seemed to be little change in the total chlorophyll content with increasing NaCl on a fresh weight and dry weight basis (Fig. 11). Per fresh weight, the chlorophyll content seemed to increase slightly from 0.3 ± 0.1 μg to 0.7 ± 0.6 μg with increasing NaCl, while the total protein content seemed to increase from 0.63 ± 0.03 μg to 1.42 ± 0.3 μg with increasing NaCl (Table 5). On a dry weight basis, the chlorophyll content seemed to decrease slightly, from 1.5 ± 0.7 μg to 0.95 ± 0.03 μg with increasing NaCl, while the total protein content seemed to increase from 1.9 ± 0.8 μg to 6.4 ± 1.9 μg (Table 5). On a leaf area basis, there seemed to be a small increase in the total protein content (Fig. 5) from 325.4 ± 39.4 μg to 362.2 ± 71.2 μg with increasing NaCl, and a decrease in the total chlorophyll content (Fig. 5) from 97.2 ± 13.9 μg to 63.8 ± 18.2 μg with increasing NaCl (Table 1). On a per leaf basis, the total protein seemed to increase with increasing NaCl (Fig. 6) from 8.9 ± 9.3 μg to 15.5 ± 0.1 μg (Table 2), while the total chlorophyll content seemed to remain relatively constant with increasing NaCl (Fig. 6) (2.7 ± 0.7 μg and 2.5 ± 1.4 μg for the treatment without NaCl and the 200 mM treatment, respectively) (Table 2).

Western blot data revealed a tendency towards an increase in all the photosynthetic enzymes examined (PEPC, PPDK, NAD-ME and Rubisco) on a protein and leaf area basis under salinity treatment (Fig. 12, 13). On a protein basis, the largest apparent increase was seen in PPDK and NAD-ME, with only a slight apparent increase in Rubisco between the treatment without NaCl and the 200 mM NaCl treatment (Fig. 14). PPDK and NAD-ME seemed to increase 110 and 89%, respectively, with increasing NaCl. Rubisco seemed to only increase by 25% with increasing NaCl. PEPC seemed to have a small decrease with increasing NaCl, (16%).

On a per leaf area basis, the largest apparent change was seen in PPDK, Rubsico and NAD-ME, with only a slight apparent increase in PEPC between the treatment without NaCl and

the 200 mM NaCl treatment (Fig. 14). PPDK seemed to increase from the treatment without NaCl to 200 mM NaCl by approximately 258 %, while Rubisco and NAD-ME seemed to increase by approximately 93 % and 110%, respectively. PEPC seemed to have the smallest increased, with only a 26 % increase from the treatment without NaCl to the 200 mM NaCl treatment.

The $\delta^{13}C$ analysis showed a a trend towards a small increase in isotope discrimination in the 200 mM NaCl treated plants compared to the plants treated without NaCl (Fig. 15), with the more negative $\delta^{13}C$ value in the 200 mM NaCl treatment (-15.3 ± 0.7 ‰) than the treatment without NaCl (-13.8 ± 0.1 ‰) (Table 6).

Discussion

The preliminary data for *S. eltonica* shows a similar succulence response to increasing NaCl as *B. sinuspersici*. The leaf size and overall fresh weight biomass seemed to increase, as well as the shoot dry weight seemed to increase. This indicates a possible increase in leaf number with increasing NaCl, as well as a positive biomass accumulation with increasing NaCl.

Gas exchange data reveals the maximum photosynthetic rates on a leaf area basis seemed to decrease with increasing NaCl. The CO_2 compensation point and carboxylation efficiency however, seemed to increase with increasing NaCl. Interestingly, there seemed to be a small increase in PEPC in *S. eltonica* with salt treatment on a leaf area basis, with a corresponding trend for an increase in C_E, which is the inverse of what is seen in *B. sinuspersici*. *S. eltonica* seems to increase its C_E under saline conditions

The $\delta^{13}C$ values show trend towards slightly more discrimination at the higher NaCl level (200 mM), indicated by its more negative isotope value, but this value is still within the normal range for C_4 plants. Both *B. sinuspersici* and *S. eltonica* had isotope values within the range of C_4 species under varying levels of salinity treatment.

Preliminary Conclusions

The overall morphological response to salinity in *S. eltonica* is similar to *B. sinuspersici*. Preliminary data shows that succulence seems to be a main response to increasing salinity in these two species. While their maximum photosynthetic responses showed similar trends, *B. sinuspersici* seemed to have around a 1.5 fold higher maximum CO_2 assimilation rate at 200 mM NaCl than *S. eltonica.* The carboxylation efficiency values for *B. sinuspersici* seemed to be around 4 fold higher than *S. eltonica* at 200 mM NaCl. Western blot data shows similar trends for changes in PEPC levels on a per leaf area basis with salt treatment (approximately a 26 and 28% increase in *S. eltonica* and *B. sinuspersici*, respectively). *B. sinuspersici* showed a apparent decrease in Rubisco and NAD-ME with increasing NaCl, while *S. eltonica* seemed to have a large increase in Rubisco and NAD-ME.

Further investigation is needed to fully understand the photosynthetic response in both species. Preliminary results in *S. eltonica* need to be confirmed with further replicates and additional NaCl levels. Further experimentation is necessary to understand not only how *S. eltonica* responds to salinity stress, but whether this Kranz-type species has differences in tolerance to salinity compared to its single-cell C_4 counterpart, *B. sinuspersici.* Experimentation into the differential effects of salinity on the regulation of the C_4 photosynthetic enzymes in these

two photosynthetic types, and the nature of NaCl sequestration in these two systems should be done in the future.

References

Bender MM, Rouhani I, Vines HM and Black CC Jr (1973) 13C/12C ratio in Crassulacean acid metabolism. Plant Physiol. 52: 427-430.

Colombo SL, Andrea CS, Chollet R (1998) The interaction of shikimic acid and protein phosphorylation with PEP carboxylase from the C_4 dicot *Amaranthus viridis*. Phytochemistry 48: 55-59.

Kapralov MV, Akhani H, Voznesenskaya EV, Edwards G, Franceschi V, Roalson RH (2006) Phylogenetic relationships in the Salicornioideae/Suaedoideae/Salsoloideae s.l. (Chenopodiaceae) clade and a clarification of the phylogenetic position of *Bienertia* and *Alexandra* using multiple DNA sequence sets. Sys. Bot. 31: 5710585.

Komarov VL, Flora of the USSR (Flora SSSR) (1970) (Translated from Russian, 1936), Izdatel'stvo Akademii Nauk SSSR, Moscow, Leningrad, pp. 1–731.

Long JJ, Wang JL, and Berry JO (1994) Cloning and analysis of the C_4 NAD-dependent malic enzyme of amaranth mitochondria. Plant Physiol. 112: 473.482.

Porra RJ, Thompson WA, Kriedemann PE (1989) Determination of accurate extinction coefficients and simultaneous equations for assaying chlorophylls a and b extracted with four different solvents: verification of the concentration of chlorophyll standards by atomic absorption spectroscopy. Biochimica et Biophysica Acta 975: 384-394.

Toqcuin P, Corbesier L, Havelange A, Pieltain A, Kurtem E, Bernier G, and Périlleux C (2003) A novel high efficiency, low maintenance hydroponic system for synchronous growth and flowering of *Arabidopsis thaliana*. BMC Plant Biol. 3: 2-12.

Table 1. Protein, chlorophyll, fresh weight and dry weight on a per leaf area basis under varying NaCl levels in *S. eltonica*. The protein and chlorophyll were extracted and quantified on a per leaf area basis. The fresh weights were measured after removal from the plant and expressed on a per leaf area basis. The dry weights were measured after leaves were placed in a 55 °C oven for 24 hours, and expressed on a per leaf area basis. The mean values are in bold ± the standard error of the mean. N = 2

NaCl (mM)	Individual Indicdent Leaf Area (cm^2)	Total chlorophyll per leaf area ($\mu g/cm^2$)	Total protein per leaf area ($\mu g/cm^2$)	Fresh weight per leaf area (mg/cm^2)	Dry weight per leaf area (mg/cm^2)
0	**0.25** ± 0.1	**97.2** ± 13.9	**325.4** ± 39.4	**47.7** ± 18.4	**13.0** ± 1.2
200	**0.3** ± 0.1	**63.8** ± 18.2	**362.2** ± 71.2	**50.9** ± 2.9	**8.9** ± 0.1

Table 2. Protein, chlorophyll, fresh weight and dry weight on a per leaf basis under varying NaCl levels in *S. eltonica*. The protein and chlorophyll were extracted and quantified on a per leaf basis. The fresh weights were measured after removal from the plant and expressed on a per leaf basis. The dry weights were measured after leaves were placed in a 55 °C oven for 24 hours, and expressed on a per leaf basis. The mean values are in bold ± the standard error of the mean. N = 2

NaCl (mM)	Total chlorophyll per leaf (µg/leaf)	Total protein per leaf (µg/leaf)	Fresh weight per leaf (mg/leaf)	Dry weight per leaf (mg/leaf)
0	**2.7** ± 0.7	**8.9** ± 9.3	**10.4** ± 1.0	**2. 4**± 0.2
200	**2.5** ± 1.4	**15.5** ± 0.1	**15.5** ± 7.5	**2.1** ± 0.9

Table 3. Root fresh and dry weights, and shoot fresh and dry weights in *S. eltonica* under varying NaCl treatments. The root and shoot dry weights were measured in *S. eltonica* between 6-8 weeks of growth. Individual plants were removed from the hydroponics system and the root and shoots were separated. Dry weight measurements were taken after the roots and shoots were placed in a 55 °C oven for several days. The mean values are in bold ± the standard error of the mean. N = 2

	Root		**Shoot**	
NaCl (mM)	**0**	**200**	**0**	**200**
Fresh Weight (g)	**14.3** ± 1.7	**17.9** ± 1.4	**22.8** ± 6.7	**37.6** ± 2.2
Dry Weight (g)	**1.2** ± 0.02	**1.5** ± 0.2	**4.7** ± 0.3	**7.7** ± 1.0
DW:FW (%)	**8.4** ± 0.9	**8.4** ± 0.3	**22.1** ± 5.1	**20.5** ± 1.5

Table 4. Summary of photosynthetic components under varying NaCl levels in *S. eltonica*. Γ is the CO_2 compensation point. C_E is the carboxylation efficiency. A_{max} is the maximum photosynthetic rate under saturating CO_2. PWUE is the photosynthetic water use efficiency. Photosynthetic components were measured at 1000 PPFD and 25 °C. The mean values are in bold ± the standard error of the mean. N = 2

NaCl (mM)	**0**	**200**
Γ(µbar)	**3.41** ± 1.8	**8.4** ± 0.9
C_E(µmol CO_2 $m^{-2}s^{-1}$ per µbar) (Ci)	**0.03** ± 0.02	**0.06**± 0.03
C_E(µmol CO_2 $m^{-2}s^{-1}$ per µbar) (Ca)	**0.01** ± 0.01	**0.03** ± 0.01
A_{max} (µmol CO_2 $m^{-2}s^{-1}$)	**7.5** ± 3.0	**5.4** ± 2.4
PWUE (µmol CO_2 fixed per mmol H_2O lost)	**5.6** ± 0.8	**5.2** ± 2.7

Table 5. Chlorophyll and protein on a per fresh and dry weight basis in *S. eltonica* under varying NaCl levels. After extraction and quantification, the total chlorophyll and protein were expressed on a fresh and dry weight basis. The mean values are in bold ± the standard error of the mean. N = 2

NaCl (mM)	µg Protein Content mg fresh weight $^{-1}$	mg Protein Content mg dry weight $^{-1}$	µg Total Chlorophyll content mg fresh weight^{-1}	µg Total Chlorophyll content mg dry weight^{-1}
0	**0.63** ± 0.03	**1.9** ± 0.8	**0.3** ± 0.1	**1.5** ± 0.7
200	**1.42** ± 0.3	**6.4** ± 1.9	**0.7** ± 0.6	**0.95** ± 0.03

Table 6. $\delta^{13}C$ analysis for *S. eltonica* under varying NaCl levels. The carbon isotope discrimination was measured under each NaCl treatment in *S. eltonica*. The isotope discrimination is measured in parts per thousand. The mean values are in bold ± the standard error of the mean. N = 2

NaCl (mM)	$\delta^{13}C$
0	**-13.8** ± 0.1
200	**-15.3** ± 0.7

Figure 1. Shoots of *S. eltonica* grown in hydroponics under varying NaCl levels. Propagated cuttings *S. eltonica* were placed in hydroponics with varying NaCl concentrations (0, and 200 mM). Pictures were taken between 6-8 weeks of growth. Scale bar = 1 cm.

0 mM

200 mM

1 cm

Figure 2. Roots of *S. eltonica* grown in hydroponics under varying NaCl levels. Propagated cuttings of *S. eltonica* were placed in hydroponics with varying NaCl concentrations (0, and 200 mM). Pictures were taken between 6-8 weeks of growth. Scale bar = 1 cm.

0 mM

200 mM

1 cm

Figure 3. *S. eltonica* leaf images. Images of *S. eltonica* grown under different NaCl concentrations (0, and 200 mM). Pictures were taken between 6-8 weeks of growth. The scale bar = 1cm.

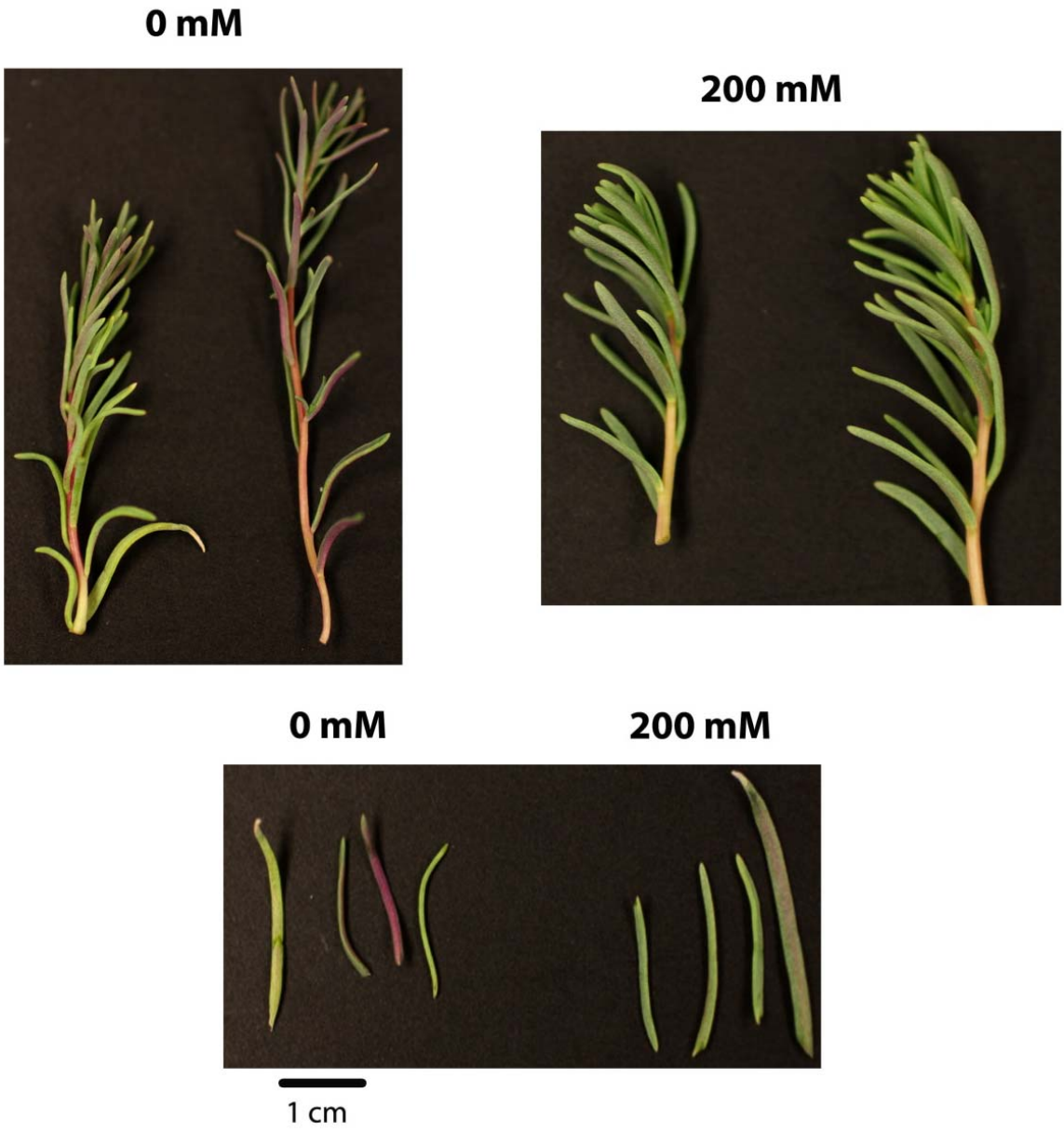
0 mM
200 mM
0 mM
200 mM
1 cm

Figure 4. Individual incident leaf area in *S. eltonica* under varying NaCl treatments. The individual incident leaf area was measured for leaves under each NaCl treatment. Error bars represent the standard error of the mean. N = 2

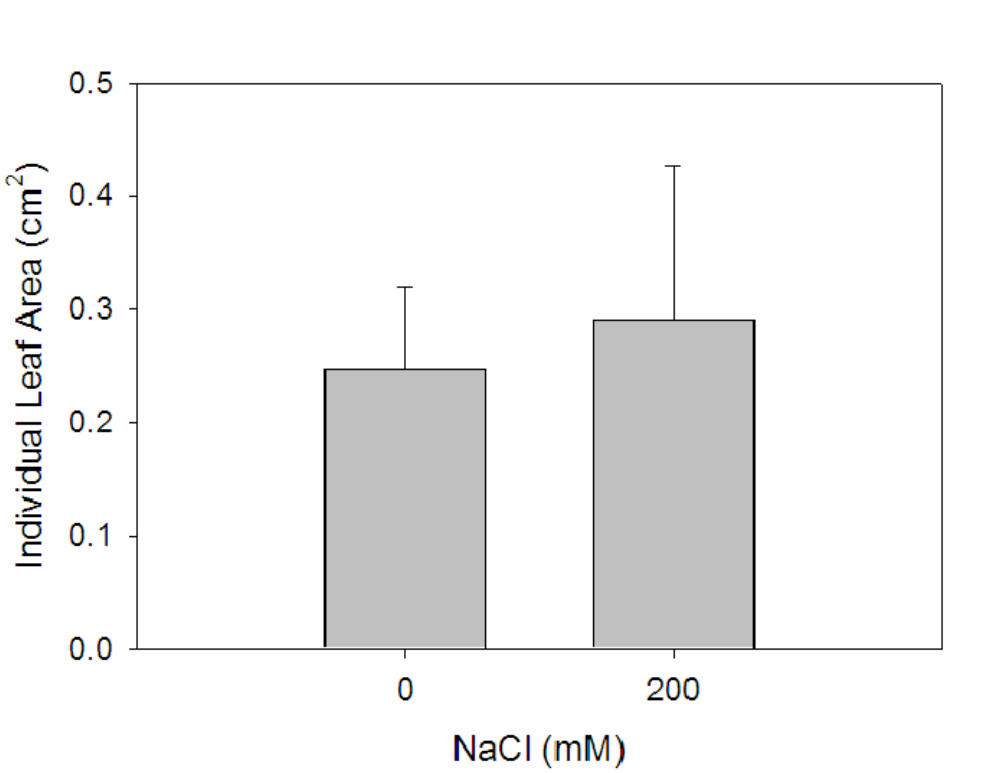

Figure 5. Effects of salt treatment on protein, chlorophyll, fresh weight and dry weight on a per leaf area basis. The protein and chlorophyll were extracted and quantified on a per leaf area basis. The fresh weights were measured after removal from the plant and expressed on a per leaf area basis. The dry weights were measured after leaves were placed in a 55 °C oven for 24 hours, and expressed on a per leaf area basis. A) fresh weight per leaf area (mg/cm^2), B) dry weight per leaf area (mg/cm^2), C) total protein per leaf area ($\mu g/cm^2$), D) total chlorophyll per leaf area ($\mu g/cm^2$). Error bars represent the standard error of the mean. N = 2

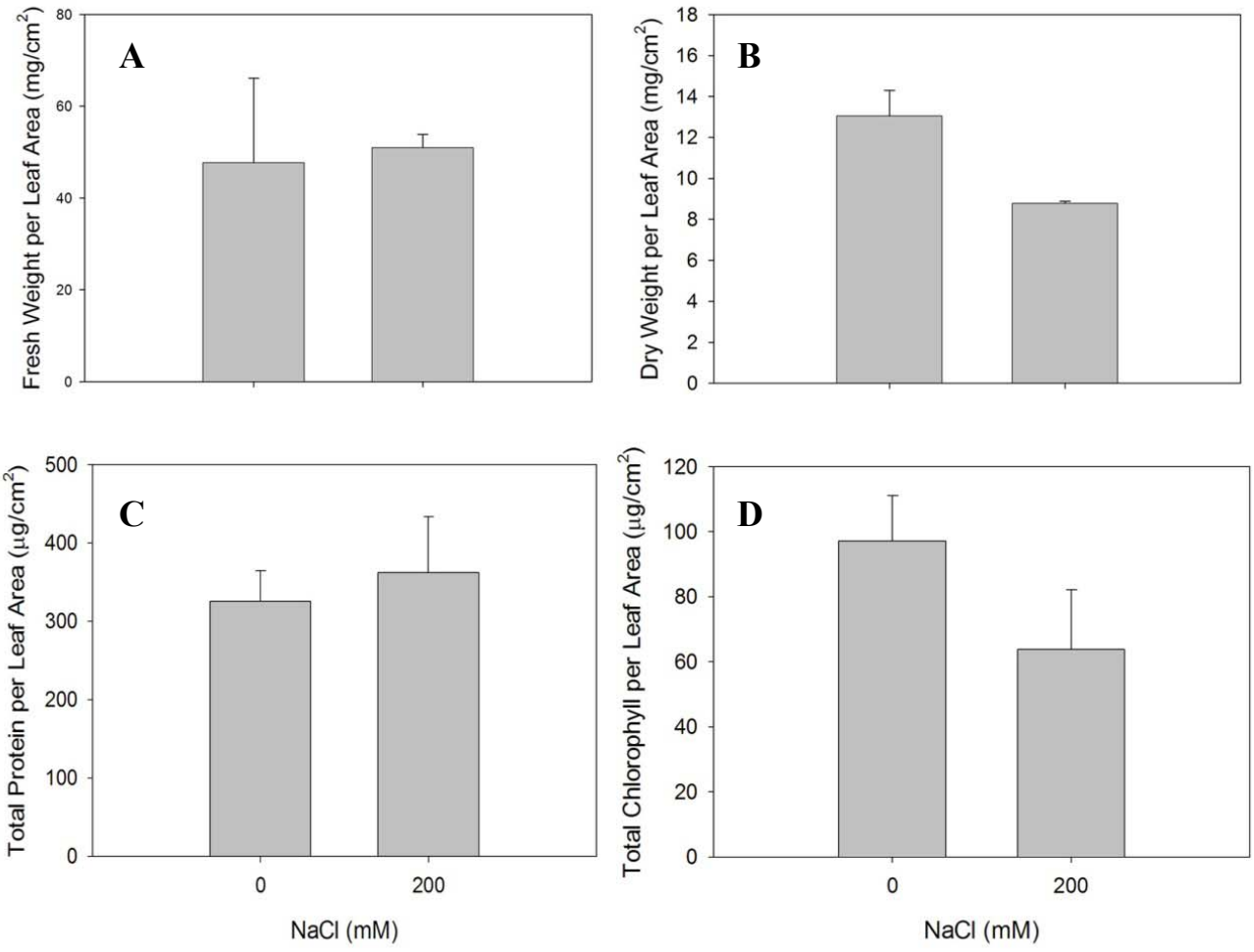
A
Fresh Weight per Leaf Area (mg/cm2)
0
20
40
60
80
B
Dry Weight per Leaf Area (mg/cm2)
0
2
4
6
8
10
12
14
16
18
C
Total Protein per Leaf Area (µg/cm2)
0
100
200
300
400
500
0
200
NaCl (mM)
D
Total Chlorophyll per Leaf Area (µg/cm2)
0
20
40
60
80
100
120
0
200
NaCl (mM)

Figure 6. The effects of salt treatment on protein, chlorophyll, fresh weight and dry weight on a per leaf basis. The protein and chlorophyll were extracted and quantified on a per leaf basis. The fresh weights were measured after removal from the plant and expressed on a per leaf basis. The dry weights were measured after leaves were placed in a 55 °C oven for 24 hours, and expressed on a per leaf basis. A) fresh weight per leaf (mg), B) dry weight per leaf (mg), C) total protein per leaf (μg), D) total chlorophyll per leaf (μg). Error bars represent the standard error of the mean. N = 2

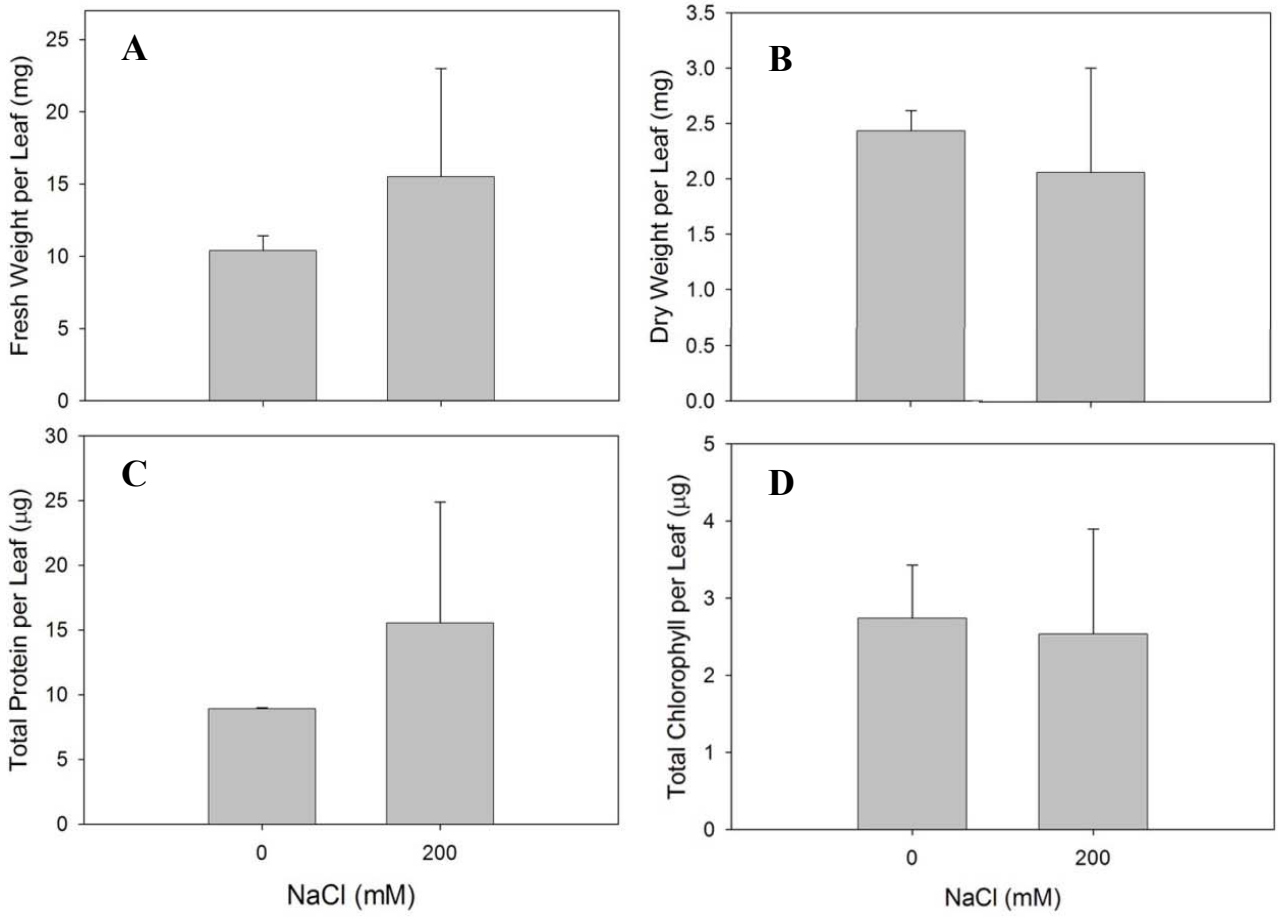
A
Fresh Weight per Leaf (mg)
25
20
15
10
5
0
B
Dry Weight per Leaf (mg)
3.5
3.0
2.5
2.0
1.5
1.0
0.5
0.0
C
Total Protein per Leaf (µg)
30
25
20
15
10
5
0
0
200
NaCl (mM)
D
Total Chlorophyll per Leaf (µg)
5
4
3
2
1
0
0
200
NaCl (mM)

Figure 7. Root fresh and dry weights, and shoot fresh and dry weights in *S. eltonica* under varying NaCl levels. The root and shoot dry weights were measured in *S. eltonica* between 6-8 weeks of growth. The entire plant was removed from the hydroponics system. The shoot and root sections were separated and the dry weights were measured. The dry weights were obtained after the shoots and roots were placed in a 55 °C oven for several days. A) root fresh weight (g), and B) shoot fresh weight (g), C) root dry weight (g), D) shoot dry weight (g), E) shoot:root fresh weight (%), F) shoot:root dry weight (%). Error bars represent the standard error of the mean. N = 2

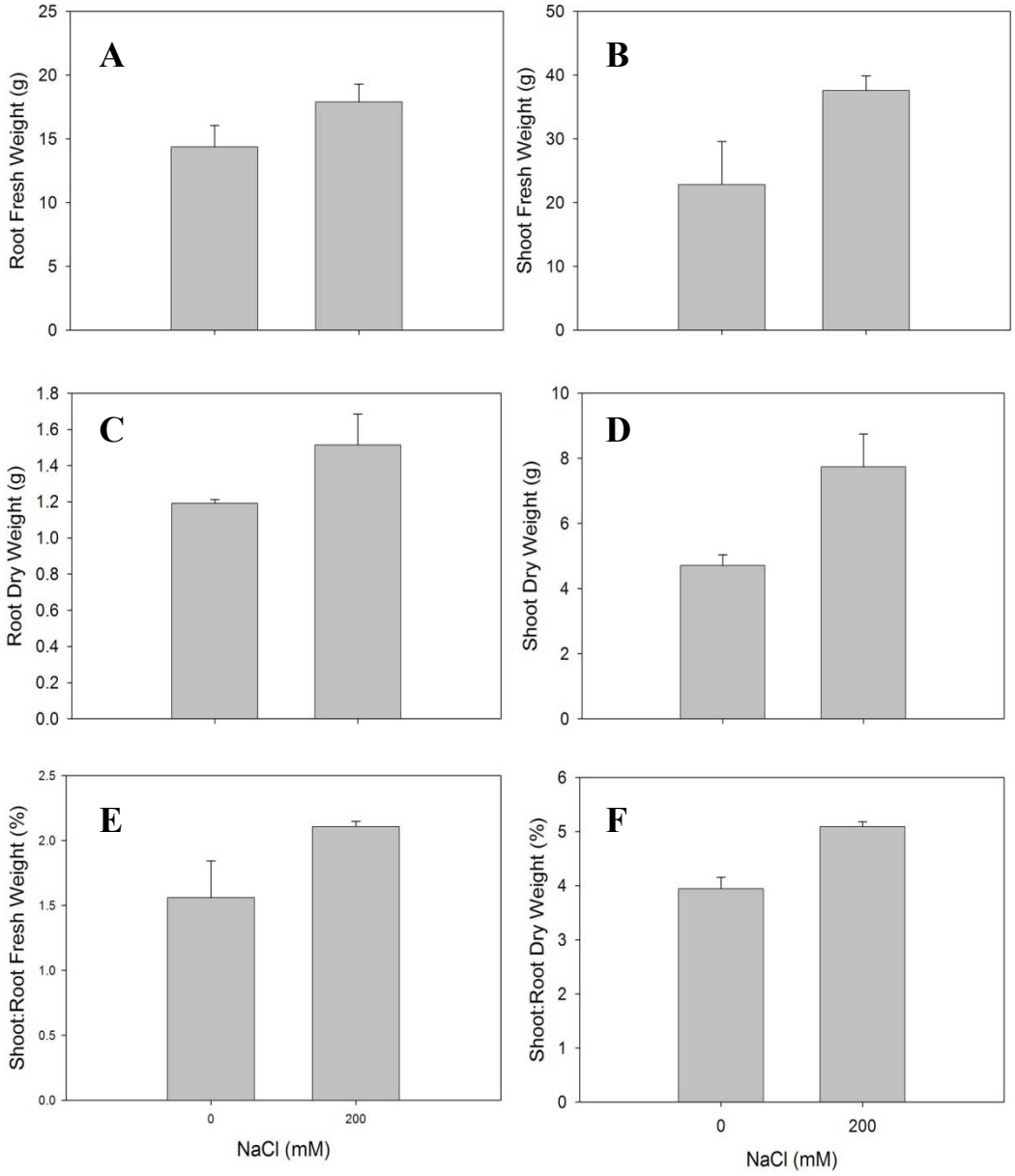
A
Root Fresh Weight (g)
25
20
15
10
5
0
B
Shoot Fresh Weight (g)
50
40
30
20
10
0
C
Root Dry Weight (g)
1.8
1.6
1.4
1.2
1.0
0.8
0.6
0.4
0.2
0.0
D
Shoot Dry Weight (g)
10
8
6
4
2
0
E
Shoot:Root Fresh Weight (%)
2.5
2.0
1.5
1.0
0.5
0.0
0
200
NaCl (mM)
F
Shoot:Root Dry Weight (%)
6
5
4
3
2
1
0
0
200
NaCl (mM)

Figure 8. Root DW:FW and shoot DW:FW in *S. eltonica* under varying NaCl levels. The root and shoot DW:FW was quantified after root and shoot dry weight and fresh weights were measured. The dry weight was obtained after the roots and shoots had been dried in a 55 ℃ oven for several days. Error bars represent the standard error of the mean. N = 2

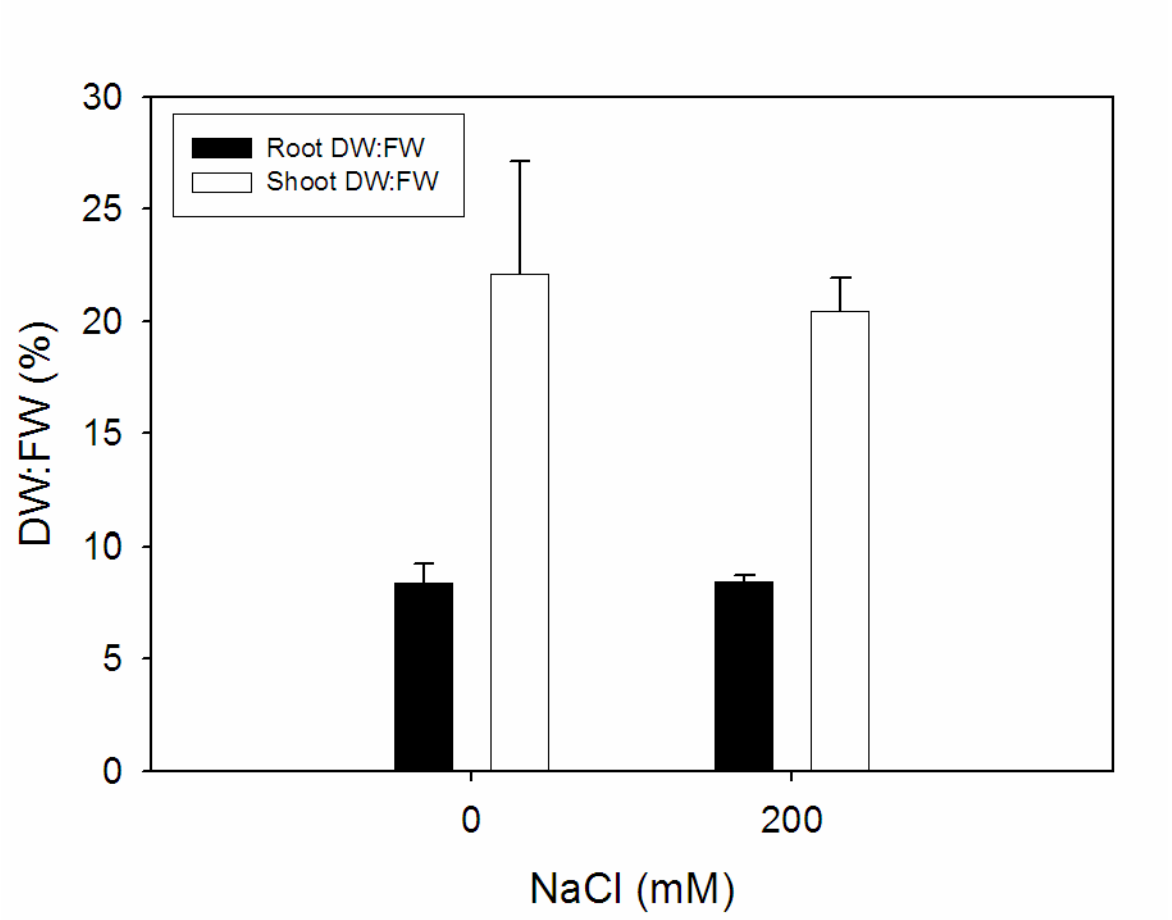

Figure 9. CO_2 response curve for *S. eltonica* under varying NaCl levels. The CO_2 response curve was performed for *S. eltonica* at each NaCl level. The photosynthetic rate is expressed in µmol CO_2 per leaf area. A represents CO_2 assimilation, Ci represents the intercellular CO_2 level. N = 2.

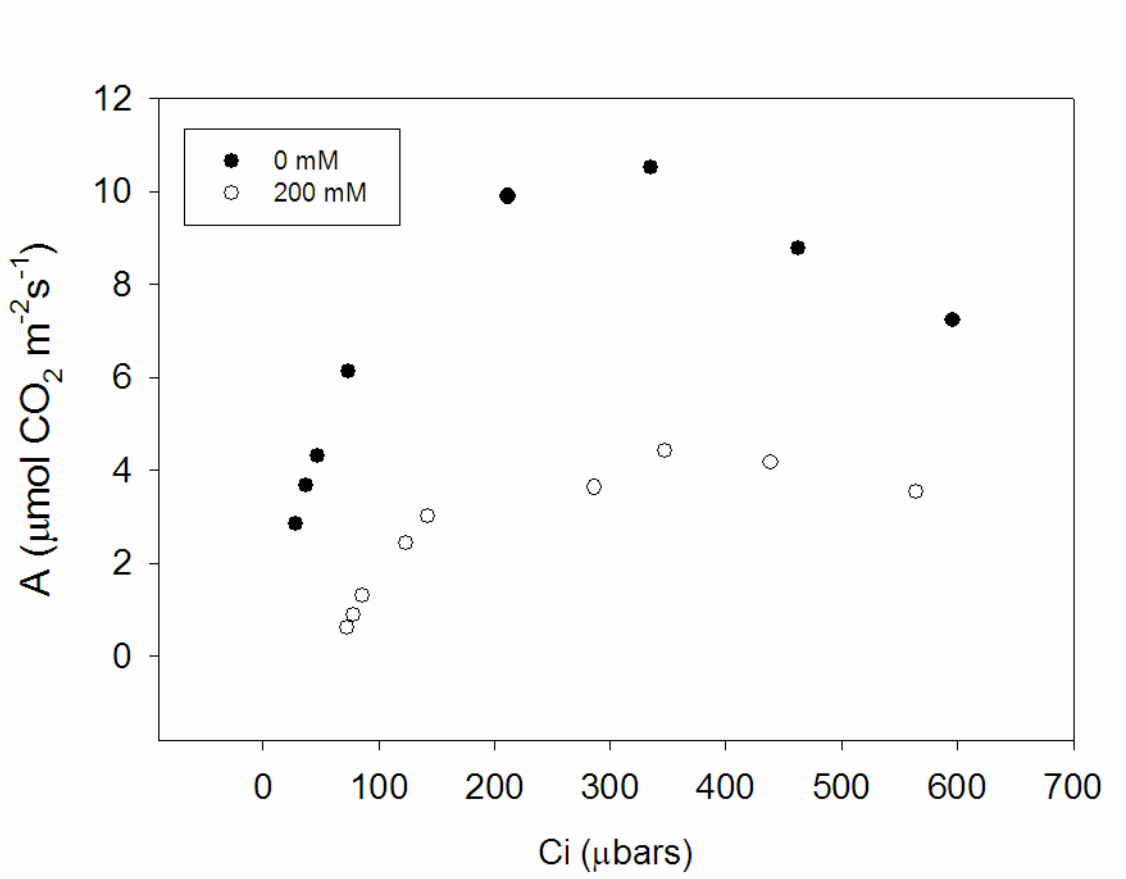

Figure 10. A_{max}, Γ, C_E, and PWUE measured under each NaCl treatment for *S. eltonica*. A_{max}, Γ , C_E, and PWUE were determined for *S. eltonica* from CO_2 response curves at each NaCl level. A) A_{max} (µmol CO_2 $m^{-2}s^{-1}$), B) Γ (µbar), C) C_E (µmol CO_2 $m^{-2}s^{-1}$/µbars), and D) PWUE (µmol CO_2 fixed mmol H_2O $lost^{-1}$). Error bars represent the standard error of the mean. N = 2.

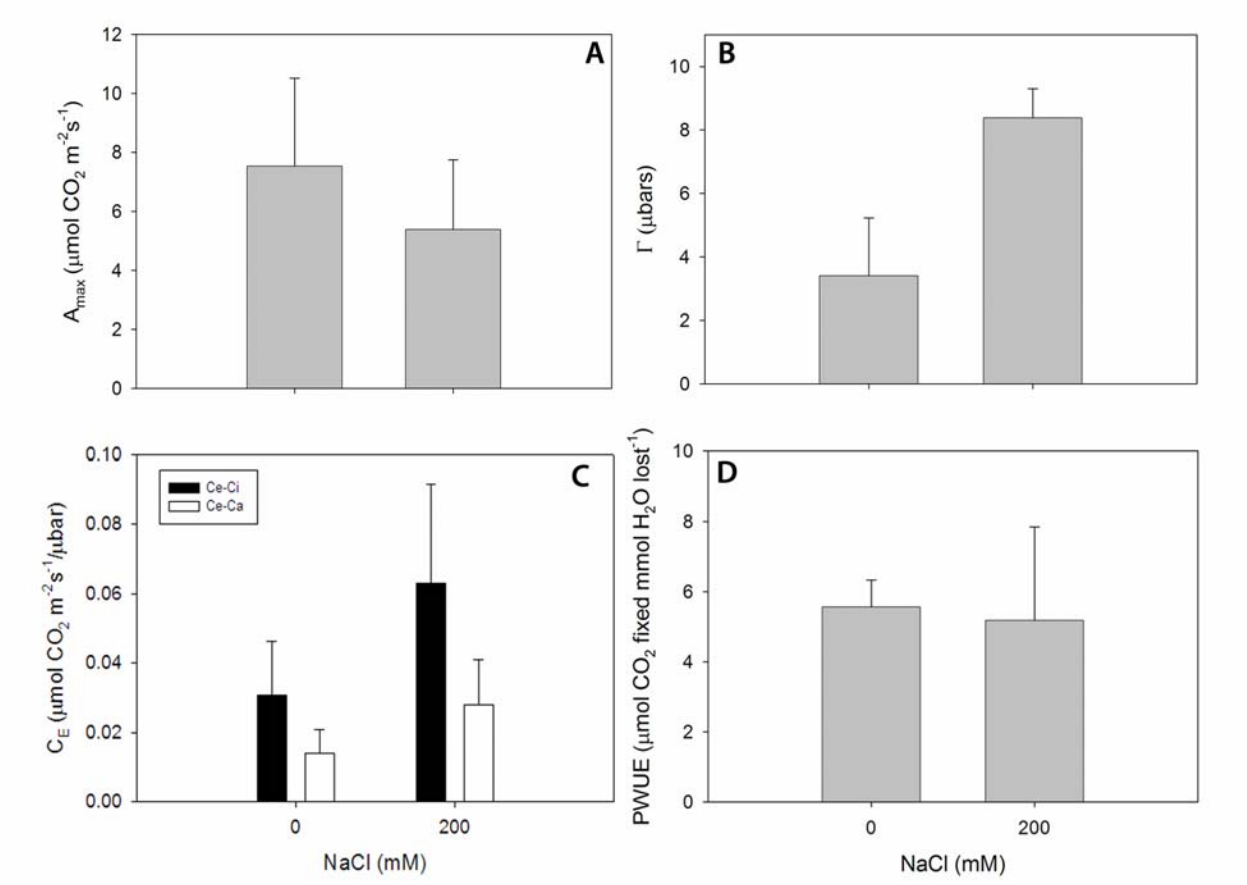
A
B
C
D
A_{max} (µmol CO_2 $m^{-2}s^{-1}$)
Γ (µbars)
C_E (µmol CO_2 $m^{-2}s^{-1}$/µbar)
PWUE (µmol CO_2 fixed mmol H_2O $lost^{-1}$)
Ce-Ci
Ce-Ca
NaCl (mM)
NaCl (mM)
0
200
0
200

Figure 11. The effect of salt on the total chlorophyll and protein on a fresh weight and dry weigh basis in *S. eltonica*. After extraction and quantification, the total chlorophyll and protein were expressed on a fresh and dry weight basis. A) total protein and chlorophyll per fresh weight (µg/mg), and B) total protein and chlorophyll per dry weight (µg/mg). The error bars represent the standard error of the mean. N = 2

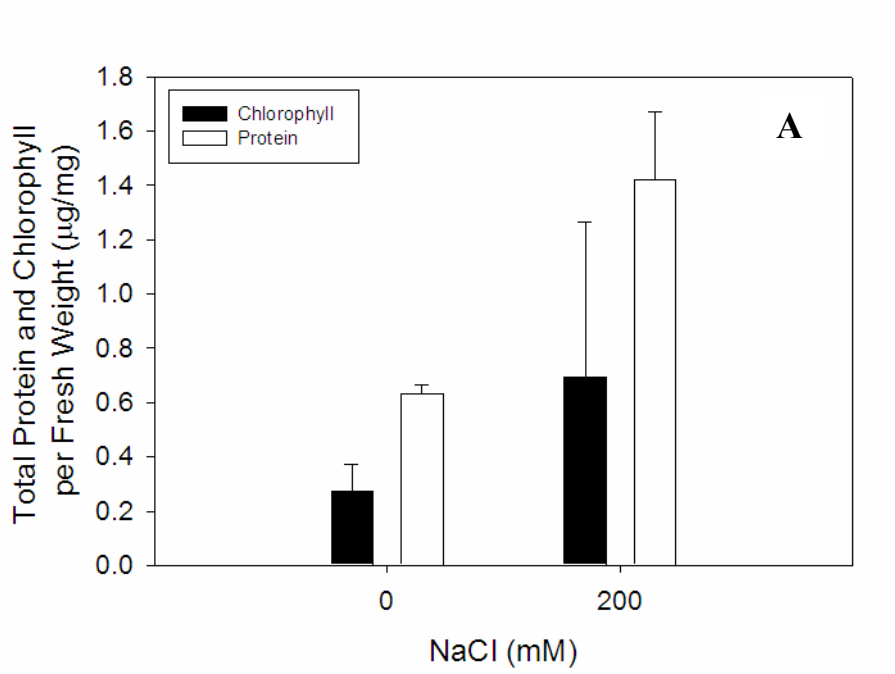
Chlorophyll
Protein
A
Total Protein and Chlorophyll per Fresh Weight (µg/mg)
1.8
1.6
1.4
1.2
1.0
0.8
0.6
0.4
0.2
0.0
0
200
NaCl (mM)

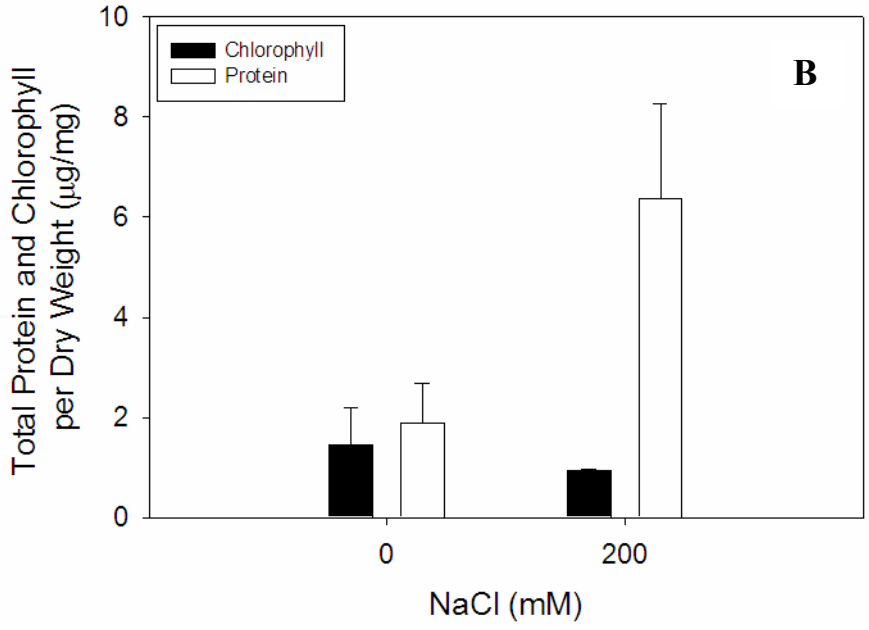
Chlorophyll
Protein
B
Total Protein and Chlorophyll per Dry Weight (µg/mg)
10
8
6
4
2
0
0
200
NaCl (mM)

Figure 12. Western blot at different NaCl levels in *S. eltonica*: Ponceau S stain. The fractionated proteins from *S. eltonica* are shown in the gel below. The molecular weights are shown beside the protein ladder. Samples were loaded onto the gel with the same amount of total protein. Two different amounts of protein were loaded to prevent over staining of high abundance proteins. R = replicate number.

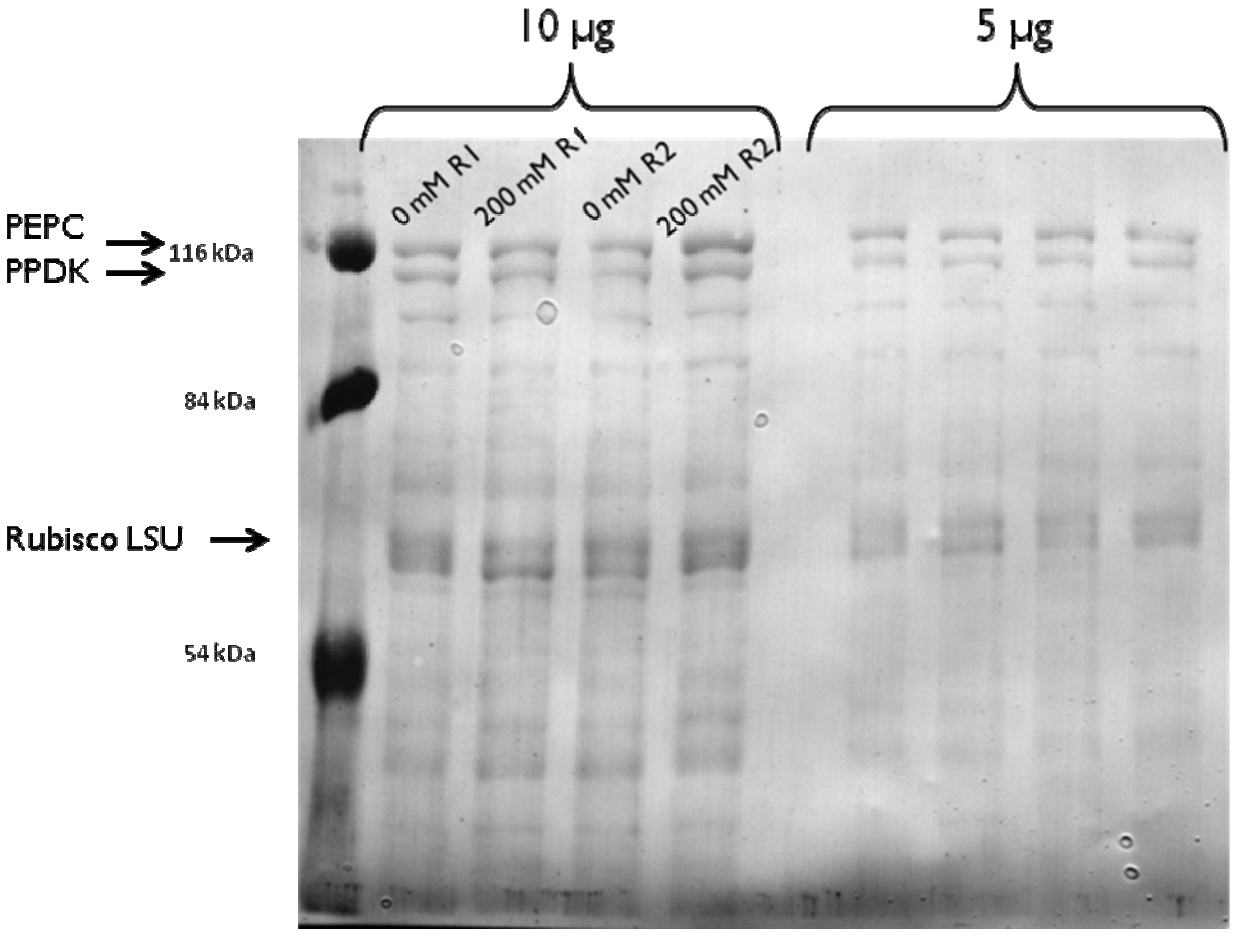

Figure 13. Western blot quantification under varying NaCl levels in *S. eltonica*. The relative intensity of each band was quantified using ImageJ analysis program. The relative intensity was compared to the treatment without NaCl, which represented 100%. Error bars represent the standard error of the mean. N= 2

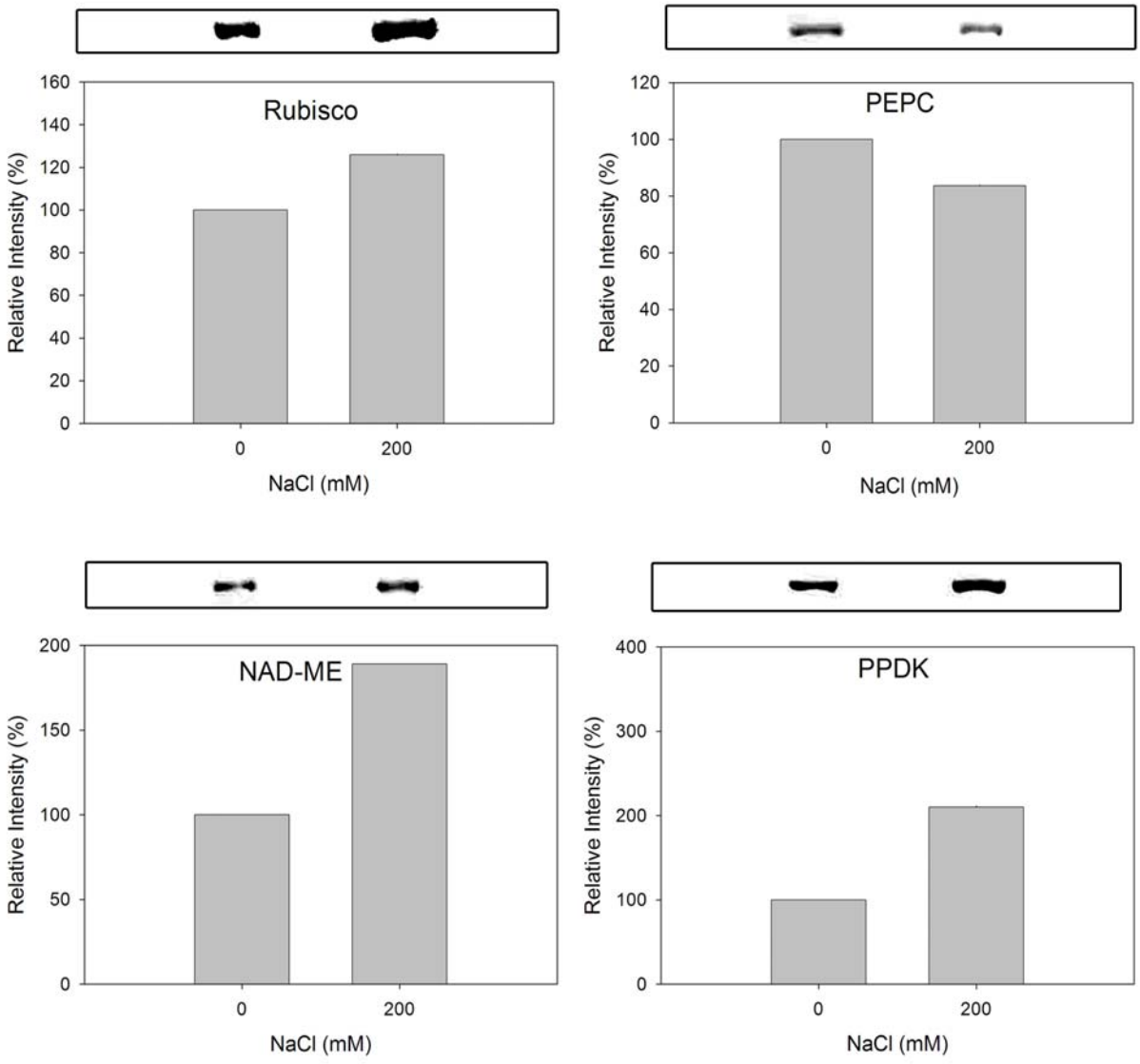
Rubisco
Relative Intensity (%)
160
140
120
100
80
60
40
20
0
0
200
NaCl (mM)
PEPC
Relative Intensity (%)
120
100
80
60
40
20
0
0
200
NaCl (mM)
NAD-ME
Relative Intensity (%)
200
150
100
50
0
0
200
NaCl (mM)
PPDK
Relative Intensity (%)
400
300
200
100
0
0
200
NaCl (mM)

Figure 14. Western blot comparison at two different NaCl levels in *S. eltonica*. The relative intensities for each enzyme were expressed on a protein and leaf area basis. The relative intensity was compared to the treatment without NaCl, which represented 100%. A) relative intensity on a protein basis (%), and B) relative intensity on a leaf area basis (%). Error bars represent the standard error of the mean. N= 2

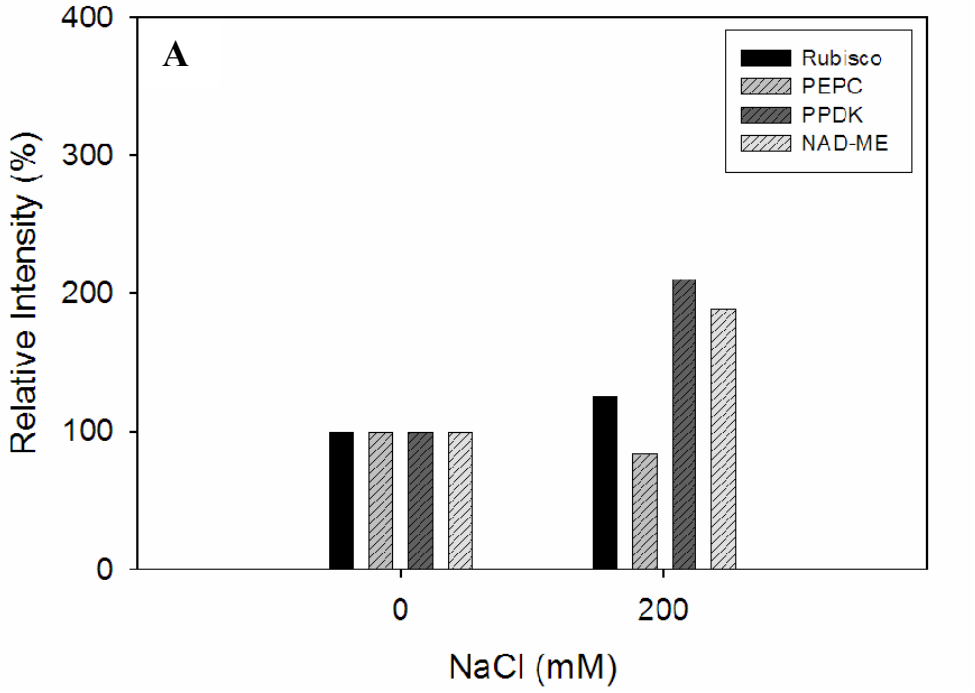
A
Rubisco
PEPC
PPDK
NAD-ME
Relative Intensity (%)
400
300
200
100
0
0
200
NaCl (mM)

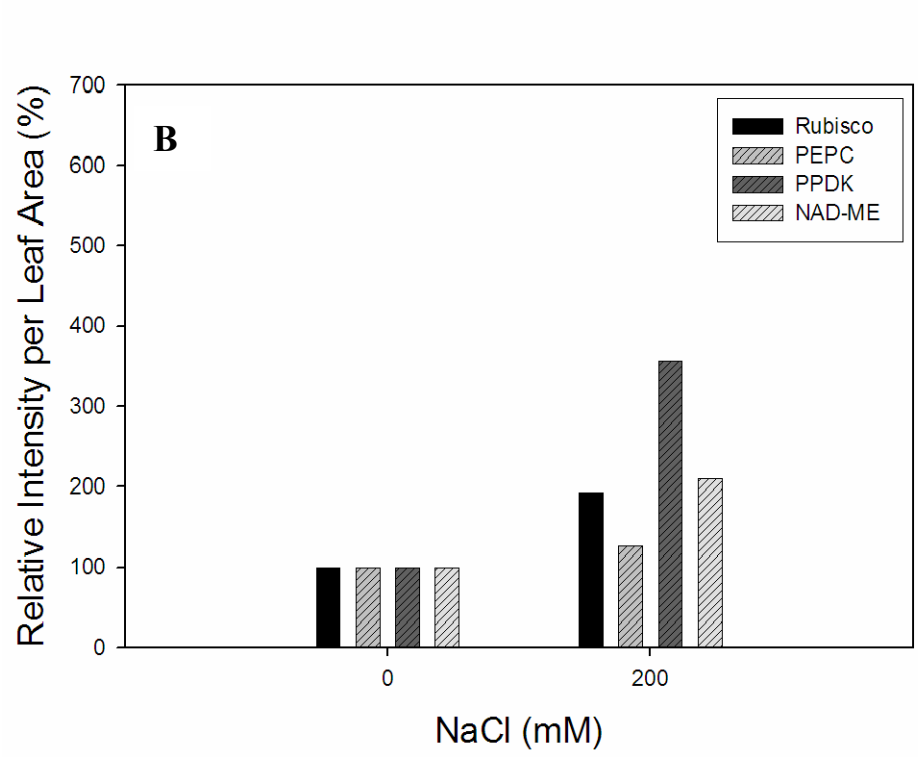
B
Rubisco
PEPC
PPDK
NAD-ME
Relative Intensity per Leaf Area (%)
700
600
500
400
300
200
100
0
0
200
NaCl (mM)

Figure 15. Carbon isotope discrimination ($\delta^{13}C$) analysis under varying NaCl levels in *S. eltonica*. The carbon isotope discrimination was measured under each NaCl treatment in *S. eltonica*. The isotope discrimination is measured in parts per thousand. Error bars represent the standard error of the mean. N= 2